Wang, Zhaohui, <u>Molecular Mechanisms of and Potential Therapies for Oxidative Damage to the Retinal Pigment Epithelium</u>. Doctor of Philosophy (Biomedical Sciences), September 2007, 161 pages, 34 illustrations, bibliography, 119 titles.

Age-related macular degeneration (AMD), the most common cause of irreversible vision loss in the elderly, results mainly from degeneration of the retinal pigment epithelium (RPE) and loss of photoreceptor cells. Oxidative stress has been acknowledged as a leading cause of RPE degeneration and concomitant photoreceptor cell loss, but the exact role of reactive oxygen species (ROS) in RPE cell death remains to be established. Moreover, while mitogen-activated protein kinases (MAPKs) are suggested to be involved in RPE degeneration induced by oxidative stress, the precise functions and molecular mechanisms of MAPKs in RPE degeneration remain elusive. In spite of the numerous therapeutic modalities proposed for AMD, the treatment of AMD remains unsatisfactory. Recent studies suggesting stem cells as a potential source for trophic factors in damaged murine hearts led us to investigate a possible role for stem/progenitor cell-derived factors in protecting RPE cells from oxidative damage. In this study, we demonstrate that p42/44 MAPK protect RPE cells from oxidative damage. Furthermore, human retinal progenitor cells promote RPE cell survival by regulating p42/p44 MAPK activity.
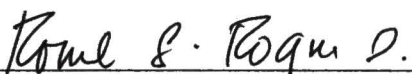
When exposed to oxidative stress produced by glucose oxidase/glucose, human RPE cells exhibited membrane blebbing and cytoskeleton remodeling in the early phase of oxidative stress. Prolonged exposure to oxidative stress induced mitochondrial

membrane potential depolarization, cell death and DNA condensation, but not DNA fragmentation. Furthermore, both p38 MAPK and p42/p44 MAPK were activated by oxidative injury. P38 MAPK inhibitor, but not p38 MAPK siRNA, inhibited RPE cell death induced by oxidative stress. Overexpression of constitutively active MEK1 inhibited RPE cell death exposed to oxidative damage. In contrast, interfering p42/p44 MAPK expression accelerated oxidative-stress induced RPE cell death. To investigate the effects of human retinal progenitor cells (hRPC) on RPE cells, we isolated and expanded hRPC *in vitro*. The hRPCs expressed markers of neuronal and retinal progenitor cells, and were capable of differentiating into neuronal phenotype in defined medium. In the presence of 10% fetal bovine serum, hRPC developed towards the glial phenotype. The conditioned medium collected from hRPC suppressed RPE cell death induced by oxidative damage. Furthermore, conditioned medium of hRPC induced activation of p42/p44 MAPK, and the protective effect of hRPC conditioned medium was suppressed by p42/p44 MAPK inhibitor. Our studies increase our understanding of the molecular mechanisms that could be employed to rescue RPE cells from degeneration and support the therapeutic potential of retinal progenitor cells. It will provide further insight into molecular mechanisms of AMD and establish a foundation for the long-term prevention and treatment of AMD
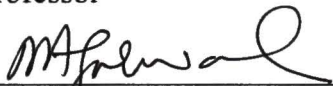
MOLECULAR MECHANISMS FOR AND POTENTIAL THERAPIES OF

OXIDATIVE DAMAGE TO THE RETINAL PIGMENT EPITHELIUM

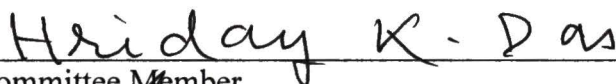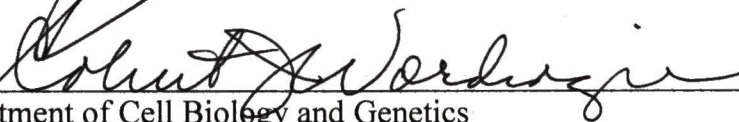Zhaohui Wang, M.S.

APPROVED:

_____
Major Professor

_____
Committee Member

_____
Committee Member

_____
Committee Member

_____
University Member

_____
Chair, Department of Cell Biology and Genetics

_____
Dean, Graduate School of Biomedical Science

MOLECULAR MECHANISMS OF AND POTENTIAL THERAPIES FOR

OXIDATIVE DAMAGE TO THE RETINAL PIGMENT EPTTHIELIUM

DISSERTATION

Presented to the Graduate Council of the

Graduate School of Biomedical Sciences

University of North Texas

Health Science Center at Fort Worth

In Partial Fulfillment of the Requirements

For the Degree of

DOCTOR OF PHILOSOPHY

By

Zhaohui Wang, M.S.

Fort Worth, Texas

September 2007

ACKNOWLEDEMENTS

TABLE OF CONTENTS

LIST OF ILLUSTRATIONS

CHAPTER I

INTRODUCTION

Retinal Pigment Epithelium (RPE)

The retinal pigment epithelium (RPE) is a monolayer of pigmented epithelial cells that separates the neural retina from choroidal circulation, thereby forming a functional blood-retinal barrier. An important function of RPE is to regenerate retinal, a metabolite of vitamin A, to maintain the excitability of photoreceptors. Photosensitization initiates the conformational change of 11-*cis*-retinal into all-*trans*-retinal, but photoreceptors could not recycle all-*trans*-retinal back to 11-cis-retinal due to lack of *cis-trans* isomerase. Therefore, all-*trans*-retinal is transported to RPE, where reisomerization to *11-cis-retinal* is completed by the participation of RPE-65, a RPE-specific protein. Newly formed 11-*cis*-retinal reenters into photoreceptors, binds to opsin and serves for light transduction.

The RPE transports materials between the retina and the choriocapillaries. The RPE carries water, ions or metabolic end products from photoreceptor outer segments to the blood. In the opposite direction, RPE transports glucose, fatty acid and other nutrients from the choroidal capillaries to the photoreceptors to provide nutrition. As described

1

above, RPE recycles retinal to maintain the visual function of photoreceptors. Similar to vitamin A, docosahexaenoic acid is also critical for the integrity of photoreceptor outer segments and inner segments. Since photoreceptors could not synthesize docosahexaenoic acid, the delivery of docosahexaenoic acid to photoreceptors by the RPE plays a critical role in visual transduction.

Photoreceptor outer segments are exposed to intense light throughout its lifetime and hence accumulate photo-damaged proteins and lipids which disturb the proper visual function of photoreceptors. Therefore, in order to maintain the photo-excitability of photoreceptors, the photoreceptor outer segments have to be renewed constantly. The tips of the photoreceptor outer segments are shed from the photoreceptors due to increased accumulation of toxic substances. The discarded photoreceptor outer segments are finally phagocytosed by the RPE.

The RPE also secretes a wide variety of growth factors to support the survival and normal function of photoreceptors. Among them are fibroblast growth factor (FGF), transforming growth factor-β (TGF-β), insulin-like growth factor (IGF), VEGF, pigmented epithelium-derived factor (PEDF). The RPE also synthesizes and releases tissue inhibitor of matrix metalloprotease (TIMP) to maintain the structural integrity of choriocapillaries and retina. Furthermore, by secreting immunosuppressive molecules, the RPE could establish the immune privilege of the retina. In addition, RPE maintains the ion homeostasis in the subretinal space by either transporting or buffering electrolytes [1]. (Figure 1.2)

Since RPE is indispensable for visual function of the retina, degeneration of RPE leads to the loss of vision.

Age-related macular degeneration (AMD)

Age-related macular degeneration (AMD) is an ocular disease characterized by progressive degeneration of the retinal pigmented epithelium (RPE) and neighboring photoreceptors in the macula of the retina (Figure1.1). This often leads to severe visual impairment and even permanent blindness. AMD is the leading cause of permanent blindness in the United States. [2] According to epidemiological studies, 11% of 65-74 years old people have AMD, with the incidence rising to 28% in people aged 75-85. About 2% of elderly suffer from blindness from AMD [2]. It is estimated that the incidence will increase 50% by 2020 [3].

Although the visual loss results from the loss of photoreceptor cells, the initial pathogenesis involves degeneration and atrophy of RPE. The progressive RPE dysfunction and eventual RPE cell death cause subsequent degeneration of rod and cone photoreceptors, perhaps due to loss of trophic support and defensive barrier. AMD patients lose both central vision and color vision due to damaged photoreceptors in the macula.

AMD is generally classified as either dry type (non-neovascular) or wet type (neovascular) according to pathological mechanisms. About 10% of AMD patients are afflicted by wet type AMD, which occurs when abnormal new vessels grow in the choroid. The newly formed vessels could penetrate the RPE layer and when torn, could

bleed and cause damage to surrounding tissues. Wet type AMD is associated with severe and abrupt vision loss, and could be treated by laser or antiangiogenic drugs in some cases. In contrast, dry type AMD causes less severe and more gradual vision loss but has proven resistant to therapy. Dry type AMD is characterized by early drusen formation beneath RPE. Drusen, the key identifier of dry AMD, are accumulations of extracellular waste materials in Bruch's membrane. The presence of a few small drusen is normal with advancing age, and most people over 40 have some hard drusen. However, the presence of larger and more numerous drusen in the macula is a common early sign of age-related macular degeneration [4].

Reactive oxygen species (ROS)

Reactive oxygen species (ROS) include hydrogen peroxide, hydroxyl radical, superoxide anion and hydroxyl radical. ROS are small but highly reactive molecules. Reactive oxygen species are natural byproducts of the normal metabolism of oxygen and play important roles as intracellular signaling molecules. Furthermore, during environmental stress intracellular ROS levels could dramatically increase, which result in oxidative damage to cellular components.

Reactive oxygen species (ROS) exist in aerobic cells in balance with antioxidants. When this ROS-antioxidant balance is disrupted, excessive ROS, or depletion of antioxidants, or both, result in the production of oxidative stress, which attacks a variety of biomolecules, including proteins, lipids and nucleic acids. In viable cells, endogenous

4

ROS are primarily derived from hydrogen peroxide and superoxide anion. Alternatively, the superoxide anion radical is converted into hydrogen peroxide by superoxide dismutase. Hydrogen peroxide might be metabolized into water by catalase or glutathione peroxidase. The induction or downregulation of the activities of these enzymes could considerably affect intracellular redox potential and cellular functions [5].

There are growing evidences that oxidative stress is involved in various degeneration diseases such as cancer, chronic inflammation, ischemia, diabetes, neural degeneration and atherosclerosis. Therefore, the potential therapeutics is directed towards development of substances that might inhibit the deleterious effects of ROS experimentally and clinically.

Oxidative stress and degeneration of RPE

Although the genetic and molecular mechanisms of AMD remain vague, studies suggest that it is a multi-factorial disease. Oxidative stress and genetic predisposition are strongly implicated in the etiology of AMD.

Prolonged light exposure and high oxygen demand of the retina render the RPE prone to oxidative stress. Intense light, high oxygen stress in the macula, the peroxidation of the shed photoreceptor outer segments and phagocytosis all contribute to the oxidative damage to the RPE. Long-term accumulation of DNA damage, especially those on the mitochondrial genome, also results in accelerated aging and exacerbates oxidative damage. On the other hand, the antioxidant capability of the RPE attenuates with aging.

The antioxidant defense system of the RPE consists of lipophilic antioxidants (such as retinoid, Vitamin E, and carotenoid), hydrophilic reducing antioxidants (such as vitamin C and glutathione), and enzymes with antioxidant capability (such as superoxide dismutase and catalase). In the human retina, the downregulation of catalase activity was observed in both macular and peripheral RPE [6]. Lipofuscin, an age-related pigment, accumulates in the RPE as a result of oxidative damage [7]. Superoxide dismutase (SOD)-deficient animals exhibit typical clinical features of age-related macular degeneration, including increased drusen formation with aging [8]. Photic injury also induces cell death of RPE *in vitro* by free-radical-associated mechanisms [9].

Inflammation, genetic factors and degeneration of RPE

Growing evidence suggests that the complement system plays a substantial role in the pathogenesis of age-related macular degeneration. Local chronic inflammatory events were shown to be involved in the formation of drusen [10]. Genetic variants of Complement factor H (CFH) have recently been identified to contribute to the pathogenesis of AMD, supporting the inflammatory hypothesis in the etiology of AMD [11] [12] [13].

The complement system comprises of three principal pathways and at least 30 enzymes and regulators. The classical, alternative and lectin pathways converge on the activation of complement C3. The activation of C3 is inhibited by CFH, a complement regulatory protein. CFH primarily inhibits the alternative complement pathway. Primarily produced by the liver, CFH is also synthesized in RPE cells. Once released to

6

extracellular space, CFH accumulates within drusen. Although genetic approaches have identified the involvement of CFH in the etiology of AMD, its precise role in AMD development remains elusive.

Drusen is the key identifier of dry type AMD. Several complement proteins, including C3, C5 and C5b9, are found in the drusen. Furthermore, fluid-phase complement regulatory proteins, such as vitronectin and clusterin, have been identified in drusen. MCP and CR1, membrane-bound complement regulator proteins, have also been found in drusen [14].

Treatment for AMD

Dry type AMD is resistant to current therapies. Since oxidative stress is largely involved in the pathogenesis of AMD, antioxidants have been utilized in the clinic to prevent the loss of RPE cells. High concentrations of zinc, vitamin C, vitamin E, or beta-carotene have all been used in clinical trials to protect the RPE from oxidative damage. However, their beneficial effects remain controversial [15, 16]. The induction of glutathione synthesis may also protect the RPE from oxidative injury. A mixture of glutamine, glycine and cysteine has been shown to significantly increase the intracellular GSH levels. Dimethylfumarate (DMF) also displays a similar positive effect on AMD patients. Recently, melatonin was shown to markedly reduce oxidative stress-induced cell death and mitochondrial DNA damage in cultured RPE cells [17].

To date, there is no effective treatment for dry AMD, whereas limited therapies are available for wet type AMD. For example, Verteporfin photodynamic therapy (PDT) is a combination of drug and laser therapy available for wet type AMD. Briefly, a photosensitive dye is administered intravenously as pro-drug to perfuse choroidal neovascular membranes. A laser light is then employed to activate the photo-sensitizer, producing an active drug that inhibits the angiogenesis. As a result, the PDT therapy inhibits the leakage of newly formed vessels. Clinical studies showed that 14% of patients had improved vision after PDT treatment, while 70% of patients had stabilized vision. However, PDT cannot restore the vision that has been lost due to AMD [18].

New treatments in the wet type AMD have been developed over the past few years as a result of the increased understanding of the pathogenesis of angiogenesis in AMD. Pegaptanib, a single strand of nucleic acid, is the first drug developed to inhibit the deregulation of VEGF, the underlying cause of wet type AMD. Pegaptanib is a pegylated anti-VEGF aptamer that specifically binds to VEGF and inhibits the angiogenesis. Originally developed as anti-cancer drug, Bevacizumab, a humanized monoclonal antibody, showed promise in the treatment of wet-type AMD by targeting VEGF and new vessel formation [19]. In 2006, ranibizuma, a humanized monoclonal antibody fragment, demonstrated an overall gain of visual acuity on wet type AMD patients in a multi-center, 2-year long, double-blind clinical trials [20].

A couple of RNAi-based therapeutics is also being pursued by biopharmaceuticals. The strategy is aimed at knocking down gene expression of VEGF or VEGF receptor. Acuity pharmaceutical developed Cand5 to abrogate VEGF mRNA

expression, showing positive results in Phase II trials. Sirna-027, siRNA therapeutics against VEGF developed by SiRNA Inc., showed 100 % visual acuity stabilization after a single intravitreal injection in Phase I trials.

Cell transplantation therapy for ocular disease has emerged as a promising experimental approach to restore retinal function and vision. RPE and human photoreceptor transplantation have been used to treat AMD and retinitis pigmentosa patients [21-23], although the results are less gratifying and beneficial. The use of neuronal/retinal stem cells to treat ocular disease exhibits similar results. For example, undifferentiated rat retinal progenitor cells were expanded *in vitro* and grafted into RCS rats in the superior quadrant close to the optic disc. Four weeks after grafting, most of the transplanted cells differentiated into glia but not neurons, regardless of the multiple differentiation potential in cell culture [24].

RPE and cell death

RPE cell death in AMD remains controversial. Reports suggest that both apoptotic and non-apoptotic cell death of the RPE occur in AMD. Apoptosis is characterized by complicated and multifaceted regulation. Apoptotic cells are identified by morphological changes including plasma membrane blebbing, cell shrinkage, chromosome condensation, and DNA fragmentation, followed by phagocytosis by neighboring cells. Mitochondrial pathway of caspase activation is triggered by the release of various proteins from mitochondria. Extrinsic stresses promote the translocation of

pro-apoptotic members of Bcl-2 family into the mitochondria, where Bax/Bak oligomers form pores for the apoptogenic proteins to pass through or destabilize the mitochondrial membrane. Of the released mitochondrial proteins, cytochrome C binds to procaspase-9 and Apaf-1 to form the apoptosome complex while AIF and Endo G induce DNA fragmentation [25].

Non-apoptotic cell death consists of necrosis, mitotic catastrophe, autophagy and senescence. The molecular mechanism that regulates non-apoptotic cell death is not fully understood, but does not appear to involve caspase activation [26]. Necrosis is the most observed and investigated in non-apoptotic cell death. In contrast to the "active" nature of apoptosis, necrosis is defined as a" passive" process of cellular destruction in response to profound cellular damage. Necrosis displays a distinctive set of morphological changes, including cellular swelling, organelle degeneration and clumping of nuclear DNA. Recently, it has been reported that necrosis might undergo regulated cell death in response to alkylating DNA damage by excessively activating PARP [27].

RPE cell death was characterized in postmortem retina from AMD patients using TUNEL staining [28]. Since TUNEL staining identifies DNA fragmentation but is not a unique marker for apoptosis, the type of RPE cell death in AMD remains undefined.

When exposed to menadione, ARPE-19, a well-established human RPE cell line, displayed features of caspase-independent cell death. The stressed RPE cells were shown to exhibit membrane blebbing, nuclear condensation but not nucleosomal fragmentation. The mitochondrial membrane depolarization, release of AIF and cytochrome C were also observed in this study [29]. Furthermore, tert-butyl-hydroperoxide(t-BHP) induced cell

death without activating caspase-3 using the same RPE cell line [30]. ARPE-19 cells exposed to hydrogen peroxide exhibited both apoptotic and necrotic morphologies as determined by electron microscopy. The redistribution of AIF from mitochondria to nucleus was observed in the same study [31].

RPE has been shown to be associated with mitochondrial apoptosis. In RPE cells damaged by oxidative stress, caspase activation and DNA fragmentation were preceded by decreased mitochondrial membrane potential[32] and increased expression of p53, caspase-3 and p21[33]. Furthermore, overexpression of Bcl-2 inhibited the apoptosis of RPE *in vitro* [34].

p38 MAPK

The mitogen-activated protein kinase (MAPK) family is a group of highly conserved protein kinases involved in multiple cellular processes, including proliferation, differentiation, cell death, inflammation and migration. MAPK family consists of extracellular-signal-regulated kinase (ERK, p42/p44 MAPK), p38 MAPK, c-Jun-amino-terminal kinase (JNK), and ERK5.

p38 MAPK plays critical roles in cell death, differentiation and inflammation in response to a wide array of environmental stresses or extracellular signals (such as oxidative stress, irradiation, osmotic stress, hypoxia, pro-inflammatory cytokines and less often growth factors). Depending on specific cell type or environmental stimuli, p38

11

differentially regulates cellular functions. Whereas p38 activation induces cell death, it may also promote cell proliferation, differentiation and inflammation.

p38 MAPK modulates cellular responses via diversified signal pathways (Figure 1.3.). Once activated by upstream kinase, p38 phosphorylates multiple downstream substrates, which initiate complex signal cascade in response to stresses. p38 MAPK mediates downstream effects by directly activating either transcription factors, such as ATF-1/2/6, SRF accessory protein (Sap1), CHOP, p53, C/EBPβ, MEF2C, MEF2A, MITF1, DDIT3, ELK1, NFAT, and high mobility group-box protein 1 (HBP1), or kinase substrates such as MAPKAPK2, lymphocyte-specific protein 1 (LSP1), cAMP response element-binding protein (CREB), transcription factor ATF1, SRF 56, and tyrosine hydroxylase [35].

p38 MAPK has four isoforms, α, β, γ, δ, with only about 60% homology among them. p38 MAPK α and p38 MAPK β are ubiquitously expressed and specifically inhibited by pyridinyl imidazole compounds, such as SB203580. In contrast, p38 MAPK γ and p38 MAPK δ are tissue-specific and could not be inhibited by pyridinyl imidazole compounds. p38 MAPK α, β, γ are activated by MEK3 and MEK6, while p38 MAPK δ is selectively activated by MEK6.

The four isoforms of p38 MAPK activate different cellular signalings and hence could play different roles, depending on specific stress in experimental model. It has been shown that p38MAPK β could specifically phosphorylate glycogen synthase in skeletal muscle, liver and brain and regulate glucose homeostasis during exercise [36]. p38 MAPK δ has been found to be the sole p38 MAPK that regulated keratinocyte differentiation by

activating AP-1 and CAATT enhancer binding protein factors. Furthermore, p38 MAPK δ could associate with p42/p44 MAPK and negatively regulate the activity of p42/44 MAPK [37].

By modulating c-JUN activity differentially, isoforms of p38 MAPK regulated AP-1 dependent transcription and subsequent cellular functions [38]. Briefly, p38 MAPK β did so by phosphorylating c-JUN, while p38 MAPK γ and p38 MAPK δ regulated AP-1 transcription to modulate cellular proliferation. p38 MAPK isoforms were involved in divergent cellular functions in heart failure. Overexpression of p38MAPK α induced apoptosis in cultured cardiomyocytes, whereas overexpression of p38 MAPK β induced cardiac hypertrophy [39].

p38 MAPK α was critical for mouse embryonic development since its inactivation caused embryonic death, while knockout mice of p38 MAPK β , γ, δ were viable. Interestingly, regardless of being largely expressed in the embryo, p38 MAPK α appeared to be only critical for placental organogenesis but not embryonic development [40]. In UVB-irradiated human keratinocyte, apoptosis signal regulating kinase-1 (Ask-1) mediated the pro-apoptotic effect of reactive oxygen species by activating p38 MAPK. In this study, p38 MAPK α[-/-] murine embryonic fibroblasts were resistant to UVB-induced apoptosis [41].

p38 MAPK β knockout animals were viable and showed no health problems. p38 MAPK β knockout animals exhibited normal immediate-early transcriptional responses, suggesting that p38 MAPK α might be the primary isoform involved in these events. Furthermore, p38 MAPK β knockout animals displayed typical symptoms of rheumatoid

arthritis and inflammatory bowel disease when hydrided with a mouse line over-expressing TNF [42]. The p38 MAPK ɣ and p38 MAPK ẟ knockout mice were viable, fertile, lack of apparent health problems. Similarly, the double knockout animals were viable, fertile and exhibited no apparent health problems [43].

In RPE cells, p38 MAPK exerts multiple functions, including TGF-β2-mediated VEGF expression [44], stimulation of interleukin -8 and monocyte chemotactic protein (MCP)-1 secretion [45], TGF-β2-mediated Type I collagen expression, [46] and PDGF-mediated cell migration [47]. p38 MAPK was also suggested to induce apoptosis in hydrogen peroxide treated ARPE-19 cell line [48], whereas p38 MAPK was shown to be cytoprotective using the same RPE line (ARVO abstract, 2006).

Heat shock protein 27(HSP27) is a specific substrate of p38 MAPK and regulates cytoskeleton reorganization in response to environmental stresses [49] (Figure1.4.). In cardiomyocytes exposed to ischemia, both p38 MAPK and HSP27 were activated and activated HSP27 disassociated from actin filament. p38 MAPK inhibitor SB203580 inhibited the ischemic injury to the cardiomyocyte [50]. On the other hand, reorganized cytoskeleton appeared to be involved in cytoprotection in cellular injury. Phosphorylation of HSP27 protected complement-induced disruption of the actin cytoskeleton and cellular injury in glomerular epithelial cells [51]. In stressed RPE cells, abrogating the activation of HSP27 accelerated the reorganization of focal adhesion and the onset of apoptosis [52].

p42/p44 MAPK

p44/p42 MAPK (ERK1/2) belong to classical MAPKs. The two isoforms share 83% homology and are ubiquitously expressed in human. Typically, p44/p42 MAPK is activated by upstream MEK1/2, members of MAPKK family. Upstream, MEK1/2 is activated by Ras and Mos, members of MAPKKK. MAPKKK is activated by either extracellular mitogens or environmental stresses. Activated p42/p44 MAPK activates a variety of substrates, including protein kinases, such as ribosomal S6 kinase (RSK), mitogen and stress activated kinase (MSK) and MAPK interacting kinase (MNK), and transcription factors, such as ELK1, c-Fos, c-Myc and Ets domain factors [53] (Figure 1.5.).

p42/p44 MAPK signaling is involved in multiple cellular functions, including proliferation, differentiation and stress responses. In response to environmental stresses, p42/p44 MAPK may be pro-apoptotic or anti-apoptotic. For example, elevated activity of p42/p44 MAPK promoted cell survival when exposed to hydrogen peroxide [54]. However, p42/p44 MAPK activation was required in cisplatin-induced apoptosis [55].

p42/p44 MAPK is localized throughout the cell, primarily bound to cytoplasmic microtubule or plasma membrane receptors. However, mitogens or environmental stresses might induce translocation of activated p42/p44 MAPK to the nucleus, where p42/p44 MAPK could phosphorylate transcription factors and nuclear proteins, differentially regulating gene expression [56].

p42/p44 MAPK pathway has been investigated by gene targeting approach. There was about 60% reduction of p42/p44 activity in B-Raf-deficient knockout animals, while knocking down Raf-1 and C-Raf exerted modest effects on p42/p44 MAPK activity. B-

Raf knock out animals developed neurological defects around day 21 compared to wild-type litters. Similarly, Raf-1 knock out animal underwent apoptosis, leading to embryonic lethality [57].

p44 MAPK invalidation is dispensable for embryonic development, but is critical for differentiation of the adipocyte and thymocyte. P42 MAPK inactivation is embryonic lethal in animal model and can not be rescued by p44 MAPK compensation. P42 MAPK was indispensable for placental development but not for proliferation and differentiation of embryonic stem cells [58].

P42/p44 MAPK was phosphorylated in RPE cell death induced by oxidative stress [59]. In another study, p42/p44 MAPK was shown to induce cell death in oxidant stressed RPE cell culture. [30]. PEDF protected RPE from oxidative stress by activating p42/p44 MAPK pathway [60]. 15-deoxy-Delta (12, 14)-prostaglandin J (2) (dPGJ(2)) also rescued RPE from hydrogen peroxide induced cell death by activating MEK-p42/p44 MAPK pathway[61].

Stem Cells

"Stem cell" is a cell that can self-renew and give rise to multiple specialized cell types. Stem cells exist at various time points during the lifespan of an individual, from embryo to adult. Stem cells are usually divided into two groups: embryonic stem cells and adult stem cells. ES cells are pluripotent and generally give rise to all cell types of the human body (Figure1.6.). Human ES cells can be isolated from blastocyst, expanded in

16

culture dishes and then administered into diseased organs to replace the damaged cells or tissues. Adult stem cells exhibit "stemness" behavior and are found in adult tissues as indicated by its name. They are more committed, and hence sometimes called "progenitor cells". Adult stem cells remain quiescent in the differentiated tissue, but still retain the potential to differentiate. The main use of adult stem cells by human body might be to maintain and repair the host tissues under stress conditions. Adult stem cells have been reported in the brain, bone marrow, peripheral blood, blood vessels, skeletal muscle, skin, liver, heart and retina. Under laboratory conditions, adult stem cells can not be expanded over a large number of generations without losing their stem cell properties. The most important application of stem cells in regenerative medicine is to repair the damaged organs via transplantation, offering the potential to treat Parkinson's disease, spinal cord injury and, as proposed in this study, AMD.

Retinal Progenitor Cells

Retinal development is initiated in the central optic cup and specialized neurons and glia are developed in a relatively fixed chronological sequence until full maturation (Figure 1.7.). During retinogenesis from the optic cup, it is the retinal progenitor cells (RPC) in the neuroblastic layer that proliferate and give rise to postmitotic progenies of the mature retina. Retinal progenitor cells possess the potential to generate most classes of retinal cells-both retinal neurons and Muller glia. In the postnatal rodent retina, retinal progenitor cells exhibit multipotent potential until the end of the development stage [62].

Cold-blood vertebrates, such as fish and amphibians, continue retinal development throughout their lifespan by adding new neurons at the ciliary margin. In 2000, it was reported that adult retinal stem cells were found in mouse pigmented ciliary margin and the adult retinal stem cells could expand as neurospheres *in vitro* and differentiate into multiple retinal cell types. Furthermore, the isolated retinal stem cells spontaneously proliferated without addition of mitogens [63].Thereafter , several groups reported the isolation of retinal stem cell from rodent retinas. Recently, human adult retinal stem cells (hRSC) were isolated from the pars plicata and pars plana of the retinal ciliary margin from early postnatal human retinas or old human retinas. Similar to mouse retinal stem cells, hRSC could self-renew, proliferate rapidly *in vitro*, and possess potential to give rise to retinal cell types. They could survive, migrate, integrate and differentiate in the postnatal diseased mouse eyes and embryonic chick eye following transplantation [64]. Recently, photoreceptor precursor cells at a certain level of maturity were transplanted into degenerating mouse retina. The engrafted photoreceptor precursors integrated with the retina, differentiated into rod photoreceptors and restored damaged visual function [65].

Secreted trophic factors of stem cells

Stem cell research has been focused on expansion and purification of stem cells and repopulation of diseased organs with differentiated stem cells. In this respect, driving stem cells into functional postmitotic cells is a tantalizing but challenging task. Recently,

Embryonic stem cells were found to release pro-survival growth factors (IGF-1 and WNT5a) to completely reverse cardiac defects in transgenic mice through either local or long-range action [66]. Furthermore, adult hippocampal neural stem/progenitor cells could secrete autocrine/paracrine factors such as SDNSF (stem-cell derived neural stem/progenitor cell supporting factor) in order to provide trophic support for neural stem/progenitor cells and maintain the capability of stem cell [67]. Moreover, it was reported that bone marrow-derived mesenchymal stem cells protected cultured cardiomyocytes from hypoxia. Moreover, the concentrated medium rescued acute myocardial infarction in animal model [68]. These findings suggest that the therapeutic potential of stem cells can be expanded to secreted growth factors and hence stem cells could serve as a reservoir of trophic factors for the protection and/or regeneration of diseased organs. This hypothesis prompted us to investigate whether human retinal progenitor cells could release pro-survival factors to treat retinal diseases such as AMD.

Specific aims and hypothesis of the study

Age-related macular degeneration (AMD) is an ocular disease with progressive degeneration of both retinal pigmented epithelium (RPE) and neighboring photoreceptors in the macula of the retina. It often leads to severe vision damage and even permanent blindness. In spite of the numerous therapeutic modalities proposed for AMD, the treatment of AMD remains unsatisfactory. Although the genetic and molecular

mechanisms of AMD remain vague, studies suggest that it is multifactorial and oxidative stress is strongly implicated.

MAPKs are a family of protein kinases that play critical roles in response to environmental stresses. Depending on specific stresses or cell lines MAPK may be pro-survival or anti-survival by initiating distinctive signal cascades. Even though extensive research effort has been input into the underlying molecular mechanisms, the exact role of MAPK in oxidative stressed RPE cells is not fully understood yet.

Cell transplantation for ocular therapies has been proposed as a promising approach to treat retinal degeneration. Among them is to transplant brain/retina neuronal stem cells (or progenitor cells) into the retina to replace damaged retinal neurons by driving the uncommitted stem/progenitor cells to differentiate into specific neurons. However, because transplanted stem/progenitor cells can replace degenerating photoreceptor cells but barely RPE cells, stem cell grafts would result in temporary short-lived neuroprotection due to the continuing RPE dysfunction. A recent study reported that stem cells could secrete trophic factors to rescue damaged murine hearts. Meanwhile, we have isolated and expanded human retinal progenitor cells (hRPC) *in vitro* and the conditioned medium collected from hRPC protected RPE cells from oxidative stress.

The overall goal of this research is to investigate the molecular mechanisms underlying oxidative stress-induced RPE degeneration and to determine the molecular basis for the efficacy of stem cell therapy in AMD, using oxidative-stress induced RPE degeneration model.

The **hypothesis** of the study is that MAPK signaling modulates oxidative stress-induced RPE degeneration. Moreover, regulation of MAPK signaling by retinal progenitor cells protects RPE cells from oxidative stress.

The **specific aims** of the study are:

1. To establish that oxidative stress promotes degeneration of cultured RPE cells.

2. To determine the role of p38 MAPK signaling in RPE cells exposed to oxidative stress.

3. To determine the role of p42/44 MAPK signaling in RPE cells exposed to oxidative stress.

4. To determine whether retinal progenitor cells promote RPE cell survival by regulating MAPK signaling.

Figure1.1. The anatomy of the macula

Macula is a small, yellowish spot near the center of the retina. The fovea, primarily composed of cone photoreceptors and retinal pigment epithelium, is localized in the center of macula and responsible for detailed central vision (www.amdcanada.com).

MACULA

OPTIC NERVE

PHOTORECEPTORS

RPE

BRUCH'S
MEMBRANE

CHOROID
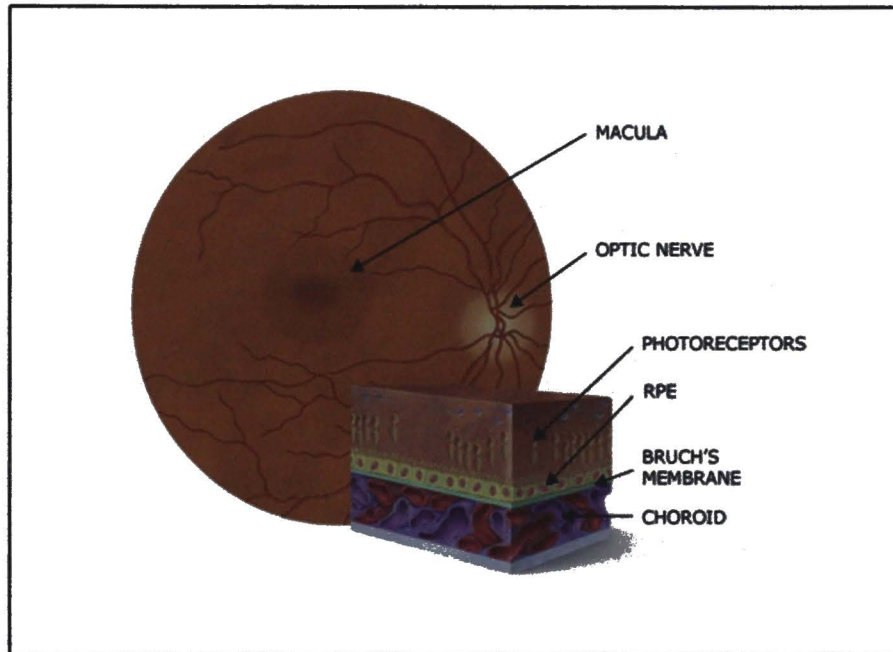
Figure1.2. Summary of the functions of retinal pigment epithelium (RPE)

The RPE separates the neural retina from the blood circulation and is an indispensable part of the retina. RPE maintains the physiological function of retina by absorbing light energy, transporting nutrients and electrolyte, recycling retinal for phototransduction, phagocytosing debris, and secreting growth factors to maintain the structural integrity of the retina. *Physiol. Rev.2005; 85: 845-881*
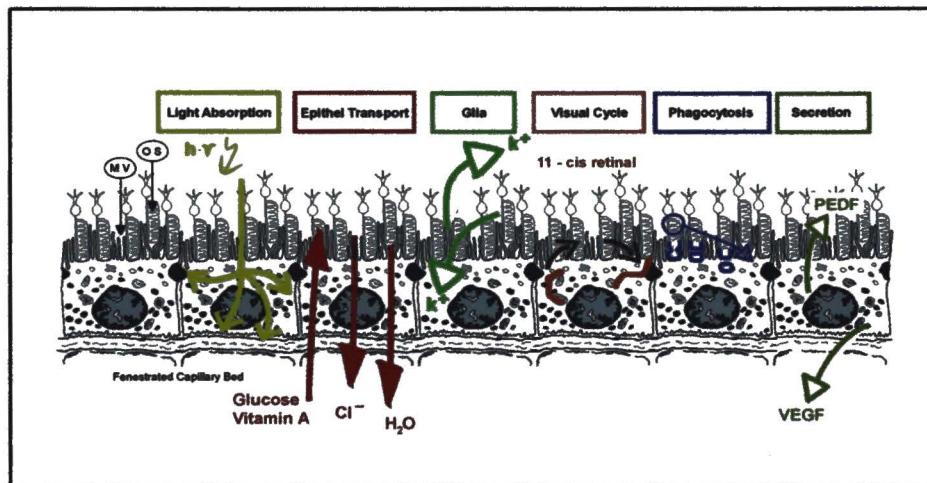
Figure1.3. Summary of p38 MAPK signal pathway

Environmental stresses activate p38 MAPK signaling by phosphorylating upstream kinases, such as (TAK1, ASK1) and MKK3/6. Once activated by MKK3/6, p38 MAPK translocates to nucleus and phosphorylates downstream transcription factors, protein kinases or other protein substrates. p38 MAPK consists of 4 isoforms, α, β, γ, δ. Only p38 MAPK α and p38 MAPK β could be inhibited by SB203580, while p38 MAPK γ and p38 MAPK δ are inhibited by BIRB0796. *Trends in Cell Biology. 2006; 16: 36-44*

TRENDS in Cell Biology
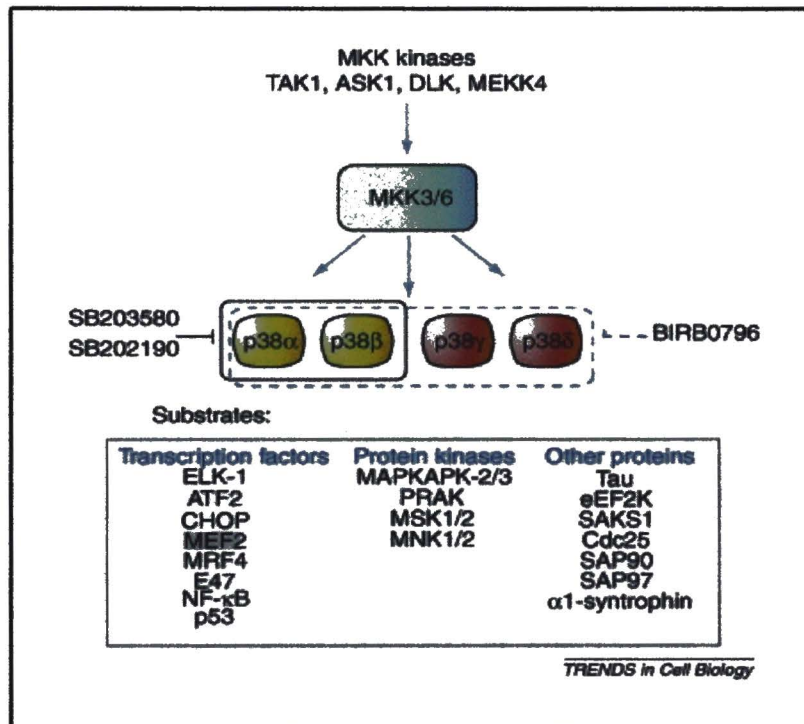
Figure1.4. Heat shock protein 27(HSP27) is activated by p38 MAPK

Aside from activating nuclear substrates, p38 MAPK phosphorylates cytoplasmic substrates and modules cellular processes post-transcriptionally. For example, p38 MAPK activates HSP27 by phosphorylating MAPKAPK2 in the cytoplasm. Activated HSP27 regulates the cytoskeleton reorganization in responses to stresses. (www.theses.ulaval.ca/2003/21038/ch03.html)

Receptors : • Tyrosine kinase
• Kinase associated
• 7 Trans-membrane domains
• Integrins
• Stress sensors
• ...

Cell Membrane

Adaptor ?
Small GTPase ?

MKKK? (PAK?)

MKK3 / MKK6

SB203580 ············· SAPK2/p38

MAPKAP k2

ATF-2

HSP 27

Nucleus

Transcription

Actin
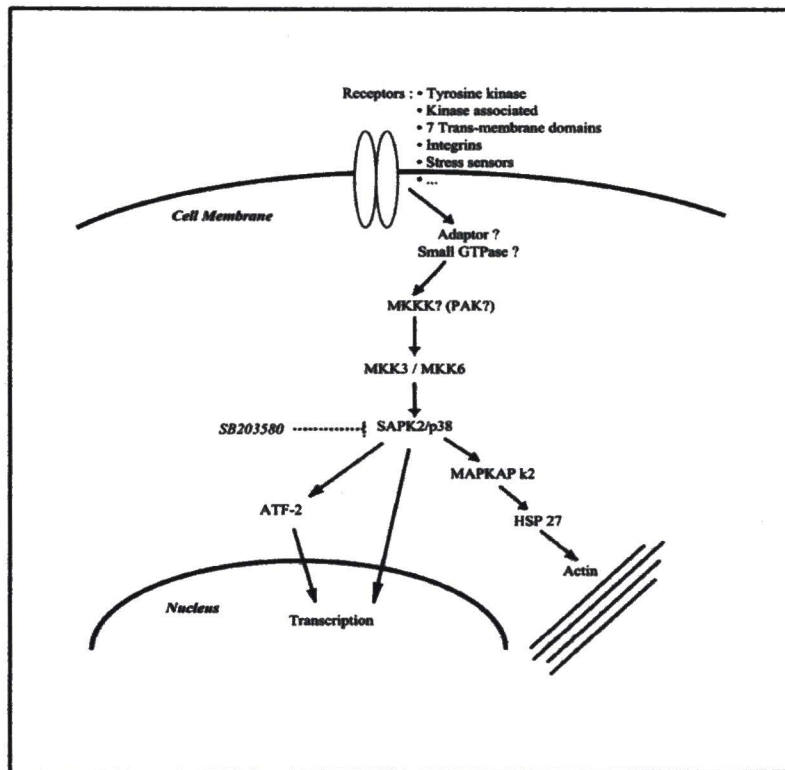
Figure1.5. Summary of Ras-Raf-MEK-p42/p44 MAPK cellular signaling

Extracellular mitogens or environmental stresses induce the activation of Ras and Raf sequentially. Activated Raf then phosphorylates p42/p44 MAPK, rendering activated p42/p44 MAPK to translocate to the nucleus. In the nucleus, activated p42/p44 MAPK regulates gene expression by acting on various substrates. p42/p44 MAPK signaling is involved in a variety of cellular events, including proliferation, differentiation and apoptosis. Expert Rev Mol Med. 2002; 25: 1-18.

The organisation and function of the Ras-Raf-MEK-ERK pathway

Expert Reviews in Molecular Medicine © 2002 Cambridge University Press
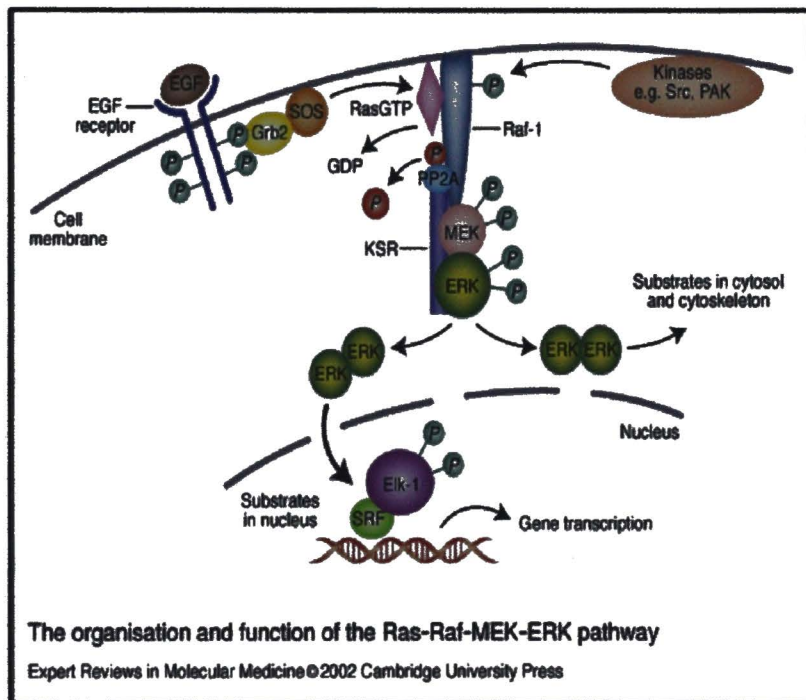
Figure1.6. Summary of pluripotent stem cells

Pluroipotent stem cells are isolated from inner mass of blastocytes and cultured *in vitro*. These unspecialized cells are characterized by properties of self-renewal and differentiation. Pluripotent stem cells have the potential to develop towards a variety of cell lineages, such as neuron, blood and muscle. (*www.csa.com*)

Pluripotent Stem Cells

Totipotent

In vivo
fertilized egg

8 cell
embryo

Cultured
undifferentiated
stem cells

Pluripotent

Blastocyst

Neural cells

Cardiac muscle

Blood cells
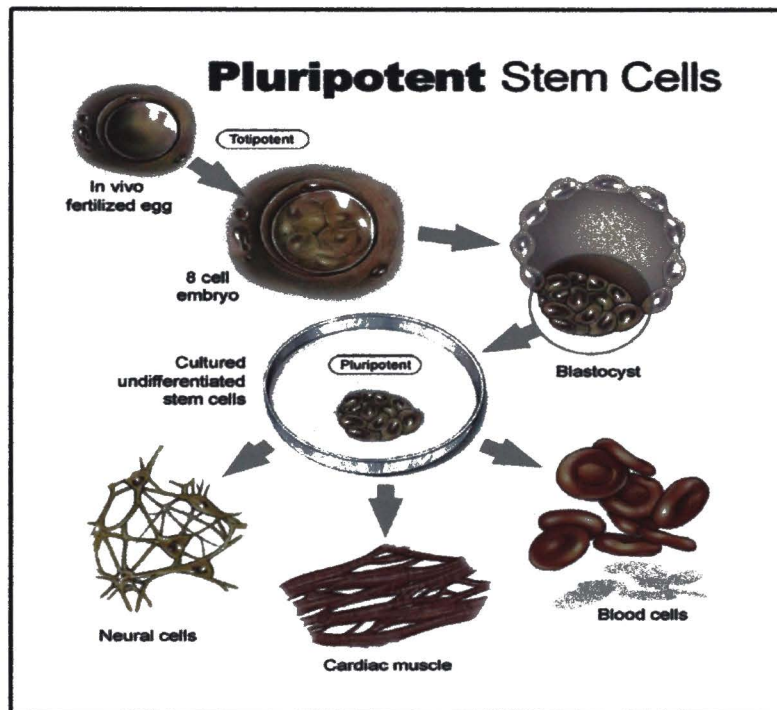
Figure1.7. Summary of retinal development

Multipotent retinal progenitor cells (RPC), residing in the inner layer of the optic cup, are the source of retinal neurons or glia, but not retinal pigment epithelium. The differentiation of retinal neurons and glia is in a relatively fixed histogenetic order. Specifically, retinal ganglion cells and horizontal cells are generated first, followed by cone photoreceptors, amacrine cells, rod photoreceptors, bipolar cells and, finally, Muller glia. The period of embryonic and postnatal days in murine development is indicated in the graph. *Trends in Neurosciences*. 2002; 25: *32-38*
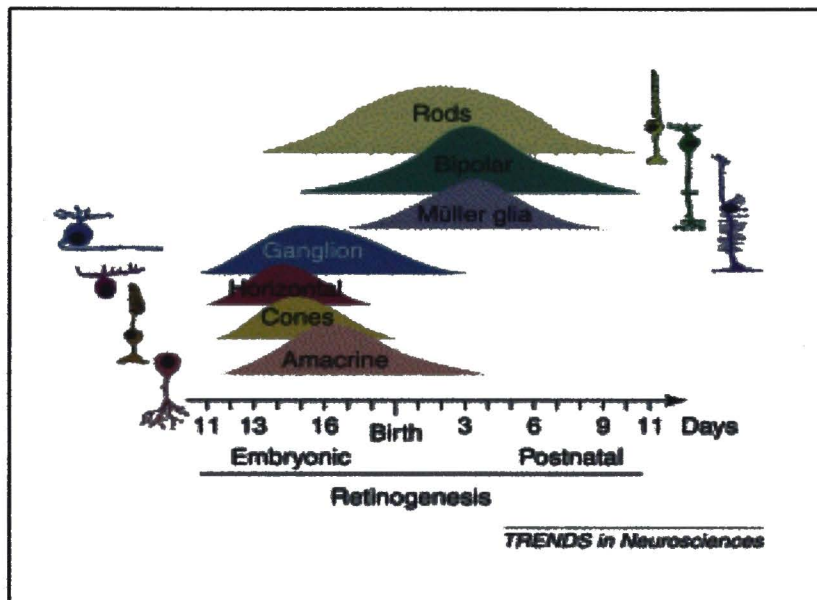
CHAPTER II

ESTABLISHMENT OF AN *IN VITRO* MODEL IN WHICH OXIDATIVE STRESS PROMOTES DEGENERATION OF RETINAL PIGMENT EPITHELIAL CELLS

Abstract

Since oxidative stress is a major factor contributing to the pathogenesis of age-related macular degeneration (AMD), many oxidants, such as hydrogen peroxide and tert-butyl hydroperoxide (t-BHP), are used to induce oxidative stress *in vitro* in order to mimic the process of RPE degeneration in AMD patient. To investigate the molecular mechanisms in RPE degeneration, we employed glucose oxidase/glucose to continuously produce hydrogen peroxide. Since it is reactive oxygen species (ROS) that directly exerts stress on RPE cells *in vivo*, we measured the production of ROS in this oxidative stress model. We found that glucose oxidase/glucose induced gradual increase of ROS level, which might simulate the gradual production and accumulation of oxidative stress in aging retina. Furthermore, we evaluated the changes in actin cytoskeleton of oxidative stressed RPE cells. Oxidative stress promoted actin reorganization and membrane blebbing, consistent with the observation from other studies [69]. Along with the prolonged

exposure of oxidative stress, the actin cytoskeleton shrank and became more concentrated around the nucleus, compared to its even distribution in untreated RPE cells. Meanwhile, glucose oxidase/glucose exposure induced RPE cell death, which was identified by calcein AM/ ethidium homodimer staining. The RPE cell degeneration induced by glucose oxidase/glucose was in a dose-dependent and time-dependent manner. The appearance of RPE cell death initiated at about 3 hours, and there was almost no cell viability at about 5 hours. So far, it is not clear whether RPE cell death in AMD patients is by necrosis or apoptosis. In addition, there are confusing reports about the phenotype of RPE cell death *in vitro*. Some studies presented the cell death as apoptosis, while others claimed that the RPE cell death was mixture of apoptosis and necrosis [31]. To determine the phenotype of RPE cell death induced by glucose oxidase/glucose, we used Hoechst 33258 to label chromatin. We found that the DNA in oxidative damaged RPE cells was condensed but not fragmented as shown in typical apoptosis. Interestingly, the condensed DNA was pushed very close to plasma membrane of oxidative damaged cells and the extruded DNA/nucleus was observed in ethidium homodimer labeled cells. Besides changes in chromatin, mitochondrial membrane potential depolarization is a key component of typical apoptosis. Since the RPE degeneration in this study did not display typical DNA fragmentation, we examined whether mitochondrial damage was involved in our model. By using JC-1 fluorescent probe, we observed increased accumulation of monomer staining for damaged mitochondria, along with decreased staining of oligomers for healthy mitochondria. The results of JC-1 fluorescence measurement suggested that the RPE cell death was accompanied by depolarization of mitochondrial membrane

37

potential. In summary, we established an oxidative stress model by which we could further explore the underlying molecular mechanism and potential therapies in RPE degeneration.

Materials and Methods

Cell Culture

ARPE-19 cell line, a spontaneously transformed human retinal pigment epithelial cell line [70], was used in this study. Since the ARPE-19 cell line maintains major characteristics of RPE cells, including specific cell markers, tight junction formation and retinoid metabolism pathways, it was extensively used in RPE cell biology. In this study, ARPE-19 cells were cultured in growth medium (Dulbecco's modified Eagle's medium, 10% fetal bovine serum, 14mM HEPES buffer and 1% penicillin/streptomycin) at 37 °C in a humidified atmosphere of 5% CO_2 and 95% air.

Reagents

Calcein AM/Ethidium homodimer-1, $H_2DCFH-DA$ and JC-1 were purchased from Invitrogen (Carlsbad, CA). MTS cell proliferation assay was purchased from Promega (Madison, WI)

Exposure of ARPE-19 cells to Glucose oxidase/Glucose (GO/G)

ARPE-19 cells were plated at a density of 16000 cells/cm^2 in growth medium. After overnight incubation, ARPE-19 cells were transferred to serum-free DMEM overnight to induce cell cycle arrest. Prior to GO/G treatment, ARPE-19 cells were washed with glucose-free medium twice and then exposed to various concentrations of glucose oxidase plus 1g/L glucose for specific period of time.

Examination of the early changes in RPE cells exposed to oxidative stress

ARPE-19 cells were exposed to 25mU/ml glucose oxidase plus 1g/L glucose for 2 hours and processed for immunocytochemistry or calcein AM/ fluorescent staining. For immunocytochemistry, the fixed ARPE-19 cells were stained with Rhodamine-phallodin following the standard immunostaining protocol. The nucleus was counterstained by DAPI. For live/dead cell fluorescent staining, treated ARPE-19 cells were stained with both 2uM calcein AM and 4 uM ethidium homodimer-1 for 2 hours. Afterwards, the immunostained cells were observed under Zeiss LSM 410 confocal microscope (Carl Zeiss Inc., Thornwood, NY.)

Immunocytochemistry

ARPE-19 cells were plated on cover slips in 24-well plate. Following treatment, ARPE-19 cells were fixed with 2% paraformaldehyde for 20min at room temperature. Fixed cells were permeabilized with 0.05% saponin in phosphate buffered saline (PBS) {10mM phosphate [pH 7.4], 150mM NaCl} for 15 minutes. The permeabilized cells were

39

blocked in 0.5% BSA ,4% normal goat serum in PBS for 1 hour at room temperature and incubated in primary antibody in PBS containing 0.5% BSA and 4% normal goat serum at 4°C overnight in a moist chamber. After several rinses with PBS, cells were incubated with anti-rabbit IgG Alexa 488/594 or anti-mouse IgG Alexa 488/594 (Molecular Probes Inc, Eugene, OR) in PBS at RT for 1h. Appropriate controls were maintained by substituting the primary antibodies with mouse or rabbit IgG to check for non-specific binding. Nucleus was counterstained with DAPI (Molecular Probes Inc, Eugene, OR) according to manufacturer's instructions after rinsing with PBS. Cover slips were mounted in aqueous mounting media and the images were captured on a Nikon microphot FXA microscope with epifluorescent attachment (Nikon Corp., Tokyo, Japan).

Live/dead cell fluorescent assay.

ARPE-19 cells after treatment were washed with DMEM and incubated with 2uM calcein AM and 4uM ethidium homodimer at 37°C for 20 minutes. The residual fluorescent dyes were washed off and the cells were observed under Olympus inverted microscope with epifluorescent attachment (Olympus Optical Co Ltd, Tokyo, Japan) and the images were captured using a digital camera.

Cell proliferation assay (MTS assay).

ARPE-19 cells were incubated for 1 hour with MTS reagent (3-4,5-dimethylthiazol-2-yl)-5-(3-carboxymethosyphenyl)-2-(4-sulfophenyl)-2H-tetrazolium) (Promega, Madison, WI) ,which was converted to a water-soluble formazan by

dehydrogenase enzyme found in metabolically active cells. The quantity of formazan product was determined by spectrophotometry using BioRad microplate reader (BioRad, Hercules, CA) at 490nm and 650nm. A standard curve was prepared for each set of experiments. Experiments were done three times.

Measurement of Mitochondrial Membrane Potential

Mitochondrial membrane potential was assessed with JC-1 fluorescent dye. ARPE-19 cells were incubated in DMEM containing 1 µg/ml JC-1 and 0.1% DMSO at 37°C for 20 minutes. Afterwards, medium was aspirated and cells were kept on ice, washed twice with ice-cold DPBS, and overlaid with colorless medium. Live cells were examined and images were captured under Olympus inverted microscope with epifluorescent attachment (Olympus Optical Co Ltd, Tokyo, Japan) and the images were captured using a digital camera.

Quantitative Measurement of Mitochondrial Membrane Potential

ARPE-19 cells were seeded in 96-well plate overnight and washed twice with serum-free DMEM. After overnight incubation, the cells were treated with oxidants or other agents at 37°C for indicated period of time. Following treatment, cells were washed once with HBSS and then incubated with 2uM JC-1 for 20 minutes. Subsequently, the residual JC-1 was washed off and the JC-1 fluorescence was examined using a fluorescent reader (Victor 3, PerkinElmer, MA)

Measurement of reactive oxygen species (ROS)

The extent of oxidative stress on RPE cells produced by glucose oxidase/glucose was determined by measuring intracellular reactive oxygen species (ROS) using the fluorescent dye H_2DCFH-DA. ARPE-19 cells were plated in 96-well plate overnight and washed twice with serum-free DMEM. After overnight incubation, the medium from each well was removed and each cell culture was loaded with 10uM H_2DCFH-DA for 30 minutes at 37 °C. After loading with H_2DCFH-DA, RPE cells were treated with oxidant for indicated periods of time. The H_2DCFH-DA fluorescence was detected by microplate reader (model FL600; Biotek, Highland Park, VT) at an excitation of 485 nm and an emission of 538 nm. Values were normalized to those in untreated control groups.

DNA gel electrophoresis

The ARPE-19 cells were rinsed with ice-cold phosphate-buffered saline (10mM phosphate [pH 7.4], 150mM NaCl), then lysed with 0.5mg/ml proteinase K in 10mM Tris-HCl, 100mM NaCl, 10mM EDTA and 0.5% SDS at 50°C overnight. Genomic DNA was extracted with phenol:chloroform:isoamylalcohol at 25:24:1 by centrifugation at 4°C for 1h at 12,000 X g. The aqueous phase was collected, treated with 1/10 v/v of 3M sodium acetate and precipitated with 2 volumes of ice-cold 100% ethanol overnight at -20°C. Genomic DNA was resuspended in TE buffer (10mM Tris-HCl and 1mM EDTA [pH 8.0]) and treated with 100 ug/ml DNase-free RNase A for 1h at 37°C. Genomic DNA was run on a 1.5% agarose gel containing 0.4g/ml ethidium bromide.

Results

Glucose oxidase/glucose induces gradual production of Reactive Oxygen Species (ROS)

Even though glucose oxidase catalyzes the production of hydrogen peroxide, it is the reactive oxygen species that directly exerts stresses on ARPE-19 cells. To measure the level of intracellular reactive oxygen species, fluorescent dye $H_2DCFH-DA$ was employed in this study. In addition, we compared the generation pattern of ROS production between hydrogen peroxide and glucose oxidase/glucose. As shown in Figure 2.1, in hydrogen peroxide group, there was an acute and significant increase of ROS fluorescence at about half an hour, followed by gradual dissipation of ROS. In contrast, when ARPE-19 cells were treated with glucose oxidase/glucose, there was gradual increase of ROS production with prolonged duration of the treatment. This study suggests that glucose oxidase/glucose induces gradual generation of reactive oxygen species, which simulates the accumulated oxidative stress in AMD patients.

Early cellular changes of RPE cells during oxidative stress

In AMD, it usually takes more than 20 years to develop RPE atrophy. Before the geographic atrophy of RPE layer, the gradual or cumulative oxidative stress affects the morphology, metabolic status, cytoskeleton remodeling, and specialized excretion of protein and lipids - major components of drusen, the key identifier in AMD. To investigate the early changes in oxidative stressed RPE cells, we examined the parameters mentioned above in this study. ARPE-19 cells were subjected to 25mU/ml

glucose oxidase plus 1g/L glucose for 2 hours. Rhodamine phallodin was used to stain filamentous actin. As shown in Figure 2.2, in treated ARPE-19 cells, the actin filament accumulated around the nucleus in contrast to its even distribution in untreated cells. We also found small round particles, positive for actin staining, localized near the stressed RPE cells. To further confirm this observation, we did the same treatment but labeled the cells with calcein AM, which only identified live cells. Similarly, green particles were found to be localized in the plasma membrane of live RPE cells. This study suggests that oxidative stress promotes early cytoskeleton remodeling and membrane blebbing in RPE cells, which might contribute to drusen formation.

Prolonged exposure to oxidative stress induces cytoskeletal remodeling and cell death

It is well known that oxidative stress induces cytoskeletal reorganization during cell death. To characterize the changes in the actin cytoskeleton, ARPE-19 cells were treated with 25mU/ml glucose plus 1g/L glucose for 3-5 hours, and Rhodamine phallodin was used to identify filamentous actin. As shown in Figure 2.3, with the increased duration of treatment, cytoskeleton remodeling was observed. Typically, in comparison to even distribution in untreated cells, the filamentous actin became concentrated around the nucleus with shrunk actin cytoskeleton separated from the plasma membrane. Along with cytoskeletal changes, RPE cell death was observed in this study. Calcein AM/ ethidium homodimer were used to measure cell viability and death. As shown in the same figure, after exposure to oxidative stress for 5 hours, there was significant increase of calcein AM staining and concomitant decrease of Ethidium Homodimer staining. The

results suggest that lethal oxidative stress induces cytoskeletal remodeling and degeneration of RPE cells.

Oxidative stress induces RPE cell death in a dose-dependent and time-dependent manner

To further characterize the cell death and optimize the experimental parameters in this RPE degeneration model, we determined whether the effects of lethal oxidative stress on RPE cells were dose-dependent and time-dependent. In both experiments, MTS assay was employed to measure cell viability. In dose-response experiments, ARPE-19 cells were exposed to 0-30mU/ml glucose oxidase plus 1g/L glucose. There was no significant decrease of cell viability with exposure to 0-15 mU/ml glucose oxidase. Starting from treatment with 20mU/ml glucose oxidase, there was 40% loss of cell viability. At 25 and 30 mU/ml, the cell viability was the lowest. We therefore used 25mU/ml glucose oxidase plus 1g/L glucose as working concentrations in later experiments. We also did the time-course to decide the optimal duration of treatment. ARPE-19 cells were exposed to 25mU/ml glucose oxidase plus 1g/L glucose for 0-5 hours, and the cell viability was measured by MTS assay. After 3 hours of exposure to oxidative stress, there was slight decrease of cell viability. The decrease in cell survival was significant with 4-hour treatment. After 5-hour exposure to oxidative stress, there was little cell viability detectable in cell culture. (Figure 2.4)

Oxidative stress induces non-classical mode of RPE cell death

To characterize the effects of oxidative injury on nuclear DNA, RPE cells were exposed to oxidative stress for 4 hours and examined for DNA changes by Hoechst 33258 staining and DNA gel electrophoresis. ARPE-19 cells demonstrated nuclear DNA shrinkage, different from DNA fragmentation found in typical apoptosis. Furthermore, similar results were confirmed by DNA gel electrophoresis. No 200bp DNA fragments were observed in oxidative damaged ARPE-19 cells. (Figure 2.5)

Oxidative stress-induced cell death involves depolarization of mitochondrial membrane potential

Since the RPE cell death in this study did not exhibit typical apoptotic characteristics, we were interested in whether mitochondrial membrane potential depolarization was associated with RPE degeneration. To test the potential changes in the mitochondrial membrane potential, we used JC-1, an extensively used fluorescent dye, to determine mitochondrial membrane integrity. ARPE-19 cells were treated by glucose oxidase/glucose for 5 hours. The JC-1 fluorescence was quantitatively measured by fluorescent reader. At treatment with 25mU/ml glucose oxidase, there was significant increase of green staining for damaged mitochondria, along with decrease of red staining for healthy mitochondria as shown in Figure 2.6.

Discussion

Functioning as retinal blood barrier, the retinal pigment epithelium (RPE) is exposed to reactive oxygen species (ROS) during the lifespan of and individual. In the aging retina, ROS is generated either from intracellular metabolism or from extracellular sources. When the defense system of the RPE could not counteract the production of ROS, excessive ROS brings about damages to DNA, protein and lipids and subsequent RPE degeneration. Since oxidative stress is a major factor contributing to the pathogenesis of AMD, a variety of oxidants are used to induce oxidative stress *in vitro* in order to simulate RPE degeneration in cell culture model. Both hydrogen peroxide and t-terbutyl peroxide are broadly used to elicit oxidative stress and induce RPE cell death. However, as shown in this study, the ROS induced by hydrogen peroxide reached maximum level at 0.5 hour and declined with increased duration of incubation. Furthermore, in order to induce RPE cell death, high concentration of hydrogen peroxide has to be used [59], which is far beyond pathophysiological level *in vivo*. The oxidative stress in aging retina is a long term accumulation of reactive oxygen species that finally causes degeneration of RPE cells. To mimic the progressive ROS production and subsequent RPE degeneration, we utilized glucose oxidase/glucose to continuously generate hydrogen peroxide. Glucose oxidase/glucose has been used to induce oxidative stress both extracellularly and intracellularly in a variety of cell culture models [71] [72] [73] [74] [75] [76] [77]. Furthermore, glucose oxidase has been successfully delivered into animals to specifically elicit oxidative stress in lung endothelial cells [78].

Before the final RPE degeneration, oxidative stress induces membrane blebbing and cytoskeleton remodeling, a part of self-defense mechanism of RPE cells. A cell sheds off part of its membrane and cytoplasm to discard damaged cellular organelles, lipid membrane or macromolecules to survive the oxidative injury. The histopathological studies on human AMD specimens or animal models implies that membrane blebbing of oxidative injuried RPE might contribute to drusen formation [79]. Therefore, several *in vitro* studies have been employed to induce membrane blebbing in order to understand the composition of shed membrane particles and investigate the molecular mechanisms [79] [80]. Likewise, our studies showed that during the early stage of lethal injury, RPE cells exhibited typical cytoskeleton remodeling and membrane blebbing.

In this study, prolonged exposure to lethal oxidative injury caused cell death in a dose-dependent or time-dependent mode. Different from classical apoptosis characterized by DNA fragmentation, stressed RPE cells displayed condensed nuclear DNA. A similar observation was shown to be accompanied by caspase-independence, PARP cleavage and AIF translocation to the nucleus [81].

The integrity of mitochondria is crucial for cells to maintain physiological functions. In apoptosis, depolarized mitochondria releases apoptotic proteins, such as cytochrome C and apoptosis-inducing factor (AIF), to initiate caspase cascade and subsequent DNA fragmentation[25]. Therefore, mitochondrial membrane potential depolarization is a hallmark of apoptosis. In addition, depolarization of mitochondria membrane potential has been shown in early phase of necrosis [82] [83]. In this study, we reported that the mitochondrial membrane potential depolarization was observed in

oxidative damaged RPE cells showing no typical characteristics of apoptosis. In summary, our results demonstrate that glucose oxidase/glucose induces RPE degeneration with characteristics of cytoskeleton remodeling, membrane blebbing, DNA condensation and depolarization of mitochondrial membrane potential.

***Figure2.1. Glucose oxidase/glucose induces production of intracellular reactive oxygen
species (ROS)***

ARPE-19 cells were loaded with 10uM fluorescent dye $H_2DCFH-DA$ for 30 minutes and
then exposed to 2 mM hydrogen peroxide or 25mU/ml glucose oxidase plus 1g/L glucose
for the indicated periods of time. The Fluorescence of H2DCFH-DA was quantified by a
fluorescent reader and the values were normalized to the percentage of untreated control
groups. Experiments were done in triplicates (n=3) and analyzed by Students't-test. Data
represent mean ± SD.
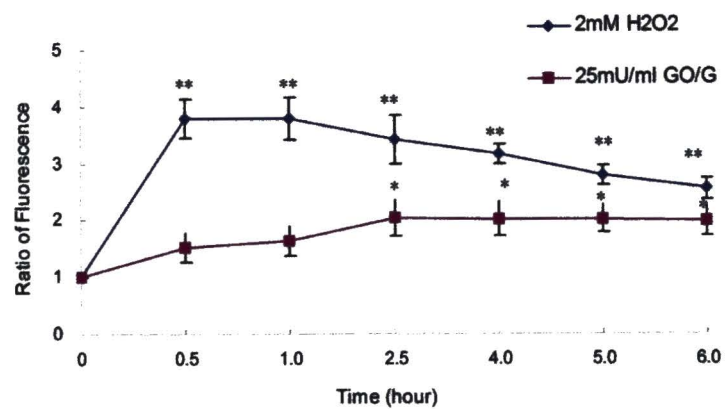
Figure2.2 oxidative stress induces membrane blebbing in the early phase

ARPE-19 cells were exposed to 25mU/ml glucose oxidase plus 1g/L glucose for 2 hours and then processed for immunocytochemistry or Calcein AM/ ethidium homodimer labeling. **A,** Rhodamine-phallodin was used to label filamentous actin. DAPI was used to counterstain the nucleus. **B,** Oxidative stressed ARPE19 cells were labeled with 2uM calcein AM to visualize membrane blebbing.

A

Control   GO/G

B

calcein AM   ethidium homodimer   merge
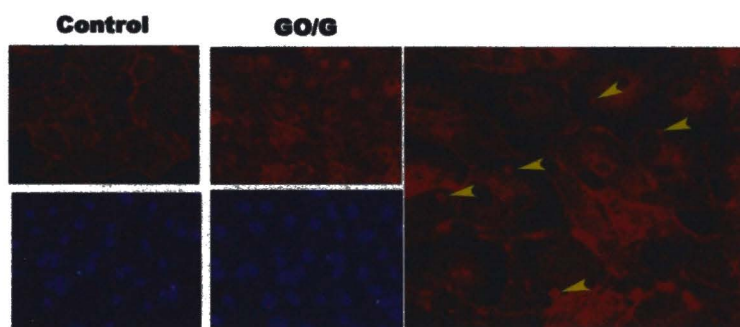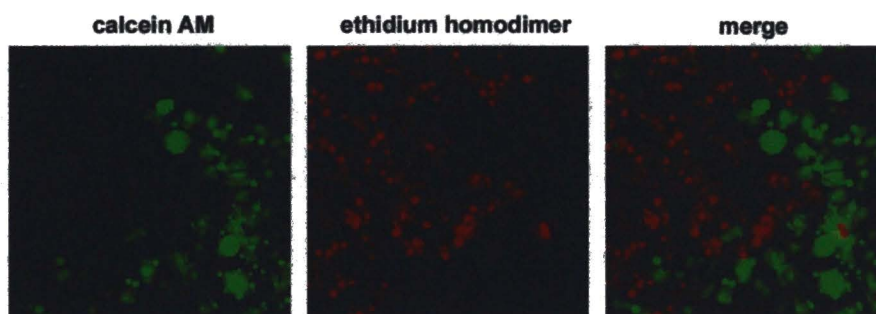
Figure2.3. Prolonged exposure to oxidative stress induces cytoskeletal remodeling

ARPE-19 cells were exposed to 25mU/ml glucose oxidase plus 1g/L glucose for indicated periods of time and then processed for immunocytochemistry. Rhodamine-phallodin was used to label filamentous actin. DAPI was used to counterstain the nucleus.

	F-Actin	DAPI	Merged
Contrl			
3hr			
4hr			
5hr			
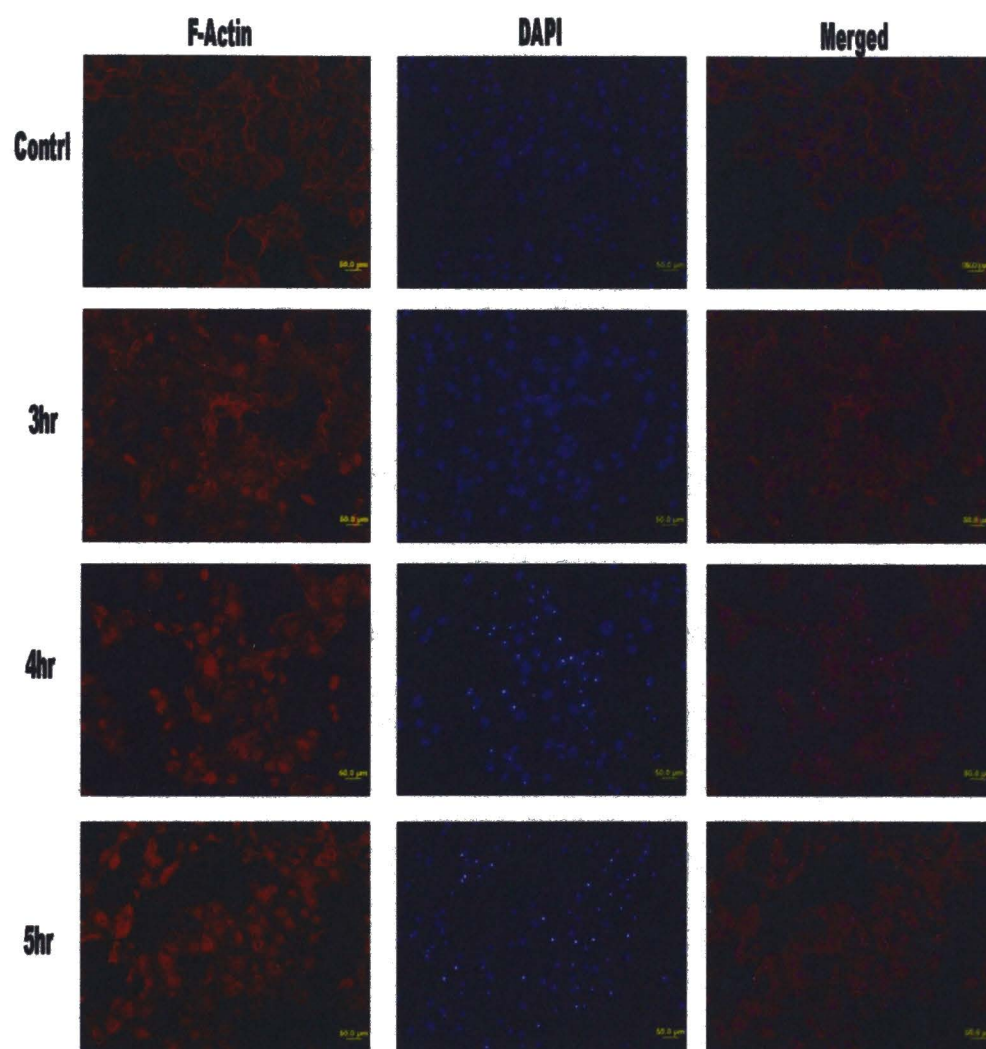
Figure2.4. Oxidative stress induces RPE cell death in a dose-dependent and time-dependent manner

A, ARPE-19 cells were exposed to different concentration of glucose oxidase (0-30 mU/ml) plus 1g/L glucose for 5 hours. 2mM ROS scavenger N-Acetylcysteine (NAC) was used to inhibit the cell death. Cell survival was examined by MTS assay. **B,** ARPE-19 cells were exposed to 25mU/ml glucose oxidase plus 1g/L glucose for indicated periods of time. MTS assay was employed to measure cell survival. Experiments were done in triplicates (n=3) and analyzed by Student's t-test. Data represent mean ± SD.

A
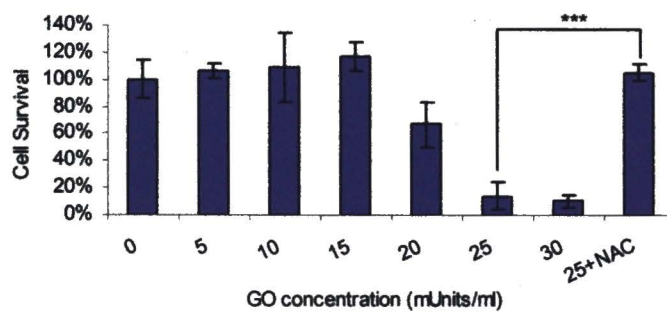
B
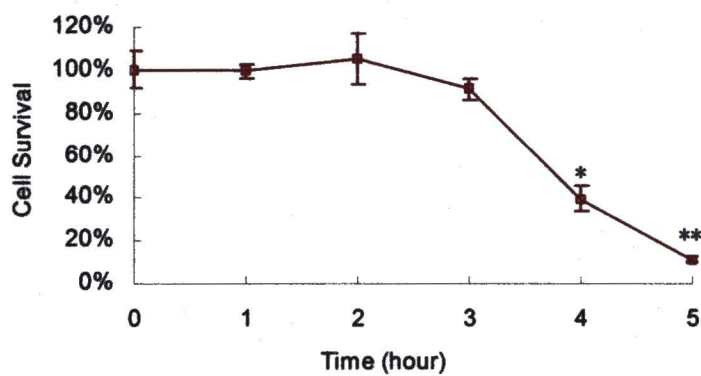
Figure2.5. GO/G induces non-classical mode of cell death in RPE cells

A, ARPE-19 cells were exposed to 25mU/ml glucose oxidase plus 1g/L glucose for 5 hours. Hoechst 33258 was used to label the nucleus. **B,** ARPE-19 cells were exposed to 25mU/ml glucose oxidase plus 1g/L glucose for 5 hours. The genomic DNA was isolated and separated on agarose gel. Untreated ARPE-19 cells were used as negative control.

A

Control   GO/G

B

Marker   RPE Ctrl   RPE+GO/G   661w+LD

3054-

1018-

517-
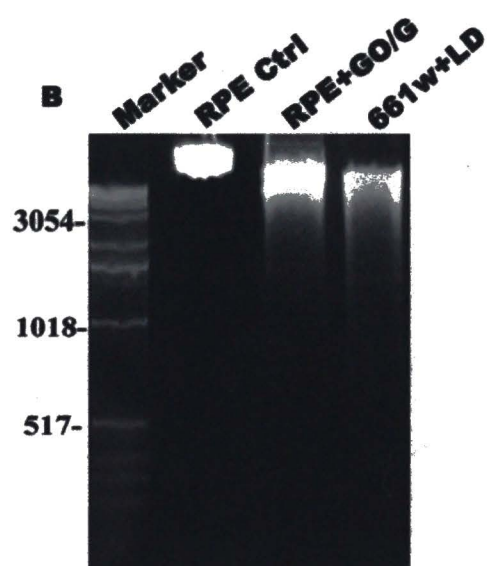
Figure2.6. Oxidative stress induces depolarization of mitochondrial membrane potential in RPE cells

ARPE-19 cells were exposed to different concentration of glucose oxidase with 1g/L glucose and then subjected to JC-1 labeling for 30 minutes. The fluorescence of JC-1 was quantitively measured by a fluorescent reader **(A)**. Experiments were done in triplicates (n=3) and analyzed by Students't-test. Data represent mean ± SD. The monomer/oligomer emission intensity ratio of JC-1 at each treatment was calculated **(B)**.

A
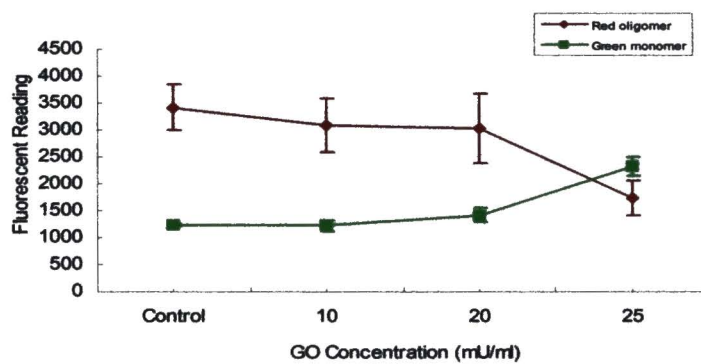
B
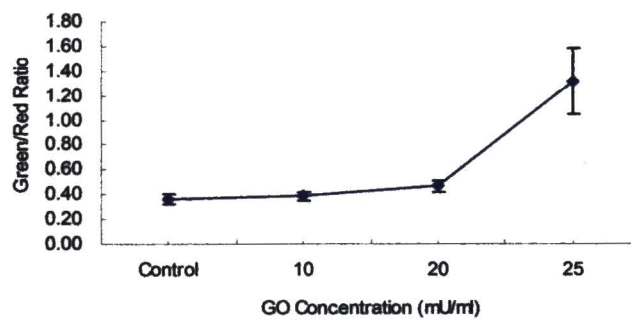
CHAPTER III

INVESTIGATIONS OF THE ROLE OF P38 MAPK SIGNALING IN RPE CELLS EXPOSED TO OXIDATIVE STRESS

Abstract

To explore the molecular mechanisms underlying RPE cell death, we tested a wide array of pharmacological inhibitors that would suppress RPE cell death from oxidative stress. Interestingly, among the pharmacological inhibitors, only SB203580, a specific p38 MAPK inhibitor, was found to significantly attenuate oxidative stress-induced cell death. Therefore, we hypothesized that p38 MAPK might play a role in RPE cell death. To test this hypothesis, we measured the expression of activated p38 MAPK at different time points following treatment by glucose oxidase/glucose. The p38 MAPK was activated at 0.5 hour, reached maximum level at 2-3 hours, and maintained higher level of expression as compared with no treatment up to 5 hours. Furthermore, nuclear translocation of activated p38 MAPK was observed in oxidative stressed cells, accompanied by increased staining in the cytoplasm, consistent with the results of immunoblotting. Besides modulating the activation of transcription factors or protein kinases, p38 MAPK phosphorylates HSP27, thereby regulating actin cytoskeleton. In this

study, HSP27 was activated by exposure to oxidative stress and the pattern of activation was consistent with that of p38 MAPK. Furthermore, the activation of HSP27 was inhibited by SB203580. Our findings suggest that p38 MAPK may regulate cytoskeleton reorganization by activating HSP27. Moreover, SB203580 inhibited RPE cell death induced by oxidative stress in a dose-dependent manner. To further explore the role of p38 MAPK, we employed specific p38 MAPK siRNA to reduce the protein expression of p38 MAPK. Interestingly, silencing p38 MAPK expression did not attenuate RPE cell death from oxidative damage. In spite of these conflicting findings, the results suggest that p38 MAPK might not be critical for RPE cell death but could play other roles, such as regulating cytoskeleton modeling in oxidative stressed RPE cells.

Materials and Methods

Reagents

Pharmacological inhibitors were purchased from Calbiochem (EMD Biosciences, San Diego, CA). p38 MAPK siRNA, anti-p38 MAPK, anti-HSP27, and anti-phospho-HSP27 were purchased from Cell Signaling (Danvers, MA). Anti-phospho-p38 MAPK was purchased from Promega (Madison, WI).

Cell Culture

ARPE-19 cells were used in this study and cultured as described in chapter II.

Exposure of ARPE-19 cells to GO/G

ARPE-19 cells were plated at a density of 15000cells/ cm^2 in DMEM with 10% FBS. After 24 hours, the cells were transferred to serum-free DMEM overnight. Prior to GO/G treatment, ARPE-19 cells were washed with glucose-free medium twice and then exposed to GO/G for specific period of time.

Immunoblotting analysis

For expression analysis, after indicated treatments, the medium was removed and the cells were lysed with RIPA buffer (50mM Tris HCl [pH 7.4], 150mM NaCl, 100mM EDTA, 1% NP-40, 0.25% sodium deoxycholate, 1g/ml aprotinin, 1mM phenylmethylsulfonyl fluoride and 1mM sodium orthovanadate) at 4°C for 15 minutes, then the lysates were centrifuged at 10,000 X g for 10 minutes. Protein concentrations were measured using the BCA (Bicinchonic acid) protein assay reagent (Pierce Chemical Company, Rockford, IL). 50ug samples were separated by SDS-PAGE and transferred to PVDF membrane for 1 hour at 100V, 250mA at 4°C. The membranes were blocked with 5% non-fat dried milk for 1 hour at room temperature and incubated with primary antibodies overnight at 4°C, followed by secondary antibodies for 1 hour at room temperature. The proteins were visualized using SuperSignal West Pico Chemiluminescent substrate (Pierce Chemical Company, Rockford, IL). The band densities were analyzed in Phosphorimager and statistical analyses were done using Student's t-test.

Immunocytochemistry

ARPE-19 cells were plated on cover slips in 24-well plates. After treatment, ARPE-19 cells were fixed with 2% paraformaldehyde for 20 minutes at room temperature. The cells were permeabilized with 0.05% saponin in phosphate buffered saline (PBS) {10mM phosphate [pH 7.4], 150mM NaCl} for 15min. The cells were blocked in 0.5% BSA ,4% normal goat serum in PBS for 1 hour at room temperature and incubated in primary antibody in PBS containing 0.5% BSA and 4% normal goat serum at 4°C overnight in a moist chamber. After several rinses with PBS, cells were incubated with anti-rabbit IgG Alexa Fluor or anti-mouse IgG Alexa Fluor (Molecular Probes Inc, Eugene, OR) in PBS at room temperature for 1 hour. Appropriate controls were maintained by substituting the primary antibodies with normal mouse or rabbit IgG to check for non-specific binding. Nucleus was counterstained with DAPI (Molecular Probes Inc, Eugene, OR) according to manufacturer's instructions after rinsing with PBS. Cover slips were mounted in aqueous mounting media and the images of representative fields were captured on a Nikon FXA microscope with epifluorescent attachment (Nikon Corp., Tokyo, Japan).

Live/dead cell fluorescent assay.

ARPE-19 cells were washed with DMEM and incubated with 2 uM calcein AM and 4 uM ethidium homodimer at 37°C for 20 minutes. The residual fluorescent dyes were washed off and the stained cells were observed under an Olympus inverted

microscope with epifluorescent attachment (Olympus Optical Co Ltd, Tokyo, Japan) and the images were captured using a digital camera.

Cell proliferation assay (MTS assay)

ARPE-19 cells were incubated for 1 hour with MTS reagent (3-4,5-dimethylthiazol-2-yl)-5-(3-carboxymethosyphenyl)-2-(4-sulfophenyl)-2H-tetrazolium) (Promega, Madison, WI), which is converted to a water-soluble formazan by dehydrogenase enzyme found in metabolically active cells. The quantity of formazan product was determined by spectrophotometry using BioRad microplate reader (BioRad, Hercules, CA) at 490nm and 650nm. A standard curve was prepared for each set of experiments. Experiments were done three times.

Small RNA interference

ARPE-19 cells were plated at a density of 15000cells/ cm^2 in 12-well plate and kept at 37 °C in a humidified incubator with 5% CO2. The day after plating, the medium was removed and ARPE-19 cells were transfected with 20 nM p38 siRNA using transfection reagent from Cell Signaling Technology, Inc., according to manufacturer's instructions. Briefly, per well of a 12-well plate, 20ng siRNA and 2ul transfection reagent were added to serum-free DMEM. The mixture of two reagents was equilibrated to room temperature for 5 minutes. One hundred microliters of the combined solution was added to each well. ARPE-19 cells were incubated with siRNA for 48 hours prior to treatment.

A fluorescein-labeled non-targeted siRNA control was used to monitor transfection efficiency and siRNA specificity.

Results

The effects of pharmacological inhibitors on RPE cell death

To investigate the potential signal cascades involved in RPE cell death during oxidative stress, we examined the effects of a wide array of pharmacological inhibitors on RPE cell death. ARPE-19 cells were pretreated with pharmacological inhibitors for 2 hours, followed by exposure to 25mU/ml glucose oxidase plus 1g/L glucose for 5 hours. The cell viability was measured by MTS assay. Other than SB203580 and antioxidant NAC, none of the pharmacological inhibitors exhibited inhibitory effects on RPE cell death. Since SB203580, a p38 MAPK inhibitor, could inhibit more than 50 percent of cell death, we hypothesized that p38 MAP signaling might mediate RPE degeneration *in vitro*. (Figure.3.1)

Oxidative stress promotes activation and nuclear translocation of p38 MAPK

To determine the role of p38 MAPK signaling in RPE cells exposed to oxidative damage, the expression of activated p38 MAPK at different time point was examined. ARPE-19 cells were exposed to 25mU/ml glucose oxidase plus 1g/L glucose for specific period of time. The activation of p38 MAPK was examined by anti-phospho-p38 MAPK

using immunoblotting. The p38 MAPK was activated at 0.5 hr after treatment and peaked at about 2-3 hours after the treatment. Levels of activated p38MAPK were maintained above control level with prolonged treatment. Typically, activated p38 MAPK translocates to nucleus to activate downstream protein substrates. To test the redistribution of p38 MAPK, we examined the localization of p38 MAPK by immunocytochemistry. ARPE-19 cells were exposed to oxidative stress for 3 hours and processed for labeling with anti-phospho-p38 MAPK. Significant accumulation of activated p38 MAPK was observed in the nucleus in contrast to little detectable nuclear staining in the control group. Furthermore, the expression of activated p38 MAPK was also upregulated in the cytoplasm, which was consistent with previous observations during immunoblotting. (Figure.3.2)

Oxidative stress induces HSP27 activation via p38 MAPK phosphorylation

Apart from regulating nuclear substrates, such as transcription factors and protein kinases, p38 MAPK also exerts effects by activating cytoplasmic substrates. For example, p38 MAPK activates heat shock protein 27 (HSP27) and hence regulates cytoskeleton remodeling in apoptosis or differentiation. Meanwhile, as a specific substrate of p38 MAPK, HSP27 was also used to determine the activity of p38 MAPK. In this study, ARPE-19 cell were exposed to 25mU/ml glucose oxidase plus 1g/L glucose for specific periods of time in the presence of or in the absence of SB203580, and the activation of HSP27 was determined by immunoblotting. As shown in Figure 3.3, HSP27 was activated with the increased duration of treatment, which is consistent with the activation

pattern of p38 MAPK. Furthermore, the activation of HSP27 was specifically inhibited by p38 MAPK inhibitor. Our results demonstrate that oxidative stress induces activation and nuclear accumulation of p38 MAPK and downstream activation of HSP27. (Figure.3.3)

SB203580 promotes RPE survival during oxidative stress

It was shown in Chapter II that SB203580, a p38 MAPK inhibitor, could rescue RPE cells from oxidative damage. To further explore the pro-survival effect of SB203580, we tested different dosages of SB203580. ARPE-19 cells were pretreated with 5, 10, 15 and 20um SB203580 for 2 hours and subjected to 25mU/ml glucose oxidase plus 1g/L glucose for 5 hours. The cell viability was measured by either MTS assay or calcein AM/ethidium homodimer. The inhibitory effect of SB203580 on RPE degeneration increased with higher dosages of SB203580. (Figure.3.4)

Knocking down p38 MAPK does not inhibit oxidative stress-induced RPE cell death

Since SB203580 inhibited RPE cell death induced by oxidative stress, we speculated that p38 MAPK might be involved in RPE degeneration induced by glucose oxidase/glucose. To further elucidate the role of p38 MAPK in RPE cell death, we utilized specific p38 MAPK siRNA to interfere with protein expression of p38 MAPK. Briefly, ARPE-19 cells were transfected with either p38 MAPK siRNA or control siRNA for 48 hours. The transfected cells were lysed and the expression of p38 MAPK was determined by immunoblotting. p38 MAPK expression was significantly lowered

compared to the control siRNA group. Furthermore, the transfected cells were exposed to oxidative stress as described above. MTS assay was employed to quantitatively measure the viable cells. In terms of cell viability, there was no statistical difference between p38 MAPK siRNA group and control siRNA group. Our findings argue that, during oxidative stress, p38 MAPK might not be critical for RPE degeneration as suggested with the use of SB203580. (Figure.3.5)

Discussion

The molecular pathway in RPE degeneration induced by oxidative jury is of interest to scientists since understanding the pathways would lay the foundation for effective therapy of age-related macular degeneration. In this study, we investigated the potential signal molecules that mediate oxidative stress-induced RPE cell death. Initially, we tested the effects of a wide array of pharmacological inhibitors on RPE cell death. We found that SB203580, an inhibitor of p38 MAPK, rescued RPE cells from oxidative damage in a mode of dose-dependent.

p38 MAPK signaling is extensively studied in cell death/ survival. In response to environmental stresses, p38 MAPK is well known for inducing cell death [84] [85]. However, some reports argue that p38 may also be protective and could inhibit cell death [86] [87]. Interestingly, the role of p38 MAPK in regulating cell death or survival is dependent on specific cell type, stimulus and even the isoform of p38 MAPK. p38 MAPK β may

attenuate the cell death induced by Fas ligation and UV irradiation, whereas p38 MAPK α promotes cell death mildly [87].

In RPE cell biology, the role of p38 MAPK is extended to differentiation, stress response and cytoprotection. p38 MAPK is suggested to induce RPE cell death in response to oxidative stress. For instance, lethal hydrogen peroxide activated p38 MAPK and promoted cell death that was inhibited by SB203580 [48]. Nevertheless, p38 MAPK was found to protect RPE cell from oxidative damage in another study using the same RPE cell line. In short, both pharmacological inhibitor (SB203580) and p38 siRNA enhanced oxidant induced cell death, while molecular interruption of MKK6 activity induced activation of p38 MAPK and subsequently inhibited RPE cell death (ARVO, 2006;47: E-Abstract 2074.). Our studies showed that even though pharmacological inhibition of p38 MAPK protected RPE cells from oxidative injury, knocking down p38 MAPK using siRNA did not exhibit protective effects.

Furthermore, oxidative stress induced activation of HSP27, which could be inhibited by SB203580. Since HSP27 has been shown to be involved in cytoskeleton reorganization in cell death and differentiation [88], we speculated that p38 MAPK might modulate actin cytoskeleton reorganization and membrane blebbing in early stages of oxidative stress.

SB203580 is a specific p38 inhibitor and extensively used to inhibit the activity of both p38 MAPK α and p38 MAPK β. This inhibitor was shown to suppress cell death induced by a variety of extracellular stresses. However, the specificity of SB203580 was reexamined recently. It was reported that SB20350 could activate Raf and downstream

MEK-p42/44 MAPK pathway. It was believed that SB203580 could directly bind to Raf and hence promotes cell survival by activating MEK-p42/p44 MAPK. Hence, the pro-survival effect of SB203580 may circumvent the p38 MAPK and instead utilize p42/p44 MAPK. Thus, it is not safe to draw conclusion on the role of p38 MAPK based on data obtained by using pharmalogical inhibitor. In other words, molecular alteration of p38 MAPK activation, either siRNA or gene targeting in animal model, may provide more convincing evidence to better understand the function of p38 MAPK in this respect. In summary, our studies show that p38 MAPK is not critical for RPE cell death, but SB203580 may provide an efficient therapy for RPE degeneration in AMD.

Figure3.1. The effects of pharmalogical inhibitors on RPE cell death

ARPE-19 cells were pretreated 2hrs with a variety of pharmalogical inhibitors and exposed to oxidative stress for 5 hours, in the presence of the same inhibitors. After overnight recovery, cell viability was measured by MTS assay. Experiments were done in triplicates (n=3) and analyzed by Student's-test. Data represent mean ± SD.
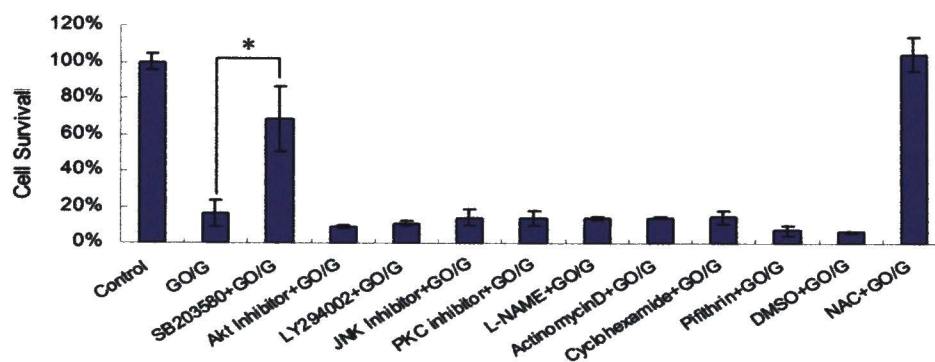
Drugs	Final Concentration
SB203580	20um
Akt Inhibitor	10um
LY294002	10um
JNK Inhibitor	20um
PKC Inhibitor	20um
L-NAME	200um
Actinomycin D	5ug/ml
Cyclohexamide	20um
Pifithrin	10um

Figure3.2. Oxidative stress promotes p38 MAPK activation and nuclear accumulation.

A, ARPE-19 cells were exposed to 25 mU/ml glucose oxidase plus 1g/L glucose for indicated periods of time and the activation of p38 MAPK was examined by immunoblotting. Total p38 was used as loading control. **B,** ARPE-19 was exposed to the same treatment for 3 hours and the distribution of activated p38 MAPK was determined by immunocytochemistry using anti-phospho-p38 antibody. DAPI was used to counterstain the nucleus.

A

GO/G

0   0.5   1   2   3   4   5 (hr)

← phospho-
p38 MAPK

← total
p38 MAPK

B

Phospho-p38   DAPI   Merged
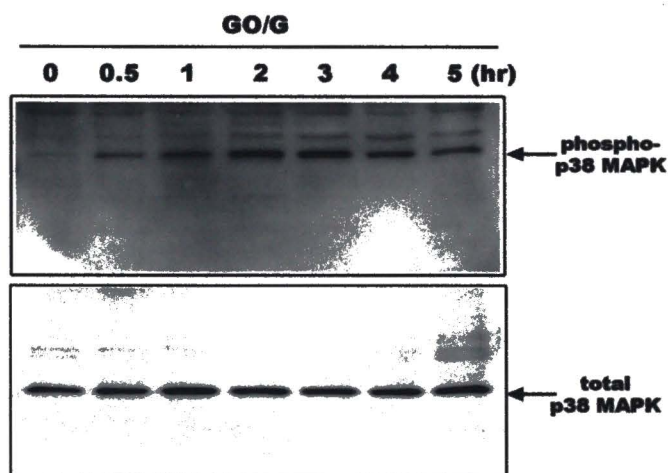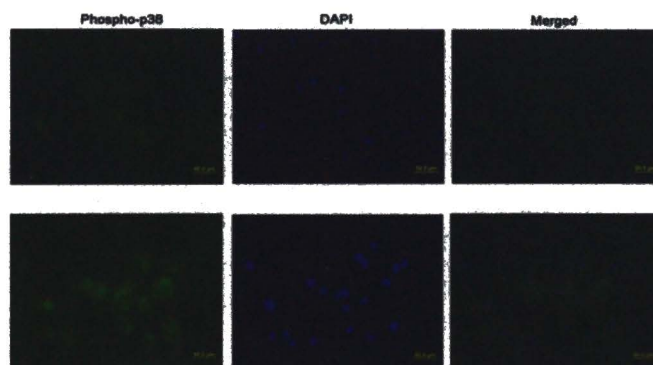
Figure3.3. p38 inhibitor, SB203580, suppresses the activation of HSP27 from oxidative stress

ARPE-19 cells were exposed to oxidative stress in the absence or presence of SB203580 for specific periods of time. The activation of HSP27 was measured by immunoblotting using anti-phospho-HSP27. Total HSP27 was used as loading control.

	0	1	2	3	0	1	2	3 (hr)
GO/G	+	+	+	+	+	+	+	+
SB203580	−	−	−	−	+	+	+	+

Phsopho-HSP27

HSP27
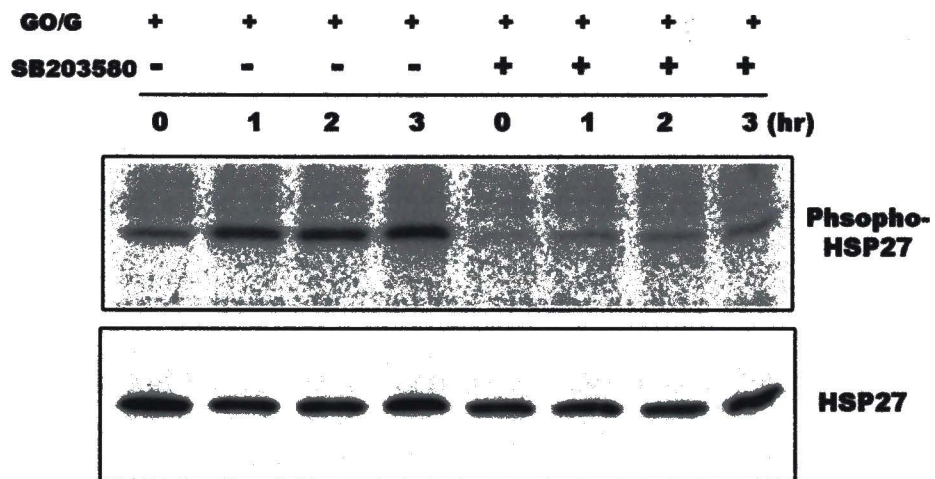
Figure3.4. SB203580, a p38 MAPK inhibitor, inhibits RPE cell death

A, ARPE-19 cells were exposed to 25mU/ml glucose oxidase plus 1g/L glucose for 5 hours in the presence of SB203580 at different concentrations (5-20uM). After overnight recovery, the cell viability was measured by MTS assay. Experiments were done in triplicates (n=3) and analyzed by Students't-test. Data represent mean ± SD. **B,** Similarly, ARPE-19 cells were exposed to 25mU/ml glucose oxidase plus 1g/L glucose for 5 hours in the presence of 20uM SB203580, followed by labeling with 2uM calcein AM and 4uM ethidium homodimer for 20mins to test cell death/survival.

A

| Control | GO/G | GO/G + SB203580 20um |
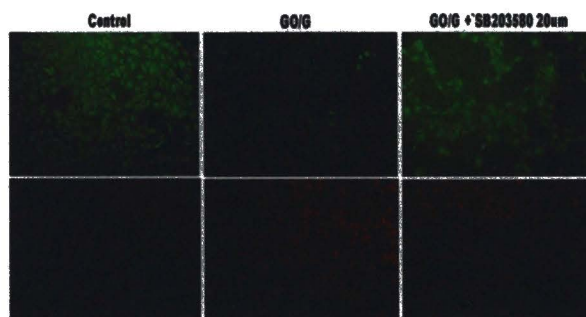
B
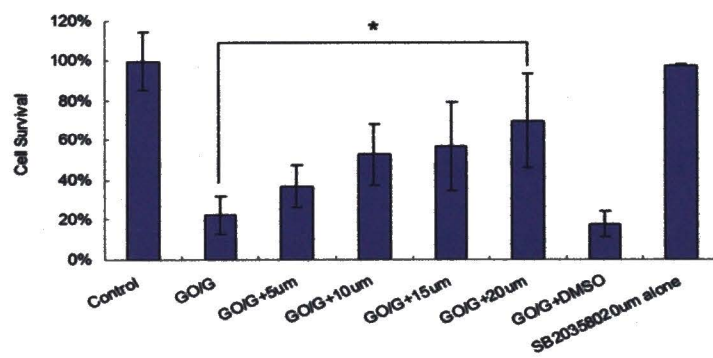
Figure3.5. Knocking down p38 MAPK gene expression does not suppress glucose oxidase/glucose induced RPE cell death

ARPE-19 cells were transiently transfected with both p38 MAPK siRNA and control SiRNA. Thereafter, the expression of p38 MAPK was examined by immunoblotting. β-tubulin was used as loading control (**A**).To test the effects of p38 MAPK interference, ARPE-19 cells were plated in 96-well plates, transfected with SiRNA and exposed to 25mU/ml glucose oxidase plus glucose for 5 hours. After overnight recovery, the cell survival was measured by MTS assay (**B**). Experiments were done in triplicates (n=3) and analyzed by Student's-test. Data represent mean ± SD.

A

W/O siRNA   Control siRNA   p38 siRNA

← total
p38 MAPK

← β–tubulin

B

■Ctrl SiRNA
■p38 SiRNA

Cell Survival

140%
120%
100%
80%
60%
40%
20%
0%

Control   GO/G
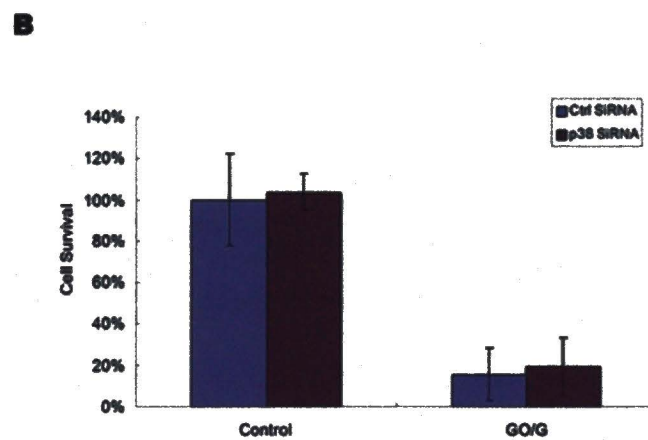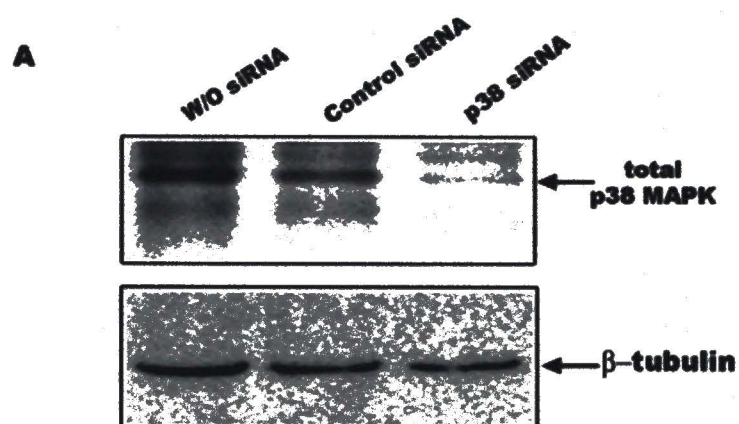
CHAPTER IV

INVESTIGATIONS ON THE ROLE OF P42/P44 MAPK SIGNALING IN RPE CELLS EXPOSED TO OXIDATIVE STRESS

Abstract

Since our studies suggested that p38 MAPK might not be involved in RPE cell death, we started to investigate another member of MAPK family, p42/p44 MAPK. p42/44 MAPK has been shown to be activated in oxidative stressed RPE cells and suggested to induce RPE cell death since pharmacological inhibitor of p42/p44 MAPK, U0126, could attenuate oxidative stress induced cell death [30]. Therefore we examined the role of p42/p44 MAPK in our oxidative damage model. We found that, during oxidative stress, p42/p44 MAPK was activated and subsequently deactivated with increased duration of treatment. However, MEK1 inhibitor U0126, did not inhibit RPE cell death as reported in other studies. Since U1026 may have other off-target effects as SB203580 does, we utilized SiRNA interference to knock down the expression of p42/p44 MAPK to further explore the role of p42/P44 MAPK. Interestingly, knocking down p42/p44 MAPK expression promoted RPE cell death in oxidative stress, in comparison to control SiRNA

83

group. Moreover, we overexpressed constitutively active MEK1 to induce activation of p42/p44 MAPK. We shown that ARPE-19 cells overexpressing MEK1 exhibited activated p42/p44 MAPK and were resistant to oxidative damage in contrast to RPE cells infected with adenovirus-β-Gal . Our studies suggest that p42/p44 MAPK may play a cytoprotective role on RPE cells exposed to oxidative stress.

Materials and Methods

Reagents

U0126 was purchased from Calbiochem (EMD Biosciences, San Diego, CA). p42 MAPK siRNA was purchased from Cell Signaling (Danvers, MA). Anti-phospho-p42/p44 MAPK and anti-p42/p44 MAPK were purchased from Santa Cruz (Santa Cruz, CA.)

Cell Culture

ARPE-19 cells were used in this study and the culture conditions were described in Chapter II.

Exposure of ARPE-19 cells to GO/G.

ARPE-19 cells were plated at a density of 5000cells/ well in DMEM with 10% FBS. 24 hours later, the cells were transferred to serum-free DMEM overnight. Prior to GO/G treatment, ARPE-19 cells were washed with glucose-free medium twice and then

exposed to GO/G for specific periods of time. To investigate the effect of U0126, ARPE-19 cells were pretreated with 20uM U0126 for 2 hours and then exposed to 25mU/ml glucose oxidase/glucose for 5 hours in the presence of 20uM U0126. After overnight incubation, MTS proliferation assay was used to quantitively measure viable cells.

Cell proliferation assay (MTS assay)

ARPE-19 cells were incubated for 1h with MTS reagent (3-4,5-dimethylthiazol-2-yl)-5-(3-carboxymethosyphenyl)-2-(4-sulfophenyl)-2H-tetrazolium) (Promega, Madison, WI) ,which was converted to a water-soluble formazan by dehydrogenase enzyme found in metabolically active cells. The quantity of formazan product was determined by spectrophotometry using BioRad microplate reader (BioRad, Hercules, CA) at 490nm and 650nm. A standard curve was prepared for each set of experiments. Experiments were done at least three times.

SiRNA interference

The p42 MAPK siRNA was obtained from Cell Signaling Technology, Inc. (Danvers, MA). ARPE-19 cells were plated at a density of 15000 cells/ $cm2$ in 12-well plate and kept at 37 °C in a humidified incubator with 5% $CO2$. The day after plating, the medium were removed and ARPE-19 cells were transfected with 20 nM of p42 MAPK siRNA using transfection reagent from Cell Signaling Technology, Inc.. Briefly, per well of a 12-well plate, 20ng siRNA and 2ul transfection reagent were added to serum-free DMEM before the mixture was allowed to stay at room temperature for 5 minutes. After

siRNA and transfection reagent was combined, 100ul mixed solution was added to each well. 24 hours later, ARPE-19 cell were transferred to DMEM with 10% FBS and incubated for another 24 hours prior to treatment. A fluorescein-labeled non-targeted siRNA control was used to monitor transfection efficiency and siRNA specificity.

Adenovirus infection

Adenovirus carrying either constitutively active MEK1 [89] or β-gal reporter was used for infections. ARPE-19 cells were seeded on 12-well plate at density of 15000 cells/ cm^2. One day after plating, ARPE-19 cells were infected at m.o.i of 100 p.f.u/cells in 1ml of Dulbecco's Modified Eagle's medium (DMEM) supplemented with 10% FBS overnight at 37 °C in a humidified incubator with 5% CO2. Subsequently, the medium with adenovirus was removed and the cells were cultured in fresh DMEM with 10% FBS for an additional 24hr prior to treatment or passage to 96 well plate. For GO/G treatment, the infected ARPE-19 cells were passaged to 96 well plates as described previously and exposed to GO/G for indicated period of time.

Immunoblotting Analysis

For protein expression analysis, 72 hours after adenovirus infection or 48 hours after siRNA transfection, the media was removed and the cells were lysed with RIPA lysis buffer (50mM Tris HCl [pH 7.4], 150mM NaCl, 100mM EDTA, 1% NP-40, 0.25% sodium deoxycholate, 1g/ml aprotinin, 1mM phenylmethylsulfonyl fluoride and 1mM sodium orthovanadate) at 4°C for 15 minutes, then the lysates were centrifuged at 10,000

X g for 10 minutes. Protein concentrations were measured using the BCA (Bicinchonic acid) protein assay reagent (Pierce Chemical Company, Rockford, IL). 50ug samples were separated by SDS-PAGE and transferred to PVDF membranes for 1h at 100V, 250mA at 4°C. The membrane was blocked with 5% non-fat dried milk for 1h at room temperature (RT) and incubated with primary antibodies overnight at 4°C, followed by secondary antibodies for 1h at RT. The protein was visualized using SuperSignal West Pico Chemiluminescent substrate (Pierce Chemical Company, Rockford, IL). The band density was analyzed using phosphorimager and statistical analysis was done by Student's t-test. The values were plotted as a ratio of protein of interest to housekeeping protein. Antibodies used in this chapter included anti-MEK1/2, antip42/p44 MAPK, anti-phospho-p42/p44 MAPK, and anti-β-tubulin.

Results

Oxidative stress promotes biphasic activation of p42/p44 MAPK

To determine whether p42/44 MAPK signaling is involved in RPE cells exposed to oxidative damage, the expression of activated p42/p44 MAPK at different time points was examined. ARPE-19 cells were exposed to 25mU/ml glucose oxidase plus 1g/L glucose for specific periods of time. The activation of p42/44 MAPK was examined by anti-phospho-p42/44 MAPK using immunoblotting. As shown in Figure.4.1, p42/44

MAPK was activated at 0.5 hour and peaked at 1-2hour. After maximum activation, the inactivation of p42/p44 MAPK was observed with the increased duration of treatment.

U0126, a MEK1 inhibitor, exhibits no protective effect on RPE cells during oxidative stress

U0126 has been shown to rescue ARPE-19 cells from oxidative damage [30]. To explore the role of p42/p44 MAPK in RPE degeneration, we examined the effects of U0126 on RPE cell death. ARPE-19 cells were pretreated with 20uM U0126 for 2 hours and subsequently exposed to 20 or 25mU/ml glucose oxidase plus 1g/L glucose for 5 hours. After overnight recovery, the cell viability was measured by MTS assay. Interestingly, U0126 did not affect oxidative stress induced RPE cell death at both concentrations as showed in Figure 4.2.

Knocking down p42/p44 MAPK expression accelerates oxidative stress-induced RPE cell death

Since U0126 did not inhibit RPE cell death during oxidative stress, we utilized specific p42 MAPK siRNA to examine the role of p42/p44 MAPK in RPE cell death. ARPE-19 cells were transfected with p42 MAPK siRNA for 48 hours. The cells were processed to detect the expression of activated p42/p44 MAPK by immunoblotting. As shown in Figure 4.3, p42/p44 MAPK expression was silenced compared to the control siRNA group. MTS cell proliferation assay was employed to investigate the effects of knocking down p42/p44 MAPK on RPE cell death. Compared to control group, knocking

88

down p42/p44 MAPK expression significantly decreased cell viability. These results demonstrate that p42/p44 MAPK are critical for RPE cell survival in oxidative stress.

Overexpression of constitutively active MEK1 protects RPE cells from oxidative stress

Since knocking down p42/p44 MAPK expression promoted RPE cell death, we hypothesized that activation of p42/p44 MAPK should protect RPE cells from oxidative damage. To test the effect of activation of p42/p44 MAPK, we infected ARPE-19 cells with constitutively active MEK-1 adenovirus for 72 hours. β-gal adenovirus was used as control in this experiment. The infected cells were processed and examined for expression of MEK1 and p42/p44 MAPK activation. Moreover, the infected cells were treated with 25mU/ml glucose oxidase plus 1g/L glucose before cell survival was measured by MTS assay. ARPE-19 cells infected with MEK1-adenovirus exhibited increased expression of MEK1 and activation of p42/44 MAPK. Furthermore, ARPE-19 cells infected with MEK1 adenovirus were resistant to oxidative stress in comparison to cells infected with β–gal adenovirus. The results demonstrate that overexpression of constitutively active MEK1 induces activation of p42/44 MAPK and rescue RPE cells from oxidative damage.

SB203580, a p38 inhibitor, promotes increased activity of p42/p44 MAPK in RPE cells

It has been shown that SB203580 might promote cell survival by activating Raf-1 and downstream MEK-p42/p44 MAPK signaling. Since SB203580 could inhibit RPE cell death dose-dependently, we speculated that SB203580 might promote p42/44 MAPK

activation. ARPE-19 cells were exposed to 20uM SB203580 for indicated periods of time, and the activation of p42/p44MAPK was examined by immunoblotting. We found that 2-hour exposure to 20uM SB203580 induced activation of p42/p44 MAPK and the activation gradually declined with increased duration of treatment. Our findings suggest that SB203580 may rescue RPE from oxidative stress by modulating p2/p44 MAPK activity.

Discussion

The roles of p42/p44 MAPK in stress response is controversial. p42/p44 MAPK may induce or inhibit cell death depending on specific stress, cell line or model of activation. p42/p44 MAPK was shown to inhibit cell death induced by oxidants. Elevated activation of p42/p44 MAPK promoted cell survival, while pharmacologic or molecular alterations resulted in increased cell death [90][91]. On the contrary, p42/p44 activation could induce apoptosis in response to oxidant damage and the induced cell death was attenuated by inhibiting p42/p44 MAPK activation [55][92].

In human RPE cells, EGF has been shown to induce p42/p44 MAPK activation and promote cell proliferation and migration [93]. Furthermore, PEDF protected RPE cells from oxidative damage by activating p42/p44 MAPK [59]. Serum deprivation induced activation of FGF1 receptor, which activated p42 MAPK and reduced apoptosis. In RPE cells exposed to hydrogen peroxide, p42/44 MAPK was phosphorylated [59]. Moreover,

p42/p44 MAPK was shown to be transiently activated in ARPE-19 cells exposed to tert-butyl hydroperoxide (t-BHP) and the RPE cell death was inhibited by U0126. Interestingly, in our study, U0126 did not inhibit ARPE-19 cell death when exposed to glucose oxidase/glucose. Furthermore, knocking down p42/p44 MAPK expression accelerated oxidative stress induced cell death. Moreover, overexpression of constitutively active MEK1 led to p42/p44 MAPK activation and protected RPE cells from oxidative damage. Our studies support the protective role of p42/44 MAPK in RPE cells exposed to oxidative damage.

The duration and magnitude of MAPK activation may be modulated at many points during environmental stresses. One of such modulations may be achieved by MAPK phosphatases (MKPs). MKPs are dual specificity (threonine/tyrosine) protein phosphatases and play important roles in regulating the MAPK activation [94]. MKP-1, an inducible phosphotase in MKPs family, is of special interest since it exhibits catalytic activity on p42/p44 MAPK, p38 MAPK and JNK MAPK [95]. As suggested by this study, the duration and magnitude of p42/44 MAPK, p38 MAPK activation and even JNK MAPK might collectively determine the fate of RPE cells during oxidative stress. Moreover, as focal modulation point, MKP-1 might modulate the fate of RPE cells by dephosphorylating MAPKs differentially. For example, in early phases of oxidative stress, MKP-1 might deactivate the inhibition of p42/p44 MAPK and leads to increased activation of p42/p44 MAPK. In late phases of oxidative stress, MKP-1 directly deactivates p42/p44 MAPK and abrogates the protective effects of p42/p44 MAPK. To further elucidate the molecular mechanisms underlying AMD, we would examine the

potential involvement of MKP-1 in MAPK regulation during oxidative stress in the future.

Figure4.1. Oxidative stress induces biphasic response in p42/p44 MAPK activity

ARPE-19 cells were exposed to 25 mU/ml glucose oxidase plus 1g/L glucose for indicated periods of time and the activation of p42/p44 MAPK was examined by immunoblotting using ant-phospho-p42/p44 MAPK. Total p42/p44 MAPK was used as loading control.
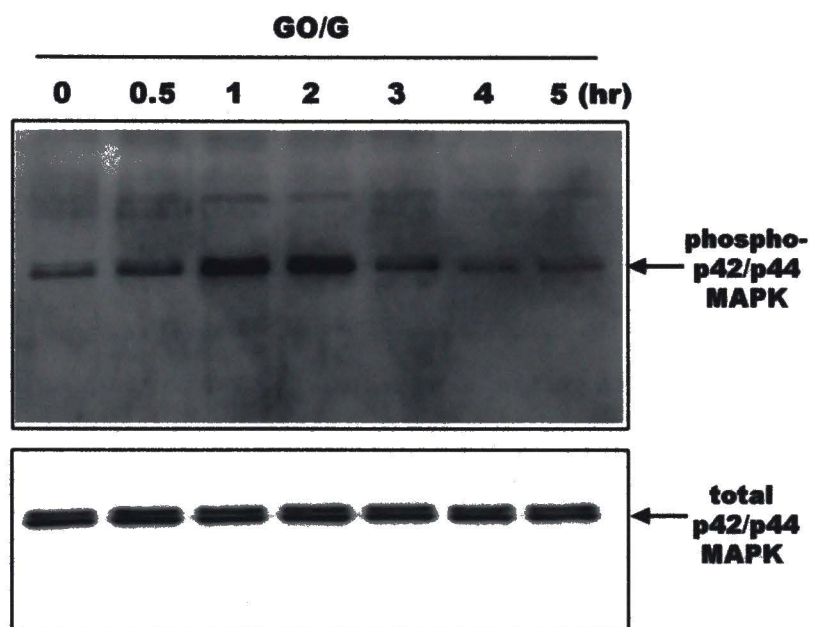
Figure4.2. U0126 has no effect on RPE cell survival during oxidative stress

ARPE-19 cells were exposed to 20 mU/ml or 25mU/ml glucose oxidase plus 1g/L glucose for 5 hours in the presence of 20uM U0126. After overnight recovery, the cell viability was measured by MTS assay. Experiments were done in triplicates (n=3) and analyzed by Student's t-test. Data represent mean ± SD.
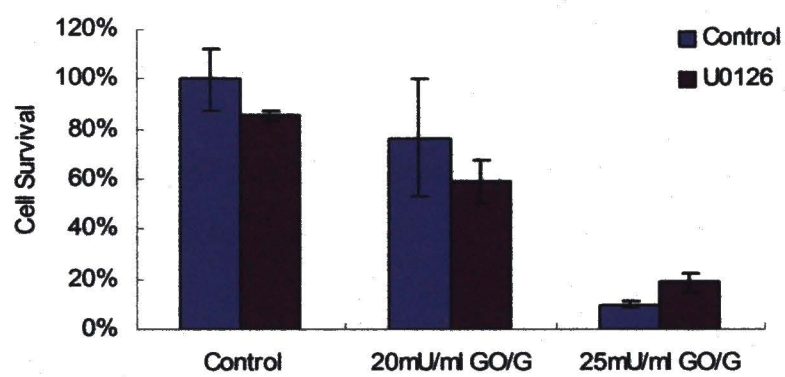
Figure4.3. Knocking down p42/p44 MAPK protein expression accelerates glucose oxidase/glucose induced RPE cell death

ARPE-19 cells were transiently transfected with both p42 MAPK siRNA and control SiRNA. Thereafter, the expression of p42/p44 MAPK was examined by immunoblotting. β-tubulin was used as loading control (**A**). To test the effect of p42/p44 MAPK interference on RPE cells, ARPE-19 cells were plated in 96-well plates, transfected with SiRNA and exposed to 25mU/ml glucose oxidase plus glucose for 5 hours. After overnight recovery, the cell survival was measured by MTS assay (**B**). Experiments were done in triplicates (n=3) and analyzed by Student's-test. Data represent mean ± SD.

A

Control siRNA   p42 MAPK siRNA   W/O siRNA

← p44 MAPK
← p42 MAPK

← β-tubulin

B

■ Control siRNA
■ p42 MAPK siRNA

Cell Surviva

140%
120%
100%
80%
60%
40%
20%
0%

Contrl   GO/G
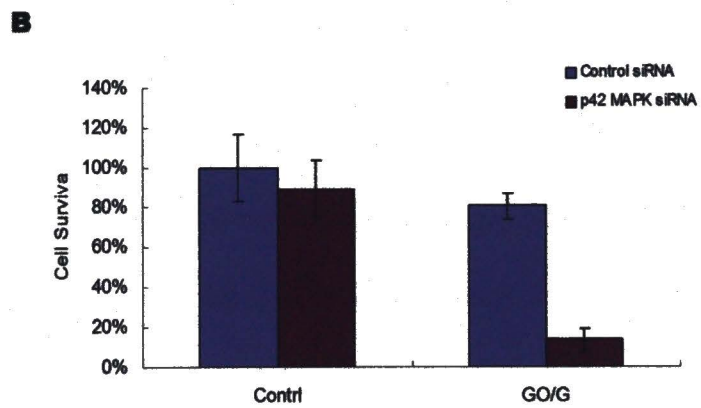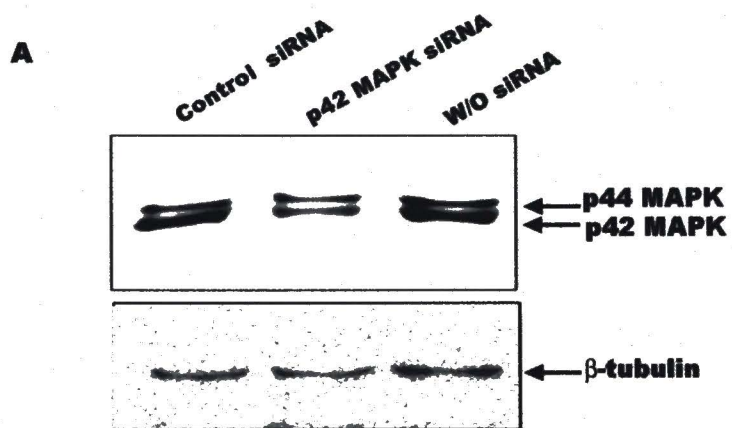
Figure4.4. Constitutively active MEK1 induces p42/p44 MAPK activation and inhibits glucose oxidase/glucose induced RPE cell death

AREP-19 cells were infected with either constitutively active MEK1 or β-gal adenovirus at MOI of 100 for 72 hours. Afterwards, the expression of MEK1 (**A**) and phosphorylated p42/p44 MAPK (**B**) were examined. To test the effect of MEK1 overexpression, infected ARPE-19 cells were passaged to 96-well plates and exposed to 25mU/ml glucose oxidase plus 1g/L glucose for 5 hours. After overnight recovery, the cell survival was measured by MTS assay (**C**). Experiments were done in triplicates (n=3) and analyzed by Student's-test. Data represent mean ± SD.

A

Adv-β-Gal Adv-MEK1 W/O Infection

← β-tubulin
← MEK1

B

Adv-β-Gal Adv-MEK1 W/O Infection

← Phospho-
p42/p44
MAPK

← p42/p44
MAPK

C

■ Adv-beta-Gal
■ Adv-MEK1

Cell Survival

140.00%
120.00%
100.00%
80.00%
60.00%
40.00%
20.00%
0.00%

Control   GO/G

**

100
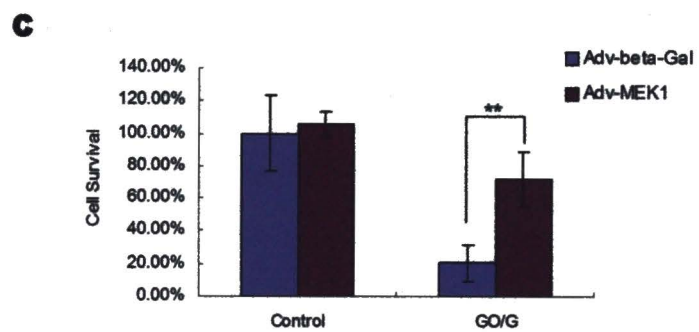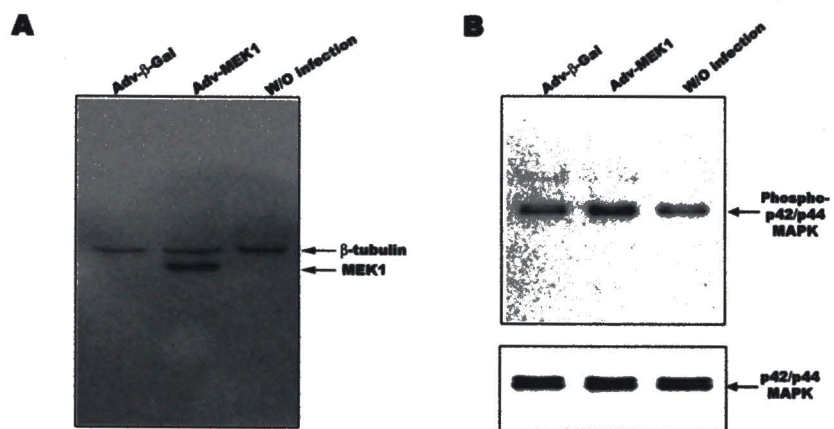
Figure4.5. SB203580 promotes p42/p44 MAPK activation in RPE cells

ARPE-19 cell were treated with 20uM SB203580 for indicated period of time and the expression of phosphorylated p42/44 MAPK was examined by immunoblotting. Total p42/p44 MAPK was used as loading control.

SB203580 (20uM)

0   2   6   12 (hr)

phospho-
p42/p44
MAPK

p42/p44
MAPK
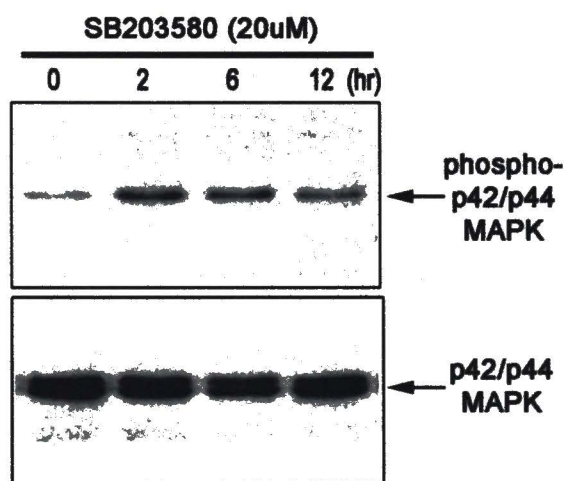
CHAPTER V

HUMAN RETINAL PROGENITOR CELLS PROMOTE RPE CELL SURVIVAL BY REGULATING MAPK SIGNALING

Abstract

Although retinal stem/progenitor cells have been employed to treat retinal degeneration in animal models, the effects have not been satisfactory and the therapeutic potential of stem cells needs to be investigated further. Stem cells have been shown to secret pro-survival molecules to rescue the heart from ischemia [6668]. Based on our previous findings, we hypothesized that retinal progenitor cells (RPC) protect RPE cells from oxidative damage by modulating p42/p44 MAPK activity. Our studies were designed to determine whether RPC-derived trophic factor(s) could inhibit cell death of cultured RPE induced by oxidative stress, and further establish the corresponding molecular mechanisms. Our findings should provide further insight into the molecular mechanisms of AMD and hence establish a foundation for the prevention and treatment of AMD.

First, we isolated progenitor cells from human retinas and expanded them *in vitro* in the presence of FGF-2 and EGF. In special neuronal progenitor medium (NPMM), RPC proliferated and formed aggregates (neurospheres). The neurospheres were reactive for proliferating cellular nuclear antigen (PCNA). We also found that neurospheres labeled for nestin, which was confirmed by RT-PCR. Furthermore, neurospheres expressed markers of retinal progenitor cells, such as Pax6 and p75NTR. Specifically, all the monolayer RPC and neurospheres labeled for Pax6. The monolayer RPC expressed GFAP while neurospheres were negative for GFAP. Aside from their self-renewal capability, RPC had the capability for differentiation. We employed NPMM plus neuronal survival factor (NSF) to induce differentiation of RPC from neurospheres. Following induction, neurospheres became flattened and neurite-containing cells migrated out of the spheres. By immunoblotting, we found that differentiated RPC lost the expression of Pax6, but displayed increased expression of neuron-specific enolase (NSE), a marker for neuronal cell. Furthermore, there were no changes in GFAP expression before and after treatment with pro-neuronal medium. When the RPC were cultured in the presence of regular 10% FBS, they lost the potential to form neurospheres but proliferated as monolayer cells, and expressed GFAP, but not Pax6 or NSE.

After the isolation of RPC, we collected conditioned medium and examined its pro-survival capability. The RPC-CM could protect RPE cells from oxidative stress. In addition, the protective capability of RPC-CM was specific and heat-resistant. Since we have shown that p42/p44 MAPK could rescue the RPE cells from oxidative damage, we investigated whether RPC-CM could regulate p42/p44 MAPK activity. RPC-CM

treatment induced activation of p42/p44 MAPK and the protective effects of RPC-CM could be inhibited by U0126. The results demonstrate that RPC-CM could protect RPE cells from oxidative damage by upregulating p42/p44 MAPK activity.

Materials and Methods

Reagents

Neuronal progenitor maintenance medium (NPMM), containing 20 ng/ml EFG and 10 ng/ml FGF-2, was purchased from Clonetics (Charles City, IA). Anti-nestin, anti-NSE, anti-Vimentin, anti-cytokeratin antibodies were purchased from Chemicon (Temecula, CA). Anti-Pax6 was purchased from Santa Cruz (Santa Cruz, CA). Anti-GFAP was purchase from Zymed (Invitrogen, Carlsbad, CA). Anti-p75NTR was a gift from Dr. Moses Chao.

Isolation and expansion of human retinal progenitor cells (RPC)

Human postnatal retina was dissected and washed briefly in ice-cold 0.1M Phosphate Buffered Saline (PBS). The tissue sections were then washed 3 times in basal medium (DMEM with 100units/ml Penicillin, 100mg/ml Streptomycin, and 15mM HEPES) to remove any residual fragments and incubated at 37°C , 5% CO_2 for 1 hour in basal medium supplemented with 0.1% collagenase/ 025% trypsin. After digestion, cells were plated in 6-well plates in neuronal progenitor maintenance medium (NPMM). After a couple of passages, the cells were cultured in NPMM and neurospheres started to form.

For passaging, cells were trypsinized and plated in 6-well plates or in T25 flasks. The medium was changed every 3 days.

Primary cultured human RPE cells

RPE cells were isolated from adult human retina. Basically, following dissection from the retina, the sheets of RPE cells were collected and transferred to 6-well plates in the presence of 10% FBS serum and antibiotics (penicillin and gentamicin). The RPE was dissociated by robust trituration using a Pasteur pipette and the resultant suspension of RPE cells was plated on collagen-coated $35mm^2$ dishes. The primary cultured RPE cells were then enriched by using DMEM with 10% FBS.

Assay of differentiation potential of RPC

Human RPC were cultured in NPMM to be expanded as neurospheres. For differentiation assay, neurospheres were collected and washed gently and briefly. Some of collected neurospheres were lysed for immunoblotting. The remaining neurospheres were plated on collagen-coated dishes with NPMM plus neural survival factor-1 (NSF-1). Neurite-containing cells migrated out from spheres and became flattened. Fourteen days after induction with NPMM plus NSF-1, the differentiated cells were processed for immunoblotting.

Immunocytochemistry

To characterize RPC, monolayer cultures or neurospheres were plated in 8-well chamber slides in the indicated media. Cells were fixed with 2% paraformaldehyde for 20 minutes at room temperature. The cells were permeabilized with 0.05M glycine containing 0.1% Triton X-100 in phosphate buffered saline (PBS) {10mM phosphate [pH 7.4], 150mM NaCl} for 15 minutes. Afterwards, the cells were blocked with 0.5% BSA ,4% normal goat serum in PBS for 1 hour at room temperature and incubated in primary antibody in PBS containing 0.5% BSA and 4% normal goat serum at 4°C overnight in a moist chamber. After several rinses with PBS, cells were incubated with anti-rabbit IgG Alexa 488 or anti-mouse IgG Alexa 488 (Molecular Probes Inc, Eugene, OR) in PBS at room temperature for 1 hour. Appropriate controls were maintained by substituting the primary antibodies with normal mouse or rabbit IgG to check for non-specific binding. Nucleus was counterstained with DAPI (Molecular Probes Inc, Eugene, OR) according to manufacturer's instructions after rinsing with PBS. Chamber slides were mounted in aqueous mounting media and the images of representative fields were captured on a Nikon microphot FXA microscope with epifluorescent attachment (Nikon Corp., Tokyo, Japan).

Immunoblotting assay

The cells maintained in media were first rinsed with ice-cold phosphate-buffered saline (10mM phosphate [pH 7.4], 150mM NaCl) and then lysed with lysis buffer (50mM Tris HCl [pH 7.4], 150mM NaCl, 100mM EDTA, 1% NP-40, 0.25% sodium

deoxycholate, 1g/ml aprotinin, 1mM phenylmethylsulfonyl fluoride and 1mM sodium orthovanadate) at 4°C for 15 minutes, then the lysates were centrifuged at 10,000 X g for 10 minutes. Protein concentrations were measured using the BCA (Bicinchonic acid) protein assay reagent (Pierce Chemical Company, Rockford, IL). 2-50ug samples were separated by SDS-PAGE and transferred to nitrocellulose membranes for 1 hour at 100V, 250mA at 4°C. The membranes were blocked with 5% non-fat dried milk for 1 hour at room temperature and incubated with primary antibodies overnight at 4°C, followed by secondary antibodies for 1 hour at room temperature. The proteins were visualized using SuperSignal West Pico Chemiluminescent substrate (Pierce Chemical Company, Rockford, IL).

Total RNA extraction

Total RNA was extracted using Ultraspec RNA (Biotecx laboratories, Houston, TX) according to product specifications. The Ultraspec RNA solution is a single, homogenous solution for the isolation of total RNA. This phenol-based reagent contains denaturants and RNase inhibitors and is used for total RNA isolation. In short, the cell sample was homogenized or disrupted in the Ultraspec reagent, followed by the addition of chloroform, and the mixture were separated into three phases by centrifugation at 10,000 X g for 15 minutes. The RNA extracts were then precipitated from the aqueous phase with isopropanol and separated by centrifugation at 10, 000 X g for 10 minutes. The total RNA was air dried and then washed twice in 70% ethanol and resuspended in nuclease-free water. The dissolved total RNA was stored at -80°C until used.

Reverse transcriptional PCR

Total RNA from above was used for cDNA synthesis by random priming. Ten micrograms of total RNA for a 100ul volume reaction were incubated with 1.5ug random primers at 85°C for 3 minutes. This was followed by the addition of 2.0ul Rnasin, 10ul 5x RT buffer, 20ul dNTPs and 4.0ul RT to the reaction mixture. RNase-free water was added to bring the final reaction volume to 100ul. The reaction mixture was incubated at 42°C for 30 minutes, and then 94°C for 2 minutes. Synthesized cDNA were stored at -80c until ready to use. PCR analysis was performed using the Taq Start Antibody Hot Start Method (Clontech laboratories Inc., Palo Alto, CA). PCR cycle parameters were 94°C 5 minutes, 40 cycles at (94°C 20 sec., 60°C 1min., 72°C 30 sec.) and a final extension at 72°C for 5 minutes. Control reactions were done for each primer pair by omitting reverse transcriptase in the cDNA synthesis. RT-PCR for β-actin was used as an internal control. RT-PCR amplified products were separated by agarose gel electrophoresis on a 1% agarose gel containing 5ug/ml ethidium bromide stain to facilitate visualization of bands under UV illumination.

Preparation of conditioned medium from RPC

Conditioned medium was collected from RPC cultured for 48 hours in basal medium consisting of Dulbecco's modified Eagles medium, 2 mM L-glutamine, 100 units/ml of Penicillin, 100ug/ml Streptomycin as described. Conditioned medium was centrifuged at 210×g for 10 minutes, filtered, and frozen at −20°C prior to use. Except for

collecting conditioned media, all cultures were maintained in NPMM (Clonetics) or DMEM with 10% FBS at 37°C under a humidified atmosphere of 95% air, 5% CO2.

Exposure of RPE cells to glucose oxidase/glucose

RPE cells were seeded at 15000 cells/ cm^2 in DMEM with 10% FBS and left overnight. Prior to glucose oxidase/glucose treatment, ARPE-19 cells were washed with glucose-free medium twice and then exposed to glucose oxidase/glucose for specific period of time.

Live/dead cell fluorescent assay

RPE cells were washed with phenol-red-free DMEM and incubated with 2uM calcein AM and 3uM ethidium homodimer at 37°C for 25 minutes. The residual fluorescent dyes were washed off and the images were captured using a fluorescence microscope.

Cell proliferation assay (MTS assay)

After indicated treatment, RPE cells were incubated for 1hour with MTS reagent (Cell Titer 96 Aqueous Cell Proliferation Assay kit, Promega, Madison, WI) ,which was converted to a water-soluble formazan by dehydrogenase enzyme found in metabolically active cells. The quantity of formazan product was determined by spectrophotometry using BioRad microplate reader (BioRad, Hercules, CA) at 490nm and 650nm. A

standard curve was prepared for each set of experiments. Experiments were done at triplicates.

Results

Isolation and expansion of human retinal progenitor cells in vitro

To test the hypothesis that human retinal progenitor cells (RPC) might be potential therapy for age-related macular degeneration, RPC was isolated from human retinas and cultured in the presence of either regular 10% FBS or neuronal progenitor medium(NPMM). In the presence of 10% FBS, RPC grew up as monolayer cells as shown in Figure 5.1. In contrast, when RPC was cultured in the presence of NPMM, the cells proliferated in the form of aggregates. As shown in the Figure 5.1, after 2-day exposure to NPMM, the cells had not formed aggregates. The appearance of small-size aggregates started at about 3 days. After exposure to NPMM for 6 days, medium-size aggregates of RPC were observed. To examine the proliferation capabilities of hRPC, neurospheres were immunostained with proliferating cellular nuclear antigen (PCNA). As shown in Figure 5.1, the neurospheres were positive for PCNA. These results demonstrate that the hRPC from human adult retina could expand in the form of neurospheres, a key characteristic of retinal progenitor cells.

Neurospheres express Nestin, a marker of neuronal progenitor cells

Since nestin is extensively used to identify neuronal progenitor cells or retinal progenitor cells, we examined the expression of nestin in human retinal progenitor cells. RPC were induced to form neurospheres and then examined for nestin expression using immunocytochemistry. Furthermore, total RNA was isolated from neurospheres and the RNA expression of nestin was examined by RT-PCR. PCR products were observed at appropriate sizes while omitting reverse transcriptase did not show any detectable bands. The results demonstrate that RPC express nestin, a marker of neuronal progenitor cells.

Neurospheres express markers of retinal progenitor cells, Pax6 and p75NTR

Besides marker of neuronal progenitor cells, we also detected the expression of retinal progenitor cells markers, such as Pax6 and p75NTR. We used immunocytochemistry and immunoblotting to determine the expression of Pax6 and p75NTR. RPC were induced to form neurospheres and subsequently processed for immunocytochemistry and immunoblotting. As shown in Figure 5.3, all neurospheres and monolayer RPC were positive for Pax6. Moreover, Pax6 expression was also confirmed by immunoblotting. In addition, P75NTR was also expressed in hRPC using immunoblotting. These results provide evidence for the progenitor expression profile of RPC.

Neurospheres do not express GFAP, a marker of glia

As shown previously, RPC were cultured in NPMM to induce the formation of neurospheres. The RPC spheres were fixed and processed for immunostaining using anti-GFAP, a marker for glia. The GFAP expression was observed only in neurospheres but not single retinal progenitor cells. (Figure 5.6)

Neuronal differentiation of RPC

Both neuronal and retinal progenitor cells have the potential to differentiate towards either neuronal or glial lineage. To test the differentiation potential of RPC, we isolated neurospheres and exposed them to special pro-neuronal medium- NPMM plus NSF-1. In the presence of pro-neuronal medium, neurite-containing cells migrated from neurospheres and gradually dominated the cultures. At this time point, the differentiated cells were lysed for protein extraction. Afterwards, the expression of Pax6, NSE, GFAP were compared between spheres and differentiated cells. As shown in Figure 5.5, compared to neurospheres expressing Pax6 but not NSE, differentiated RPC lost the expression of Pax6 but exhibited increased expression of NSE. Moreover, there was no change of GFAP expressions in both cultures. These results suggest that RPC possess the differentiation potential towards neuronal lineage.

Glial progenitor cell from RPC (default pathway)

While we used NPMM plus NSF-1 to induce neuronal differentiation, we cultured RPC in DMEM plus 10% FBS to induce glial differentiation. In this experiment, we

incubated RPC in 10% FBS for 14 days. Afterwards, we examined the expression of GFAP, Vimentin, Pax6, and NSE. As shown in Figure 5.6, when incubated in 10% FBS, RPC exhibited increased expression of GFAP, with undetectable expression of Pax6 and NSE.

Summary of RPC expansion and differentiation

RPC were isolated from adult human retina and found to express markers of neuronal progenitor cells and retinal progenitor cells, including Nestin, Pax6 and p75NTR. In the presence of FGF-2 and EGF, RPC proliferated as cellular aggregates, i.e. neurospheres, which were positive for nestin and Pax6 but not GFAP. When exposed to NPMM plus neuronal survival factor (NSF-1), the neurospheres differentiated towards neurite-containing cells with increased expression of NSE. In contrast, in the presence of 10% FBS, RPC differentiated towards GFAP-positive cell lineage. (Figure 5.7)

Conditioned medium of RPC protect RPE cells from oxidative damage

To test the hypothesis that RPC may secrete pro-survival molecules to rescue RPE cells from oxidative damage, we collected conditioned medium from early RPC. Prior to exposure to 25mU/ml glucose oxidase plus 1g/L glucose, ARPE-19 cells were pretreated with RPC-CM overnight. After exposure to glucose oxidase/glucose, RPE cell viability was measured by MTS cell proliferation assay. Compared to control group, RPC-CM significantly inhibited RPE degeneration induced by oxidative stress as seen in Figure 5.8.

RPC-CM protects primary cultures of human RPE cells from oxidative damage

Apart from ARPE-19 cells, we also tested the effect of RPC-CM on primary cultured RPE cells. The primary culture of human RPE cells was examined for expression of cytokeratin, a marker for retinal epithelial cells. Similarly, prior to exposure to 25mU/ml glucose oxidase plus 1g/L glucose, human RPE cells were pretreated with RPC-CM overnight. After exposure to oxidative stress, cell survival was measured by MTS assay. RPC-CM significantly inhibited RPE cell death induced by oxidative stress as shown in Figure 5.9.

Specificity of RPC-CM on RPE cell death

To examine the specificity of RPC-CM on ARPE-19 cells, RPC-CM was compared to conditioned medium from Muller cells and BHR cells (a human RPE cell line). ARPE-19 cells were pretreated with conditioned medium mentioned above and subjected to oxidative damage in the presence of corresponding conditioned medium. As shown in Figure 5.10, only RPC-CM promoted RPE cell viability, whereas conditioned medium from Muller cells or BHR cells did not inhibit RPE cell death induced by oxidative stress. Furthermore, the heat liability of RPC-CM was examined. RPC-CM was boiled for 5 minutes and resultant precipitation was removed. The heat treatment did not affect the protective effects of RPE-CM on RPE cell death. Moreover, according to silver staining of SDS-PAGE gels, there was no difference observed on the protein components of RPC-CM and boiled RPE-CM.

115

RPC-CM inhibits RPE cell death by activating p42/44 MAPK

In Chapter IV, we showed that p42/44 MAPK played a protective role in the RPE degeneration model. Furthermore, RPC-CM protected ARPE-19 cells from oxidative damage. Thus, we examined whether p42/p44MAPK was involved in the protective activity of RPC-CM. First, we treated ARPE-19 cells with either RPC-CM or glucose-free medium in the presence of 1g/L glucose for 12 hours. The treated cells were then processed for immunoblotting using anti-phospho p42/p44 MAPK. As shown in Figure 5.11, activation of p42/p44 MAPK was observed in cells treated with RPC-CM. Moreover, we employed a pharmacological inhibitor, U0126, to test the potential linkage between p42/44 MAPK and the cytoprotection of RPC-CM. Prior to pretreatment with RPC-CM overnight, ARPE-19 cells were pretreated with 20um U0126 for 2 hours. After the pretreatment with RPC-CM, ARPE-19 cells were subjected to oxidative damage as described before. The viability of RPE cells were measured by MTS assay. In contrast to inhibitory effects of RPC-CM, the presence of U0126 attenuated cell viability during oxidative damage. The results suggest that RPC-CM may protect RPE cells from oxidative damage by activating p42/p44 MAPK signaling.

Discussion

As an integral part of the central nervous system, retinal development is initiated in central optic cup and progresses into functional neurons and glia in a relatively fixed chronological sequence until full maturation.

Retinal neurons and Müller glia are derived from a common population of retinal progenitor cells (RPC) that possess multi-lineage differentiation potential and contribute to the generation of different retinal cell types in a defined histogenetic order. The elaborate regulation system of retinal development is controlled by the interplay of mechanisms that regulate proliferation, differentiation, and especially cell death of RPC. Retinal progenitor cells, i.e. neuroepithelial cells, are localized on the surface of the neural tube, or retinal ventricular zone. Newly derived postmitotic cells migrate variable distances to corresponding layers. To maintain effective information processing and patterning, newborn neurons have to precisely form synapses with other neurons.

Human retinal progenitor cells have been isolated from adult human retina and enriched in FGF-2 and EGF. For example, under pro-neuronal differentiation conditions, isolated RPC formed neurospheres and exhibited the expression of β-tubulin III, a neuronal marker [96]. In another study, retinal progenitor cells were isolated from adult human retina and shown to form nestin-positive neurospheres, from which retinal neurons were generated [97]. Retinal stem cells have been identified in the pigmented epithelium of the ciliary margin in rodent and human [98]. The isolated retinal stem cells could renew and generate retinal neurons and glia. Furthermore, neuronal precursor cells

were identified in choroid and sclera region of adult human retina. Nestin-positive cells were found in the adult human retina and epiretinal membrane [99].

In response to mitogens, such as FGF-2 and EGF, retinal stem cells or retinal progenitors grow as cell aggregates, commonly referred to as neurospheres. Neurospheres are multipotent and possess the potential to develop towards neurons and glia [100] [101]. Neurospheres are heterogeneous aggregates with different sizes, granularity and even at different stages of cell cycle and differentiation. For instance, the heterogeneous population of neurospheres from brain consists of distinct molecular phenotypes and different expression profile of protein markers [102].

Neuronal progenitor cells or retinal progenitor cells are usually characterized by an expression profile of protein markers since each marker itself may be expressed in postmitotic cells elsewhere in the retina. The expression of a combination of markers may help to better characterize retinal progenitor cells. Nestin, a type VI intermediate filament (IF) protein, is usually expressed in a variety of tissues during development but also present in specific adult tissues. It is extensively used to identify neuronal stem/progenitor cells and retinal progenitor cells in stem cell biology. Pax6, a paired domain and homeodomain containing transcription factor, is crucial for retinal development. Loss of Pax6 arrested retinal development at early optic vesicle stage. Furthermore, Pax6 is indispensable for retinal progenitor cells to maintain multipotential phenotypes [103]. Conditional gene inactivation of Pax6 rendered retinal progenitor cells to develop only into amacrine neurons instead of other cell lineages. Moreover, retinal stem cells with abrogated Pax6 expression had problem with proliferation *in vitro* [104]. Low-

affinity neurotrophin receptor p75NTR is also used to characterize retinal progenitor cells. P75NTR is expressed in retinal development to induce programmed cell death of RPC in order to modulate the quantity of retinal progenitor cells [105].

Though the unlimited self-renewal property and the multiple differentiation potential prepare stem cells/progenitor cells a promising therapy to repair diseased organs, the disadvantages should be considered in regenerative medicine. The disadvantages including surgical damage, uncontrolled differentiation and tumor formation [106] limit the use of retinal stem cells/progenitors in development of cell transplantation therapy for retinal diseases. Recently, the therapeutic potential of stem cell therapy has been expanded to the paracrine protective effect of stem cells/progenitor cells. It was shown that stem cells could secrete pro-survival molecules to protect damaged tissues [66] [68107]. In this study, our findings demonstrate that human retinal progenitor cells secrete pro-survival molecules to protect RPE cells from oxidative damage by modulating p42/p44 MAPK signaling.

Figure5.1. Isolation and expansion of human retinal progenitor cells in vitro

A, Human retinal progenitor cells were isolated from human retina and formed aggregates (neurospheres) when cultured in NPMM. **B,** Phase-contrast images of sphere-forming cells. When cultured in NPMM, RPC showed development of neurospheres with increased duration of treatment (2-6 days). **C,** Neurospheres were examined for expression of proliferating cell nuclear antigen (PCNA) by immunocytochemistry. DAPI was used to counterstain nucleus.
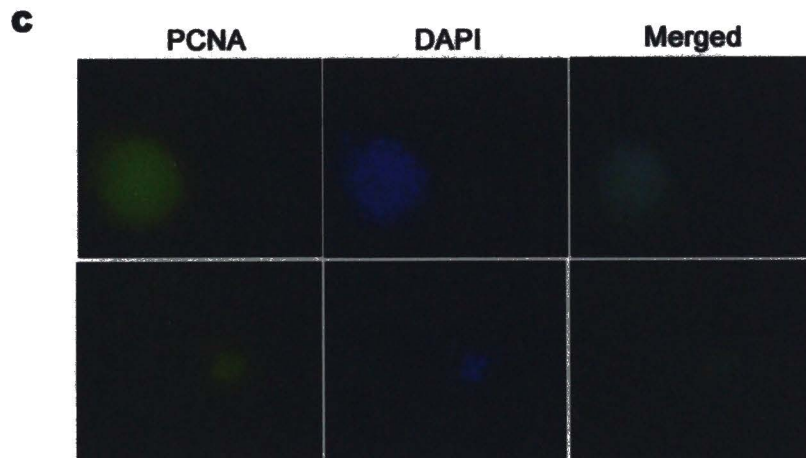
A

1% Serum

NPMM

B

2d 3d

4d 6d

C

PCNA DAPI Merged
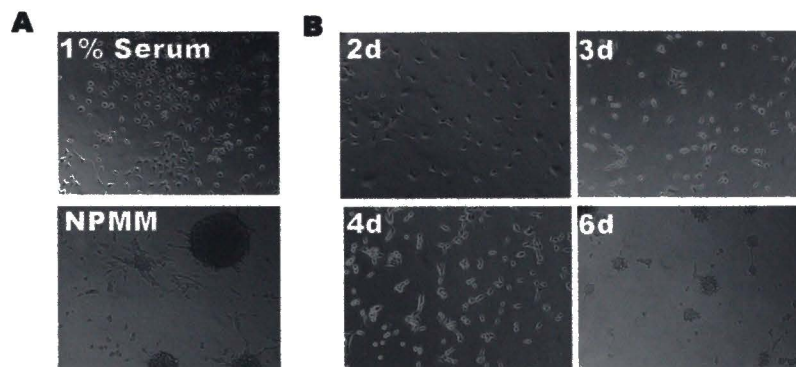
Figure5.2. Neurospheres express nestin, a marker of neuronal progenitor cells

A, Human retinal progenitor cells (top panel) and neurospheres (low panel) were examined for expression of nestin (green) using immunocytochemistry. DAPI (blue) was used to counterstain nucleus. **B,** Total RNA was isolated from RPC neurospheres and the RNA expression of nestin was determined by RT-PCR. β-actin was used as positive control while omission of reverse transcriptase was used as negative control.

A
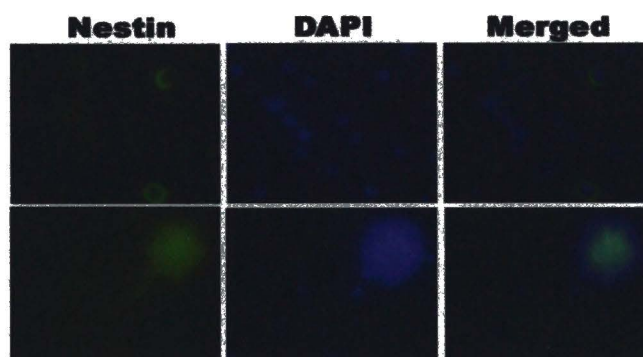
B
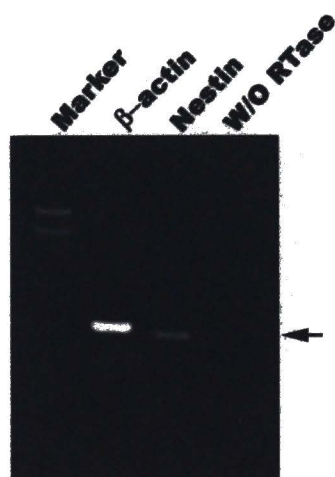
Figure5.3. Human retinal progenitor cells (hRPC) express Pax6 and p75NTR, markers of retinal progenitor cells

RPC neurospheres were examined for Pax6 expression using immunocytochemistry (**A**) and immunoblotting (**B**). DAPI (blue) was used to counterstain nucleus. The expression of p75NTR in RPC neurospheres was examined using immunoblotting (**C**).

A

Pax6   DAPI   Merged

B   C

Pax6

p75NTR
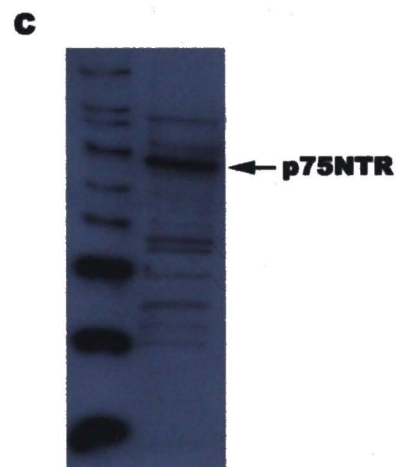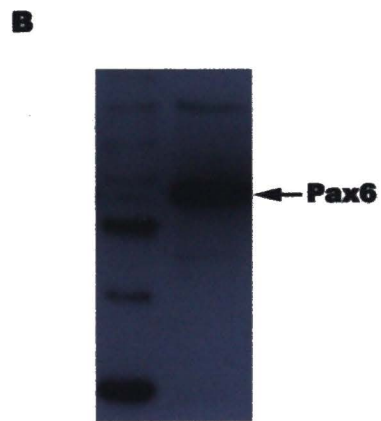
Figure5.4. Neurospheres do not express GFAP, a glial marker

The hRPC were exposed to NPMM medium to induce neurosphere formation and then examined for GFAP expression using immunocytochemistry. DAPI (blue) was used to counterstain nucleus.

GFAP   DAPI   Merged
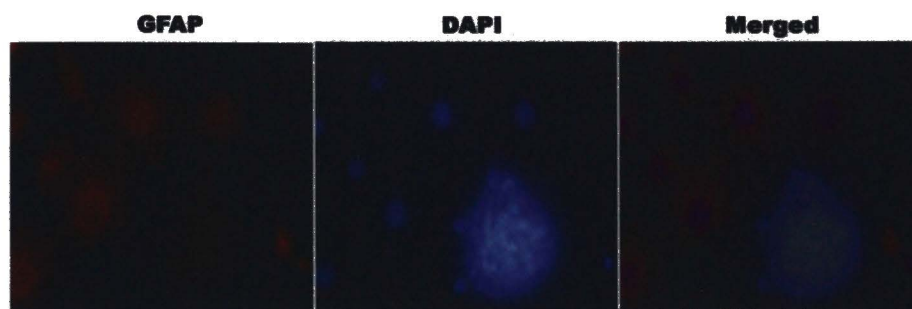
Figure5.5. RPC differentiates towards neuron-specific enolase (NSE)-positive cells

Neurospheres were collected and cultured in the presence of NPMM plus NSF-1 for 14 days, and the expression of Pax6, neuron-specific enolase (NSE), GFAP were examined using immunoblotting. β-actin was used as loading control.

Pax6 NSE GFAP Actin

1 2 1 2 1 2 1 2

1: Neurosphere

2 NPMM+ NSF-1
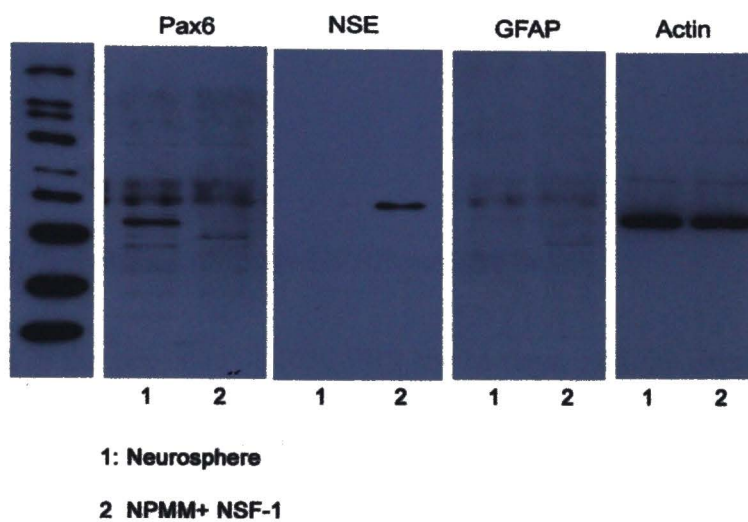
Figure5.6. RPC differentiates towards GFAP-positive cells

RPC was cultured in the presence of 10% FBS for 14 days, and the expression of GFAP, Vimentin, Pax6 and NSE were examined using immunoblotting. Homogenates from human retina were used as positive control
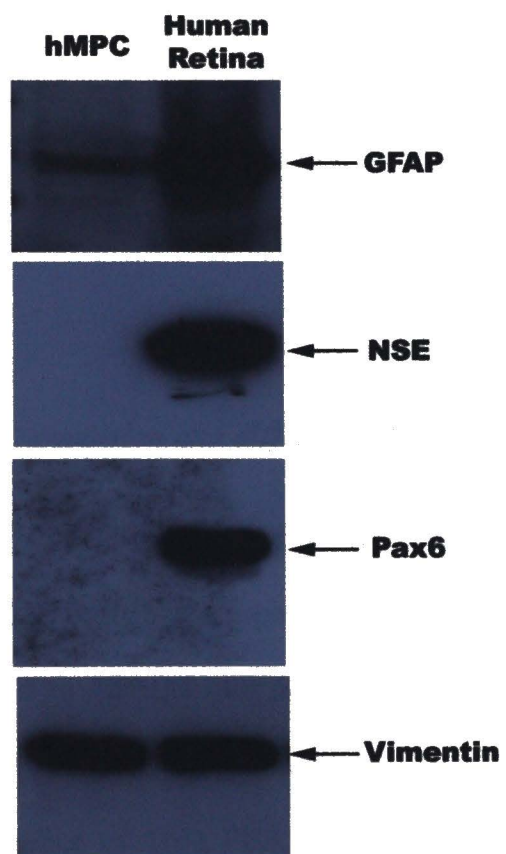
Figure5.7. Summary of hRPC expansion and differentiation

Isolated RPC expressed markers of neuronal progenitor cells and retinal progenitor cells, including nestin, Pax6 and p75NTR. The neurospheres were positive for nestin and Pax6 but not GFAP. When exposed to NPMM plus neuronal survival factor (NSF-1), the neurospheres differentiated towards neurite-containing cells with increased expression of NSE. In contrast, in the presence of 10% FBS, RPC differentiated towards GFAP-positive cell lineage.

Retinal Progenitors
(Nestin⁺,Pax6⁺,p75NTR⁺)

NPMM

10% FBS

Spheres
(Nestin⁺,Pax6⁺,GFAP⁻,NSE⁻)

10% FBS

Glia
(GFAP⁺,Vimentin⁺,Pax6⁻,NSE⁻)

NPMM+NSF-1

Neurons (NSE⁺, Pax6⁻, GFAP⁻)
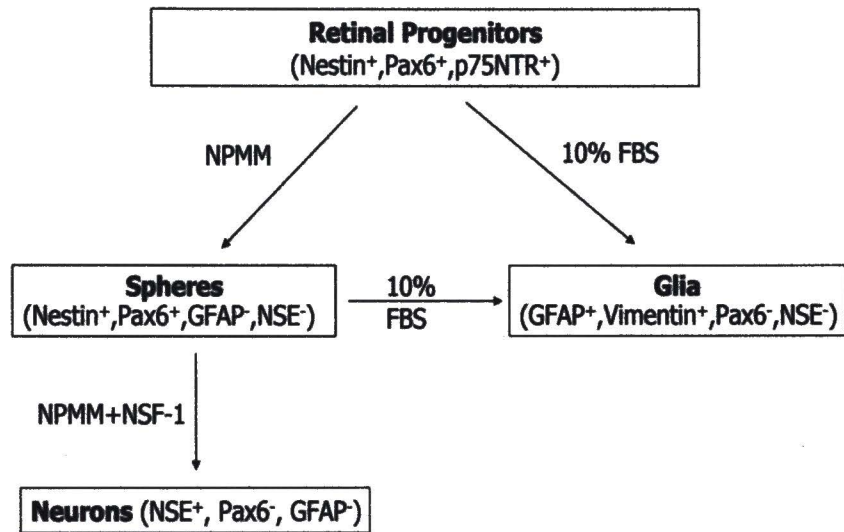
Figure5.8. Conditioned medium of RPC protects RPE cells from oxidative damage

Conditioned medium was collected from RPC that was cultured in serum-free DMEM for 48 hours. ARPE-19 cells were exposed to 25mU/ml glucose oxidase plus 1g/L glucose for 5 hours in the presence of RPC-CM. After overnight recovery, calcein AM/ethidium homodimer was used to assay live/dead cells (**A**). MTS cell proliferation assay was used to measure the viability of ARPE-19 cells (**B**).

A

Control   GO/G   hRPC-CM+GO/G
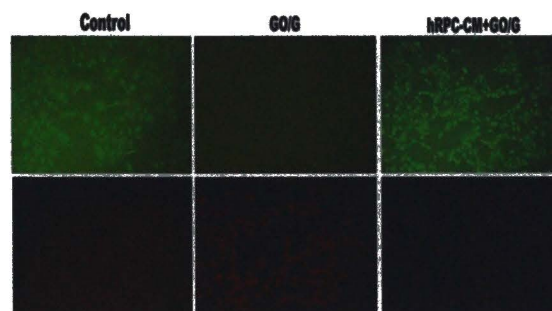
B
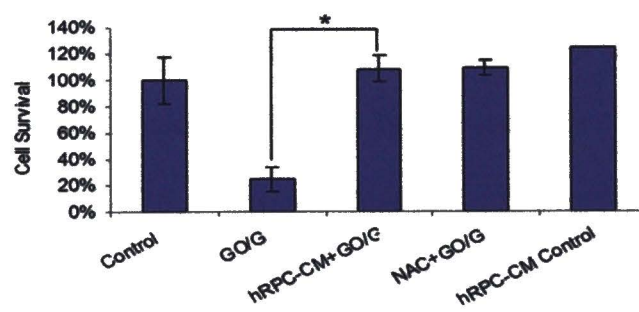
Figure5.9. RPC-CM protects primary cultured human RPE cells from oxidative damage

RPE cells were isolated from human retina and maintained as primary culture. **A,** Primary cultured RPE cells were examined for cytokeratin expression. **B,** RPE cells were incubated with 30mU/ml glucose oxidase plus 1g/L glucose for 6 hours in the presence of or in the absence of RPC-CM. Calcein AM/ethidium homodimer was used to assay live/dead cells. **C,** Moreover, MTS cell proliferation assay was used to measure the viability of ARPE-19 cells.

A Cytokeratin

B Control   GO/G   hRPC-CM+GO/G

C
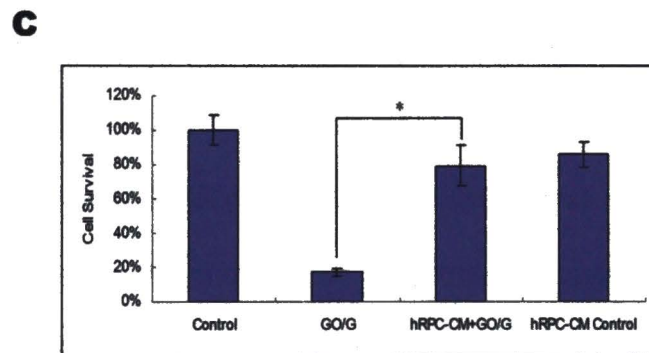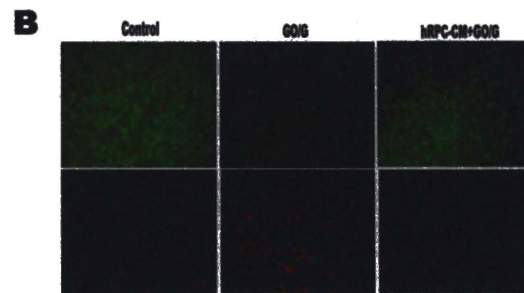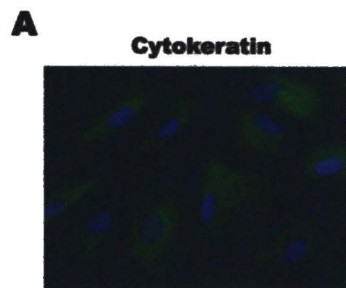
Figure5.10. Specificity of RPC-CM on ARPE-19 cells

A, ARPE-19 cells were treated with 25mU/ml glucose oxidase plus 1g/L glucose for 5 hours in the presence of conditioned media of RPC, conditioned media of human Muller cells or conditioned media of BHR cells. The cell viability was measured by MTS assay. **B,** RPC-CM was boiled for 10 minutes and its protection capability in RPE cells was compared to non-boiled RPC-CM. **C,** The protein components of RPC-CM and boiled RPE-CM were compared using silver staining of SDS-PAGE gel.
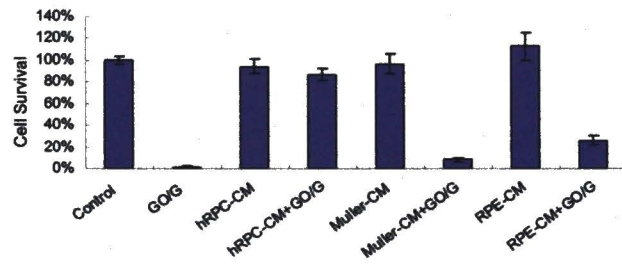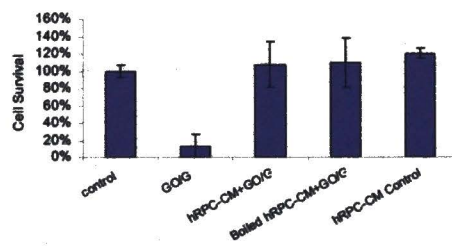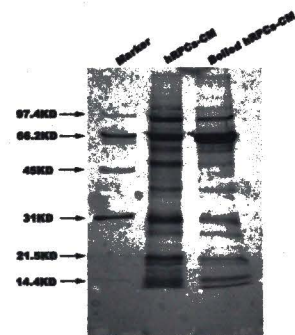
Figure5.11. RPC conditioned medium inhibits RPE cell death by activating p42/44 MAPK

A, ARPE-19 cells were treated with hRPC-CM for 12 hours and the expression of activated p42/44 MAPK was examined using immunoblotting. Total p42/p44 MAPK was used as loading control. **B,** ARPE-19 cells were exposed to 25mU/ml glucose oxidase plus 1g/L glucose for 5 hours in the presence of RPC-CM or in the presence of U0126 and RPC-CM. After exposure to oxidative stress, the cell viability was measured by MTS assay.

A

0 hr   hRPC-CM12hr   DMEM12hr

← phospho-
p42/p44 MAPK

← p42/p44 MAPK

B

Cell Survival

120%
100%
80%
60%
40%
20%
0%

Control   GO/G   hRPC-CM+GO/G   U0126+hRPC-CM+GO/G   hRPC-CM Control

*
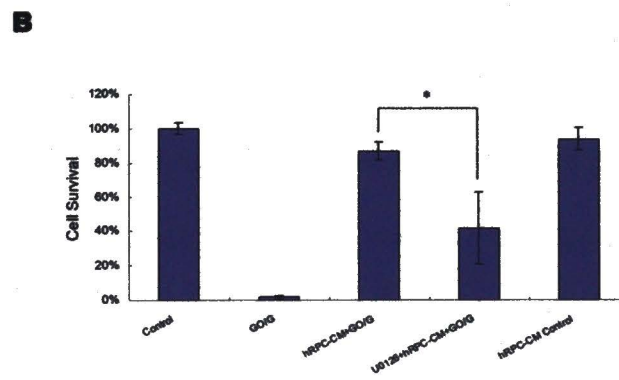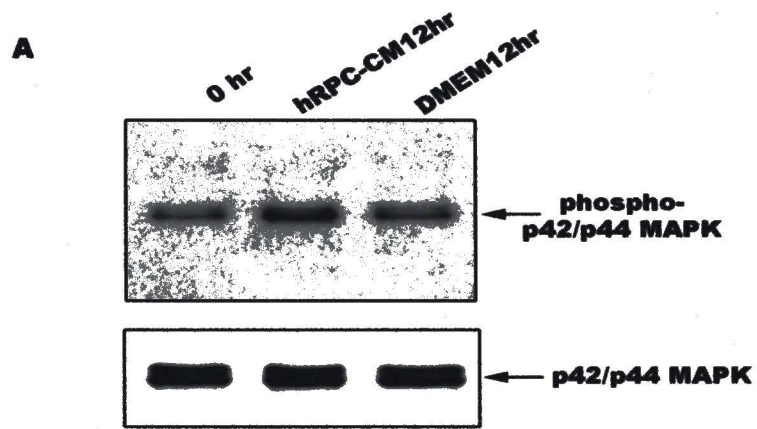
CHAPTER VI

SUMMARY

Age-related macular degeneration (AMD) is a leading cause of permanent vision loss in the developed countries, which is divided into two groups, dry form AMD and wet form AMD. The primary cause of wet type AMD is angiogenesis-deregulation of VEGF signal transduction. Hence, most of the new treatments for wet type AMD are developed to inhibit deregulated angiogenesis events. In contrast, the dry form of AMD does not have effective treatments and the underlying mechanism is still not fully understood. Several mechanisms have been proposed to explain the pathogenesis of RPE degeneration in dry AMD, including oxidative stress and inflammation. In these studies, we established a model of oxidative injury to RPE cells and demonstrated that p42/p44 MAPK promoted RPE cell survival. Furthermore, we showed that human retinal progenitor cells promoted RPE cell survival by regulating p42/p44 MAPK pathway.

Long term exposure to light, high oxygen demand , lipid peroxidation, and other factors have contributed to the oxidative damage to the human retina, whereas the antioxidant defense system of RPE cells attenuates with aging. For example, abrogation of superoxide dismutase (SOD) gene expression in animal model led to typical clinical

142

characteristics of age-related macular degeneration, including increased accumulation of drusen [8]. In human retina, the decline of catalase activity was found in both macular and peripheral RPE layers [6]. All the observations suggest that oxidative stress to retinal pigment epithelial cells might be a suitable model to study RPE degeneration. In this study, to investigate the molecular mechanisms and potential therapies in RPE degeneration *in vitro*, we established an oxidative stress model to induce RPE cell death utilizing glucose oxidase/glucose. In addition, ARPE-19 cell line is a spontaneously immortalized cell line obtained from human retina donor in the early 1990s. ARPE-19 has been demonstrated in a variety of studies to maintain characteristics of retinal pigment epithelium, including polarized epithelial monolayer with tight junctions and barrier properties, expression of RPE-specific markers CRALBP and RPE65 and binding and internalization of rod outer segments for phagocytosis[108].

To induce RPE degeneration *in vitro*, a variety of oxidants, such as hydrogen peroxide, t-terbutyl-hydroperoxide and menadione, are used to exert oxidative stress on RPE cells. In this study, we used glucose oxidase/glucose to continuously generate reactive oxygen species (ROS), which we believe simulates the chronic accumulation of oxidative stress in the aging retina. Furthermore, since the generation of ROS is chronic in our model, it is convenient to determine the optimal timing to induce non-lethal oxidative injury.

It is well known that RPE geographic atrophy is associated with cell death in AMD development, but the phenotype of cell death is not clear yet. A clinical study

proposed that, the degenerating RPE cells was apoptotic in AMD patients using TUNEL staining. Since TUNEL staining is a marker for DNA fragmentation, but not for apoptosis, the cell death of RPE may not be apoptotic as suggested by the authors. In cell culture models, the phenotype of cell death is also controversial. The RPE cell death induced by oxidative stress was claimed to be apoptotic in some studies using TUNEL staining and flow cytometry [48] [30]. Other studies suggested that the degeneration of the RPE was a combination of apoptosis and necrosis [31]. However, RPE cell death induced by menadione exhibited only chromatin condensation and nuclear DNA from damaged RPE cells did not demonstrate typical 200bp nucleosomal fragments [81]. **In our studies, we showed that RPE cell death exposed to lethal oxidative stress exhibited DNA condensation, but not DNA fragmentation.**

Cellular membrane blebbing is a defensive mechanism when cells are exposed to a wide range of injuries, including toxic drugs, oxidants, and environment stresses. By doing so, the cells could shed off damaged organelles, plasma membrane and cytosolic proteins so as to survive the damages. Membrane blebbing has been proposed to contribute to drusen formation in animal models [109][110]. Presently, our research efforts are focused on inducing membrane blebbing to mimic drusen formation *in vitro,* which would aid in understanding the mechanisms of drusen formation and the molecular components within the drusen. Both non-lethal and lethal oxidative injury could induce membrane blebbing and might be used to investigate sub-RPE deposit accumulations [69] [81]. **In this study, we demonstrated that non-lethal oxidative injury promotes membrane blebbing and cytoskeleton remodeling.**

p38 is a member of MAPK family and involved in a variety of complex signaling cascades. p38 has been extensively studied in cell death, proliferation and differentiation. In RPE cell biology, p38 plays a wide array of roles, such as mediating VEGF expression, stimulating expression of IL-8, and regulating collagen expression and cell migration. Besides, p38 has been shown to induce RPE cell death in tissue culture models. In ARPE-19 cell line, hydrogen peroxide induced p38 activation and downstream substrates, while the cell death was inhibited by p38 MAPK inhibitor, SB203580 [48]. In another study, p38 was shown to be protective rather than pro-degeneration using the same RPE cell line. In short, both SB203580 and p38 siRNA promoted cell death and hence p38 was suggested to be protective (ARVO, 2006, E-Abstract 2074.). Besides regulating cell death or survival, p38 could modulate cytoskeleton reorganization by activating HSP27 [111], [112]. Furthermore, activation of p38 could contribute to membrane blebbing associated with cell death [49]. **In this study, HSP27 was shown to be activated by oxidative stress and the activation of HSP27 was inhibited by p38 MAPK inhibitor, suggesting that p38 might be involved in HSP27 mediated cytoskeleton remodeling. Furthermore, our study showed that knocking down p38 MAPK expression did not rescue RPE cell death from oxidative stress, but pharmacological inhibition of p38 MAPK protected RPE cells from oxidative damage.**

Pharmacological inhibitors are widely used in biomedical research in view of their convenience, efficiency and specificity. However, their off-target effects on certain substrates may bring about controversial results and .limit their use in cell biology, especially with the advancement of RNAi technology. SB203580 is widely used in

investigating the role of p38 MAPK in regulating transcription, translation and other cellular functions. It efficiently inhibits p38 MAPKα and p38 MAPK β, but not other p38 MAPK isoforms. Recently, however, its side effects on other signal proteins were examined. SB203580 was shown to activate Raf-1 in a dose-dependent mode in quiescent smooth muscle cells [113]. SB203580 enhanced transcriptional activity of NF-kB by activating p42/p44 MAPK in the erythroleukaemic cell line [114]. In rabbit aortic vascular smooth muscle cells, SB203580, but not other p38 MAPK inhibitors, activated p42/p44 MAPK and cytosolic phospholipase A2 [115]. In THP-1 monocytic cells and U937 cells, SB203580 induced sustained activation of c-Raf, MEK1/2 and p42/p44 MAPK [116]. In addition, SB203580 induced differentiation of human promyelocytic HL-60 cells, a cellular event closely associated with activation of p42/p44 MAPK, but not p38 MAPK. In 3T3 cells and 293 cells, SB203580 at micromolar concentrations activated both c-Raf and MEK1 independent of p38 MAPK inhibition [117]. **In this study, we identified that SB203580 inhibited RPE cell death evoked by oxidative injury. We also reported that SB203580 activated p42/p44 MAPK and might play a protective role by modulating p42/p44 MAPK signaling.**

p42/p44 MAPK is another member of MAPK family and modulates various cellular functions, such as proliferation, differentiation and cell death. In response to environment stresses, p42/p44 MAPK may either inhibit or promote cell death by modulating different downstream signaling cascades. Once activated by environmental stresses or extracellular mitogens, p42/p44 MAPK translocate to the nucleus, where p42/p44 MAPK phosphorylate a group of transcription factors and differentially regulate

146

transcription of target genes. p42/p44 MAPK are indispensable for RPE cell proliferation in response to mitogenic stimuli as shown in a variety of studies. Both EGF and FGF promoted RPE proliferation by activating p42/p44 MAPK signaling [93]. On the contrary, cAMP inhibited the proliferation of RPE cells by deregulating p42/p44 MAPK [118]. Moreover, 15-deoxy-Delta(12,14)-prostaglandin J(2) (dPGJ(2)) and PDGF protected RPE cells from oxidative injury by elevating p42/p44 MAPK activity [60]. Nevertheless, p42/p44 MAPK has been suggested to induce RPE cell death in response to oxidative stress, based on that U0126 inhibited oxidative-stress induced cell death. **In this study, U0126 did not inhibit the cell death induced by glucose oxidase/glucose, and knocking down p42/p44 MAPK expression accelerated RPE cell death during oxidative stress. Furthermore, overexpression of constitutively active MEK1 protected RPE cells from oxidant injury.**

Stem cells or progenitor cells are unspecialized cells with potential to self-renew and give rise to post-mitotic cells that are critical for physiological functions of human beings. The most attractive use of stem cells/progenitor cells is to maintain and repair the damaged tissues caused by environmental stresses. Clinically, stem cell transplantation may be a promising therapeutic approach for Parkinson's disease, spinal cord injury and retinal degeneration.

During retinal development, retinal progenitor cells (RPC) in the neuroblastic layer proliferate and generate postmitotic progenies of the mature neuronal retina. In the rodent, RPC showed multipotent potential till postnatal stage. In contrast, the

147

development of human retina reaches maturity just before birth, suggesting that adult human retina may not possess retinal progenitor cells. However, retinal stem cells/retinal progenitor cells were recently isolated from adult human retina. For instance, adult retinal stem cells with the potential to generate retinal neurons were isolated from pigmented ciliary margin from human retina donors [119]. Moreover, human retinal progenitor cells isolated from human retina could proliferate, form neurospheres and give rise to retinal neurons [97]. **In this study, we isolated and expanded adult human retinal progenitor cells *in vitro*. The human RPC proliferated as neurospheres and expressed markers of neuronal progenitor cells and retinal progenitor cells, such as nestin, Pax6 and p75 NTR. Furthermore, isolated human RPC demonstrated differentiation potential towards both neuronal and glia lineage under different culture conditions.**

Regenerative medicine is primarily focused on driving stem cells towards appropriate cell lineages so as to repair damaged organs. This approach is challenged by uncontrolled differentiation, potential surgical damage and tumor formation. For instance, transplantation of retinal progenitor cells led to tumor formation in the retina after engraftment into rhodopsin$^{-/-}$ animals [106]. Until recently, it was proposed that stem cells could secrete pro-survival molecules to protect injured organs rather than undergo differentiation. For instance, stem cells reversed cardiac defects in animal models by secreting IGF-1 and WNT5a [66]. In addition, bone marrow-derived mesenchymal stem cells rescued cardiomyocytes from hypoxia both *in vivo* and *in vitro* [68]. Hence, stem cells might serve as a resource of survival factors and protect damaged organs including diseased human retina. **In this study, we demonstrated that hRPC secreted pro-**

survival molecules to protect RPE cells from oxidative damage by activating p42/p44 MAPK signaling pathway.

In conclusion, we demonstrate that MAPKs play different roles in RPE degeneration induced by oxidative stress. Activation of p42/p44 MAPK promotes RPE cell survival, whereas p38 MAPK is not involved in RPE cell death. Meanwhile, human retinal progenitor cells protect RPE cells from oxidative damage by activating p42/p44 MAPK signaling.

In this study, we demonstrate that SB203580 rescues RPE cell death from oxidative damage, which suggests that SB203580 might be a candidate compound for AMD therapy. Therefore, future studies would be designed to test the beneficial effects of SB203580 on AMD animal models. We have isolated human retinal progenitor cells and demonstrate that RPC possesses the potential to differentiate towards both neurons and glia *in vitro*. Furthermore, the RPC could be protective by secreting pro-survival molecules and activating p42/p44 MAPK. The potential of differentiation and protection of RPC will be examined in animal models. Light damaged rat will be used as animal model in this study. Both RPC and conditioned medium of RPC will be injected into the retina and the therapeutic effects will be examined and compared after exposing rat to light for specific period of time.

APPENDIX

LIST OF ABBREVIATIONS USED

AIF = apoptosis inducing factor

ATP = adenosine triphosphate

BSA = bovine serum albumin

DAPI = 4',6-diamidino-2-phenylindole

DMSO = dimethyl sulfoxide

DTT = dithiothreitol

EGF = Epidermal growth factor

ERK = extracellular signal-regulated kinase

FBS = Fetal bovine serum

FGF = Fibroblast growth factor

β-Gal = β-galactosidase

GFAP = glial fibrillary acidic protein

GO/G = glucose oxides/glucose

HBSS = Hank's balanced salt solution

RPC = retinal progenitor cells

HSP27 = heat shock protein 27

IGF = insulin growth factor

JC-1 = 5,5',6,6'-tetrachloro-1,1',3,3' tetraethylbenzimidazolylcarbocyanine iodide

JNK = c-jun N-terminal kinase

MAPK = mitogen activated protein kinase

MEK = MAPK/ERK kinase

NPMM = neural progenitor maintenance medium

NSE = neurons specific enolase

NSF-1 = neural survival factor-1

P75NTR = p75 neurotrophin receptor

PAGE = polyacrylamide gel electrophoresis

Pax6 = paired box 6

PBS = phosphate Buffered Saline

PCNA = proliferating Cellular Nuclear Antigen

PDT = photodynamic therapy

PKC = protein kinase C

RNAi = RNA interference

PVDF = polyvinylidene fluoride

ROS = reactive oxygen species

RPC = retinal progenitor cells

RPE = retinal pigment epithelium

RT-PCR = reverser transcription-PCR

SDS = sodium dodecyl sulphate

siRNA = small interference RNA

TGFβ = transforming growth factor beta

TUNEL = terminal deoxynucleotidyl transferase-mediated dUTP nick end labeling

TIMP =tissue inhibitor of matrix metalloprotease

VEGF = vascular endothelial growth factor

BIBLIOGRAPHY

1. Strauss, O. The retinal pigment epithelium in visual function. *Physiol. Rev.* **85**, 845-881 (2005).

2. Congdon, N. *et al.* Causes and prevalence of visual impairment among adults in the United States. *Arch. Ophthalmol.* **122**, 477-485 (2004).

3. Friedman, D. S. *et al.* Prevalence of age-related macular degeneration in the United States. *Arch. Ophthalmol.* **122**, 564-572 (2004).

4. Petrukhin, K. New therapeutic targets in atrophic age-related macular degeneration. *Expert Opin. Ther. Targets* **11**, 625-639 (2007).

5. Waris, G. & Ahsan, H. Reactive oxygen species: role in the development of cancer and various chronic conditions. *J. Carcinog.* **5**, 14 (2006).

6. Liles, M. R., Newsome, D. A. & Oliver, P. D. Antioxidant enzymes in the aging human retinal pigment epithelium. *Arch. Ophthalmol.* **109**, 1285-1288 (1991).

7. Cai, J., Nelson, K. C., Wu, M., Sternberg, P.,Jr & Jones, D. P. Oxidative damage and protection of the RPE. *Prog. Retin. Eye Res.* **19**, 205-221 (2000).

8. Imamura, Y. *et al.* Drusen, choroidal neovascularization, and retinal pigment epithelium dysfunction in SOD1-deficient mice: a model of age-related macular degeneration. *Proc. Natl. Acad. Sci. U. S. A.* **103**, 11282-11287 (2006).

9. Seko, Y., Pang, J., Tokoro, T., Ichinose, S. & Mochizuki, M. Blue light-induced apoptosis in cultured retinal pigment epithelium cells of the rat. *Graefes Arch. Clin. Exp. Ophthalmol.* **239**, 47-52 (2001).

10. Anderson, D. H., Mullins, R. F., Hageman, G. S. & Johnson, L. V. A role for local inflammation in the formation of drusen in the aging eye. *Am. J. Ophthalmol.* **134**, 411-431 (2002).

11. Klein, R. J. *et al.* Complement factor H polymorphism in age-related macular degeneration. *Science* **308**, 385-389 (2005).

12. Edwards, A. O. *et al.* Complement factor H polymorphism and age-related macular degeneration. *Science* **308**, 421-424 (2005).

13. Haines, J. L. *et al.* Complement factor H variant increases the risk of age-related macular degeneration. *Science* **308**, 419-421 (2005).

14. Sivaprasad, S. & Chong, N. V. The complement system and age-related macular degeneration. *Eye* **20**, 867-872 (2006).

15. Rose, R. C., Richer, S. P. & Bode, A. M. Ocular oxidants and antioxidant protection. *Proc. Soc. Exp. Biol. Med.* **217**, 397-407 (1998).

16. Mares-Perlman, J. A. *et al.* Association of zinc and antioxidant nutrients with age-related maculopathy. *Arch. Ophthalmol.* **114**, 991-997 (1996).

17. Liang, F. Q., Green, L., Wang, C., Alssadi, R. & Godley, B. F. Melatonin protects human retinal pigment epithelial (RPE) cells against oxidative stress. *Exp. Eye Res.* **78**, 1069-1075 (2004).

18. Photodynamic therapy of subfoveal choroidal neovascularization in age-related macular degeneration with verteporfin: one-year results of 2 randomized clinical trials--TAP report. Treatment of age-related macular degeneration with photodynamic therapy (TAP) Study Group. *Arch. Ophthalmol.* **117**, 1329-1345 (1999).

19. Avery, R. L. *et al.* Intravitreal bevacizumab (Avastin) for neovascular age-related macular degeneration. *Ophthalmology* **113**, 363-372.e5 (2006).

20. Rosenfeld, P. J. *et al.* Ranibizumab for neovascular age-related macular degeneration. *N. Engl. J. Med.* **355**, 1419-1431 (2006).

21. Kaplan, H. J., Tezel, T. H., Berger, A. S., Wolf, M. L. & Del Priore, L. V. Human photoreceptor transplantation in retinitis pigmentosa. A safety study. *Arch. Ophthalmol.* **115**, 1168-1172 (1997).

22. Kaplan, H. J., Tezel, T. H. & Del Priore, L. V. Retinal pigment epithelial transplantation in age-related macular degeneration. *Retina* **18**, 99-102 (1998).

23. Weisz, J. M. *et al.* Allogenic fetal retinal pigment epithelial cell transplant in a patient with geographic atrophy. *Retina* **19**, 540-545 (1999).

24. Yang, P., Seiler, M. J., Aramant, R. B. & Whittemore, S. R. Differential lineage restriction of rat retinal progenitor cells in vitro and in vivo. *J. Neurosci. Res.* **69**, 466-476 (2002).

25. Wang, X. The expanding role of mitochondria in apoptosis. *Genes Dev.* **15**, 2922-2933 (2001).

26. Okada, H. & Mak, T. W. Pathways of apoptotic and non-apoptotic death in tumour cells. *Nat. Rev. Cancer.* **4**, 592-603 (2004).

27. Zong, W. X., Ditsworth, D., Bauer, D. E., Wang, Z. Q. & Thompson, C. B. Alkylating DNA damage stimulates a regulated form of necrotic cell death. *Genes Dev.* **18**, 1272-1282 (2004).

28. Dunaief, J. L., Dentchev, T., Ying, G. S. & Milam, A. H. The role of apoptosis in age-related macular degeneration. *Arch. Ophthalmol.* **120**, 1435-1442 (2002).

29. Strunnikova, N. *et al.* Survival of retinal pigment epithelium after exposure to prolonged oxidative injury: a detailed gene expression and cellular analysis. *Invest. Ophthalmol. Vis. Sci.* **45**, 3767-3777 (2004).

30. Glotin, A. L. *et al.* Sustained versus transient ERK1/2 signaling underlies the anti- and proapoptotic effects of oxidative stress in human RPE cells. *Invest. Ophthalmol. Vis. Sci.* **47**, 4614-4623 (2006).

31. Yang, P., Peairs, J. J., Tano, R. & Jaffe, G. J. Oxidant-mediated Akt activation in human RPE cells. *Invest. Ophthalmol. Vis. Sci.* **47**, 4598-4606 (2006).

32. Cai, J., Wu, M., Nelson, K. C., Sternberg, P.,Jr & Jones, D. P. Oxidant-induced apoptosis in cultured human retinal pigment epithelial cells. *Invest. Ophthalmol. Vis. Sci.* **40**, 959-966 (1999).

33. Jin, G. F., Hurst, J. S. & Godley, B. F. Hydrogen peroxide stimulates apoptosis in cultured human retinal pigment epithelial cells. *Curr. Eye Res.* **22**, 165-173 (2001).

34. Godley, B. F., Jin, G. F., Guo, Y. S. & Hurst, J. S. Bcl-2 overexpression increases survival in human retinal pigment epithelial cells exposed to H(2)O(2). *Exp. Eye Res.* **74**, 663-669 (2002).

35. Zarubin, T. & Han, J. Activation and signaling of the p38 MAP kinase pathway. *Cell Res.* **15**, 11-18 (2005).

36. Kuma, Y., Campbell, D. G. & Cuenda, A. Identification of glycogen synthase as a new substrate for stress-activated protein kinase 2b/p38beta. *Biochem. J.* **379**, 133-139 (2004).

37. Efimova, T., Broome, A. M. & Eckert, R. L. A regulatory role for p38 delta MAPK in keratinocyte differentiation. Evidence for p38 delta-ERK1/2 complex formation. *J. Biol. Chem.* **278**, 34277-34285 (2003).

38. Pramanik, R. *et al.* p38 isoforms have opposite effects on AP-1-dependent transcription through regulation of c-Jun. The determinant roles of the isoforms in the p38 MAPK signal specificity. *J. Biol. Chem.* **278**, 4831-4839 (2003).

39. Wang, Y. *et al.* Cardiac muscle cell hypertrophy and apoptosis induced by distinct members of the p38 mitogen-activated protein kinase family. *J. Biol. Chem.* **273**, 2161-2168 (1998).

40. Adams, R. H. *et al.* Essential role of p38alpha MAP kinase in placental but not embryonic cardiovascular development. *Mol. Cell* **6**, 109-116 (2000).

41. Van Laethem, A. *et al.* Apoptosis signal regulating kinase-1 connects reactive oxygen species to p38 MAPK-induced mitochondrial apoptosis in UVB-irradiated human keratinocytes. *Free Radic. Biol. Med.* **41**, 1361-1371 (2006).

42. Beardmore, V. A. *et al.* Generation and characterization of p38beta (MAPK11) gene-targeted mice. *Mol. Cell. Biol.* **25**, 10454-10464 (2005).

43. Sabio, G. *et al.* p38gamma regulates the localisation of SAP97 in the cytoskeleton by modulating its interaction with GKAP. *EMBO J.* **24**, 1134-1145 (2005).

44. Bian, Z. M., Elner, S. G. & Elner, V. M. Regulation of VEGF mRNA expression and protein secretion by TGF-beta2 in human retinal pigment epithelial cells. *Exp. Eye Res.* **84**, 812-822 (2007).

45. Bian, Z. M., Elner, V. M., Yoshida, A., Kunkel, S. L. & Elner, S. G. Signaling pathways for glycated human serum albumin-induced IL-8 and MCP-1 secretion in human RPE cells. *Invest. Ophthalmol. Vis. Sci.* **42**, 1660-1668 (2001).

46. Kimoto, K., Nakatsuka, K., Matsuo, N. & Yoshioka, H. p38 MAPK mediates the expression of type I collagen induced by TGF-beta 2 in human retinal pigment epithelial cells ARPE-19. *Invest. Ophthalmol. Vis. Sci.* **45**, 2431-2437 (2004).

47. Hollborn, M., Bringmann, A., Faude, F., Wiedemann, P. & Kohen, L. Signaling pathways involved in PDGF-evoked cellular responses in human RPE cells. *Biochem. Biophys. Res. Commun.* **344**, 912-919 (2006).

48. Ho, T. C. *et al.* Activation of mitogen-activated protein kinases is essential for hydrogen peroxide -induced apoptosis in retinal pigment epithelial cells. *Apoptosis* **11**, 1899-1908 (2006).

49. Huot, J. *et al.* SAPK2/p38-dependent F-actin reorganization regulates early membrane blebbing during stress-induced apoptosis. *J. Cell Biol.* **143**, 1361-1373 (1998).

50. Okada, T. *et al.* Role of F-actin organization in p38 MAP kinase-mediated apoptosis and necrosis in neonatal rat cardiomyocytes subjected to simulated ischemia and reoxygenation. *Am. J. Physiol. Heart Circ. Physiol.* **289**, H2310-8 (2005).

51. Aoudjit, L., Stanciu, M., Li, H., Lemay, S. & Takano, T. P38 Mitogen-Activated Protein Kinase Protects Glomerular Epithelial Cells from Complement-Mediated Cell Injury. *Am. J. Physiol. Renal Physiol.* **285**, F765-74 (2003).

52. de Graauw, M. *et al.* Heat shock protein 27 is the major differentially phosphorylated protein involved in renal epithelial cellular stress response and controls focal adhesion organization and apoptosis. *J. Biol. Chem.* **280**, 29885-29898 (2005).

53. Lewis, T. S., Shapiro, P. S. & Ahn, N. G. Signal transduction through MAP kinase cascades. *Adv. Cancer Res.* **74**, 49-139 (1998).

54. Guyton, K. Z., Liu, Y., Gorospe, M., Xu, Q. & Holbrook, N. J. Activation of mitogen-activated protein kinase by H2O2. Role in cell survival following oxidant injury. *J. Biol. Chem.* **271**, 4138-4142 (1996).

55. Wang, X., Martindale, J. L. & Holbrook, N. J. Requirement for ERK activation in cisplatin-induced apoptosis. *J. Biol. Chem.* **275**, 39435-39443 (2000).

56. Rubinfeld, H., Hanoch, T. & Seger, R. Identification of a cytoplasmic-retention sequence in ERK2. *J. Biol. Chem.* **274**, 30349-30352 (1999).

57. Galabova-Kovacs, G. *et al.* ERK and beyond: insights from B-Raf and Raf-1 conditional knockouts. *Cell. Cycle* **5**, 1514-1518 (2006).

58. Aouadi, M., Binetruy, B., Caron, L., Le Marchand-Brustel, Y. & Bost, F. Role of MAPKs in development and differentiation: lessons from knockout mice. *Biochimie* **88**, 1091-1098 (2006).

59. Garg, T. K. & Chang, J. Y. Oxidative stress causes ERK phosphorylation and cell death in cultured retinal pigment epithelium: prevention of cell death by AG126 and 15-deoxy-delta 12, 14-PGJ2. *BMC Ophthalmol.* **3**, 5 (2003).

60. Tsao, Y. P., Ho, T. C., Chen, S. L. & Cheng, H. C. Pigment epithelium-derived factor inhibits oxidative stress-induced cell death by activation of extracellular signal-regulated kinases in cultured retinal pigment epithelial cells. *Life Sci.* **79**, 545-550 (2006).

61. Qin, S., McLaughlin, A. P. & De Vries, G. W. Protection of RPE cells from oxidative injury by 15-deoxy-delta12,14-prostaglandin J2 by augmenting GSH and activating MAPK. *Invest. Ophthalmol. Vis. Sci.* **47**, 5098-5105 (2006).

62. Turner, D. L. & Cepko, C. L. A common progenitor for neurons and glia persists in rat retina late in development. *Nature* **328**, 131-136 (1987).

63. Tropepe, V. *et al.* Retinal stem cells in the adult mammalian eye. *Science* **287**, 2032-2036 (2000).

64. Coles, B. L. *et al*. Facile isolation and the characterization of human retinal stem cells. *Proc. Natl. Acad. Sci. U. S. A.* **101**, 15772-15777 (2004).

65. MacLaren, R. E. *et al*. Retinal repair by transplantation of photoreceptor precursors. *Nature* **444**, 203-207 (2006).

66. Fraidenraich, D. *et al*. Rescue of cardiac defects in id knockout embryos by injection of embryonic stem cells. *Science* **306**, 247-252 (2004).

67. Toda, H. *et al*. Stem cell-derived neural stem/progenitor cell supporting factor is an autocrine/paracrine survival factor for adult neural stem/progenitor cells. *J. Biol. Chem.* **278**, 35491-35500 (2003).

68. Gnecchi, M. *et al*. Paracrine action accounts for marked protection of ischemic heart by Akt-modified mesenchymal stem cells. *Nat. Med.* **11**, 367-368 (2005).

69. Marin-Castano, M. E. *et al*. Repetitive nonlethal oxidant injury to retinal pigment epithelium decreased extracellular matrix turnover in vitro and induced sub-RPE deposits in vivo. *Invest. Ophthalmol. Vis. Sci.* **47**, 4098-4112 (2006).

70. Dunn, K. C., Aotaki-Keen, A. E., Putkey, F. R. & Hjelmeland, L. M. ARPE-19, a human retinal pigment epithelial cell line with differentiated properties. *Exp. Eye Res.* **62**, 155-169 (1996).

71. Kim, Y. S. & Kim, S. U. Oligodendroglial cell death induced by oxygen radicals and its protection by catalase. *J. Neurosci. Res.* **29**, 100-106 (1991).

72. Dhanasekaran, A. *et al*. Supplementation of endothelial cells with mitochondria-targeted antioxidants inhibit peroxide-induced mitochondrial iron uptake, oxidative damage, and apoptosis. *J. Biol. Chem.* **279**, 37575-37587 (2004).

73. Bae, G. U. *et al*. Hydrogen peroxide activates p70(S6k) signaling pathway. *J. Biol. Chem.* **274**, 32596-32602 (1999).

74. Song, J. Y., Lim, J. W., Kim, H., Morio, T. & Kim, K. H. Oxidative stress induces nuclear loss of DNA repair proteins Ku70 and Ku80 and apoptosis in pancreatic acinar AR42J cells. *J. Biol. Chem.* **278**, 36676-36687 (2003).

75. Mueller, S., Pantopoulos, K., Hubner, C. A., Stremmel, W. & Hentze, M. W. IRP1 activation by extracellular oxidative stress in the perfused rat liver. *J. Biol. Chem.* **276**, 23192-23196 (2001).

76. Corna, G., Santambrogio, P., Minotti, G. & Cairo, G. Doxorubicin paradoxically protects cardiomyocytes against iron-mediated toxicity: role of reactive oxygen species and ferritin. *J. Biol. Chem.* **279**, 13738-13745 (2004).

77. Gow, A. J. *et al*. Immunotargeting of glucose oxidase: intracellular production of H(2)O(2) and endothelial oxidative stress. *Am. J. Physiol.* **277**, L271-81 (1999).

78. Christofidou-Solomidou, M. *et al*. Immunotargeting of glucose oxidase to endothelium in vivo causes oxidative vascular injury in the lungs. *Am. J. Physiol. Lung Cell. Mol. Physiol.* **278**, L794-805 (2000).

79. Green, W. R. Histopathology of age-related macular degeneration. *Mol. Vis.* **5**, 27 (1999).

80. Strunnikova, N. *et al*. Regulated heat shock protein 27 expression in human retinal pigment epithelium. *Invest. Ophthalmol. Vis. Sci.* **42**, 2130-2138 (2001).

81. Zhang, C., Baffi, J., Cousins, S. W. & Csaky, K. G. Oxidant-induced cell death in retinal pigment epithelium cells mediated through the release of apoptosis-inducing factor. *J. Cell. Sci.* **116**, 1915-1923 (2003).

82. Kroemer, G., Dallaporta, B. & Resche-Rigon, M. The mitochondrial death/life regulator in apoptosis and necrosis. *Annu. Rev. Physiol.* **60**, 619-642 (1998).

83. Pastorino, J. G., Simbula, G., Gilfor, E., Hoek, J. B. & Farber, J. L. Protoporphyrin IX, an endogenous ligand of the peripheral benzodiazepine receptor, potentiates induction of the mitochondrial permeability transition and the killing of cultured hepatocytes by rotenone. *J. Biol. Chem.* **269**, 31041-31046 (1994).

84. Zhuang, S., Demirs, J. T. & Kochevar, I. E. P38 Mitogen-Activated Protein Kinase Mediates Bid Cleavage, Mitochondrial Dysfunction, and Caspase-3 Activation during Apoptosis Induced by Singlet Oxygen but Not by Hydrogen Peroxide. *J. Biol. Chem.* **275**, 25939-25948 (2000).

85. Shimizu, H. *et al*. Activation of p38 mitogen-activated protein kinase and caspases in UVB-induced apoptosis of human keratinocyte HaCaT cells. *J. Invest. Dermatol.* **112**, 769-774 (1999).

86. Shimizu, H. *et al*. Activation of p38 mitogen-activated protein kinase and caspases in UVB-induced apoptosis of human keratinocyte HaCaT cells. *J. Invest. Dermatol.* **112**, 769-774 (1999).

87. Nemoto, S., Xiang, J., Huang, S. & Lin, A. Induction of apoptosis by SB202190 through inhibition of p38beta mitogen-activated protein kinase. *J. Biol. Chem.* **273**, 16415-16420 (1998).

88. Dalle-Donne, I., Rossi, R., Milzani, A., Di Simplicio, P. & Colombo, R. The actin cytoskeleton response to oxidants: from small heat shock protein phosphorylation to changes in the redox state of actin itself. *Free Radic. Biol. Med.* **31**, 1624-1632 (2001).

89. Klesse, L. J., Meyers, K. A., Marshall, C. J. & Parada, L. F. Nerve growth factor induces survival and differentiation through two distinct signaling cascades in PC12 cells. *Oncogene* **18**, 2055-2068 (1999).

90. Ikeyama, S., Kokkonen, G., Shack, S., Wang, X. T. & Holbrook, N. J. Loss in oxidative stress tolerance with aging linked to reduced extracellular signal-regulated kinase and Akt kinase activities. *FASEB J.* **16**, 114-116 (2002).

91. Peus, D. & Pittelkow, M. R. Reactive oxygen species as mediators of UVB-induced mitogen-activated protein kinase activation in keratinocytes. *Curr. Probl. Dermatol.* **29**, 114-127 (2001).

92. Jimenez, L. A. *et al.* Role of extracellular signal-regulated protein kinases in apoptosis by asbestos and H2O2. *Am. J. Physiol.* **273**, L1029-35 (1997).

93. Yan, F., Hui, Y. N., Li, Y. J., Guo, C. M. & Meng, H. Epidermal growth factor receptor in cultured human retinal pigment epithelial cells. *Ophthalmologica* **221**, 244-250 (2007).

94. Raman, M., Chen, W. & Cobb, M. H. Differential regulation and properties of MAPKs. *Oncogene* **26**, 3100-3112 (2007).

95. Slack, D. N., Seternes, O. M., Gabrielsen, M. & Keyse, S. M. Distinct binding determinants for ERK2/p38alpha and JNK map kinases mediate catalytic activation and substrate selectivity of map kinase phosphatase-1. *J. Biol. Chem.* **276**, 16491-16500 (2001).

96. Klassen, H., Ziaeian, B., Kirov, I. I., Young, M. J. & Schwartz, P. H. Isolation of retinal progenitor cells from post-mortem human tissue and comparison with autologous brain progenitors. *J. Neurosci. Res.* **77**, 334-343 (2004).

97. Mayer, E. J. *et al.* Neural progenitor cells from postmortem adult human retina. *Br. J. Ophthalmol.* **89**, 102-106 (2005).

98. Tropepe, V. *et al.* Retinal stem cells in the adult mammalian eye. *Science* **287**, 2032-2036 (2000).

99. Mayer, E. J., Hughes, E. H., Carter, D. A. & Dick, A. D. Nestin positive cells in adult human retina and in epiretinal membranes. *Br. J. Ophthalmol.* **87**, 1154-1158 (2003).

100. Caldwell, M. A. *et al.* Growth factors regulate the survival and fate of cells derived from human neurospheres. *Nat. Biotechnol.* **19**, 475-479 (2001).

159

101. Horrocks, G. M., Lauder, L., Stewart, R. & Przyborski, S. Formation of neurospheres from human embryonal carcinoma stem cells. *Biochem. Biophys. Res. Commun.* **304**, 411-416 (2003).

102. Suslov, O. N., Kukekov, V. G., Ignatova, T. N. & Steindler, D. A. Neural stem cell heterogeneity demonstrated by molecular phenotyping of clonal neurospheres. *Proc. Natl. Acad. Sci. U. S. A.* **99**, 14506-14511 (2002).

103. Marquardt, T. *et al.* Pax6 is required for the multipotent state of retinal progenitor cells. *Cell* **105**, 43-55 (2001).

104. Xu, S. *et al.* The proliferation and expansion of retinal stem cells require functional Pax6. *Dev. Biol.* **304**, 713-721 (2007).

105. Frade, J. M. & Barde, Y. A. Genetic evidence for cell death mediated by nerve growth factor and the neurotrophin receptor p75 in the developing mouse retina and spinal cord. *Development* **126**, 683-690 (1999).

106. Arnhold, S., Klein, H., Semkova, I., Addicks, K. & Schraermeyer, U. Neurally Selected Embryonic Stem Cells Induce Tumor Formation after Long-Term Survival following Engraftment into the Subretinal Space. *Invest. Ophthalmol. Vis. Sci.* **45**, 4251-4255 (2004).

107. Klassen, H. J. *et al.* Multipotent retinal progenitors express developmental markers, differentiate into retinal neurons, and preserve light-mediated behavior. *Invest. Ophthalmol. Vis. Sci.* **45**, 4167-4173 (2004).

108. Cai, H. & Del Priore, L. V. Gene expression profile of cultured adult compared to immortalized human RPE. *Mol. Vis.* **12**, 1-14 (2006).

109. Burns, R. P. & Feeney-Burns, L. Clinico-morphologic correlations of drusen of Bruch's membrane. *Trans. Am. Ophthalmol. Soc.* **78**, 206-225 (1980).

110. Ishibashi, T., Sorgente, N., Patterson, R. & Ryan, S. J. Pathogenesis of drusen in the primate. *Invest. Ophthalmol. Vis. Sci.* **27**, 184-193 (1986).

111. Pichon, S., Bryckaert, M. & Berrou, E. Control of actin dynamics by p38 MAP kinase - Hsp27 distribution in the lamellipodium of smooth muscle cells. *J. Cell. Sci.* **117**, 2569-2577 (2004).

112. Hollborn, M., Bringmann, A., Faude, F., Wiedemann, P. & Kohen, L. Signaling pathways involved in PDGF-evoked cellular responses in human RPE cells. *Biochem. Biophys. Res. Commun.* **344**, 912-919 (2006).

113. Kalmes, A., Deou, J., Clowes, A. W. & Daum, G. Raf-1 is activated by the p38 mitogen-activated protein kinase inhibitor, SB203580. *FEBS Lett.* **444**, 71-74 (1999).

114. Birkenkamp, K. U. *et al.* The p38 MAP kinase inhibitor SB203580 enhances nuclear factor-kappa B transcriptional activity by a non-specific effect upon the ERK pathway. *Br. J. Pharmacol.* **131**, 99-107 (2000).

115. Fatima, S., Khandekar, Z., Parmentier, J. H. & Malik, K. U. Cytosolic phospholipase A2 activation by the p38 kinase inhibitor SB203580 in rabbit aortic smooth muscle cells. *J. Pharmacol. Exp. Ther.* **298**, 331-338 (2001).

116. Numazawa, S. *et al.* Regulation of ERK-mediated signal transduction by p38 MAP kinase in human monocytic THP-1 cells. *J. Biochem. (Tokyo)* **133**, 599-605 (2003).

117. Ishii, Y., Sakai, S. & Honma, Y. Pyridinyl imidazole inhibitor SB203580 activates p44/42 mitogen-activated protein kinase and induces the differentiation of human myeloid leukemia cells. *Leuk. Res.* **25**, 813-820 (2001).

118. Hecquet, C., Lefevre, G., Valtink, M., Engelmann, K. & Mascarelli, F. cAMP inhibits the proliferation of retinal pigmented epithelial cells through the inhibition of ERK1/2 in a PKA-independent manner. *Oncogene* **21**, 6101-6112 (2002).

119. Coles, B. L. *et al.* Facile isolation and the characterization of human retinal stem cells. *Proc. Natl. Acad. Sci. U. S. A.* **101**, 15772-15777 (2004).